AD-A057 329 BELL HELICOPTER TEXTRON FORT WORTH TEX F/G 1/3
VIBRATORY ICE PROTECTION FOR HELICOPTER ROTOR BLADES.(U)
JUN 78 H E LEMONT, H UPTON DAAJ02-76-C-0051
UNCLASSIFIED USAAMRDL-TR-77-29 NL

1 OF 2
AD
A057329

(18) USAAMRDL-TR-77-29

(19) LEVEL II

(11)

(6) VIBRATORY ICE PROTECTION FOR HELICOPTER ROTOR BLADES

(10) H. E. Lemont
H. Upton
Bell Helicopter Textron
P.O. Box 482
Fort Worth, Texas 76101

(11) June 1978

(12) 174 p.

(9) Final Report.

(15) DAAJ02-76-C-0051

(16) 1F262209AH76

(17) 00

Prepared for

APPLIED TECHNOLOGY LABORATORY
U. S. ARMY RESEARCH AND TECHNOLOGY LABORATORIES (AVRADCOM)
Fort Eustis, Va. 23604

APPLIED TECHNOLOGY LABORATORY POSITION STATEMENT

The primary purpose of this effort was to assess, through analyses, the feasibility of the vibratory concept for helicopter rotor blade ice protection to provide a sound basis for further development or abandonment of the concept. The primary concern was the effect of induced rotor blade vibrations on blade fatigue life and other airframe and subsystem components. Also of significance in determining feasibility for further development are features such as system weight, cost, reliability, maintainability, aircraft performance penalties, and countermeasures. This effort has resulted in analytically derived estimates of these features.

This Laboratory concurs in the findings presented in this report and recommends use of the information contained herein for further R&D planning purposes. The information contained herein should not be used for design of production systems, since test verification has not been accomplished.

This Laboratory plans to continue investigations to verify the feasibility of the vibratory concept for rotor blade ice protection and to further develop the concept if feasibility can be verified.

The Project Engineer for this effort was Richard I. Adams of the Systems Support Division.

Unclassified

SECURITY CLASSIFICATION OF THIS PAGE (When Data Entered)

REPORT DOCUMENTATION PAGE		READ INSTRUCTIONS BEFORE COMPLETING FORM
1. REPORT NUMBER USAAMRDL-TR-77-29	2. GOVT ACCESSION NO.	3. RECIPIENT'S CATALOG NUMBER
4. TITLE (and Subtitle) VIBRATORY ICE PROTECTION FOR HELICOPTER ROTOR BLADES		5. TYPE OF REPORT & PERIOD COVERED Final 6. PERFORMING ORG. REPORT NUMBER
7. AUTHOR(s) H. E. Lemont H. Upton		8. CONTRACT OR GRANT NUMBER(s) DAAJ02-76-C-0051
9. PERFORMING ORGANIZATION NAME AND ADDRESS Bell Helicopter Textron P. O. Box 482 Fort Worth, Texas 76101		10. PROGRAM ELEMENT, PROJECT, TASK AREA & WORK UNIT NUMBERS 62209A 1F262209AH76 165EK
11. CONTROLLING OFFICE NAME AND ADDRESS Applied Technology Laboratory, U. S. Army Research and Technology Laboratories (AVRADCOM) Fort Eustis, Virginia 23604		12. REPORT DATE June 1978 13. NUMBER OF PAGES 167
14. MONITORING AGENCY NAME & ADDRESS(if different from Controlling Office)		15. SECURITY CLASS. (of this report) Unclassified 15a. DECLASSIFICATION/DOWNGRADING SCHEDULE

16. DISTRIBUTION STATEMENT (of this Report)

Approved for public release; distribution unlimited.

17. DISTRIBUTION STATEMENT (of the abstract entered in Block 20, if different from Report)

18. SUPPLEMENTARY NOTES

19. KEY WORDS (Continue on reverse side if necessary and identify by block number)

Deicing	Helicopter Rotors
Vibration	Fatigue
Helicopters	Hubs
Airloads	Gearbox

20. ABSTRACT (Continue on reverse side if necessary and identify by block number)

This report presents the results of a study on vibrational deicing of main and tail rotor blades through higher harmonic shaking of the blades with aerodynamic, mechanical, and hydraulic shakers. Studies were made of various locations for mounting shakers, the forces and frequencies to deice, types of shakers, concept effectiveness, energy requirements, system reliability, system maintainability, weights, costs, aircraft performance penalties, impact on countermeasure methods, effects on aircraft components, and applicability

over

DD FORM 1 JAN 73 1473 EDITION OF 1 NOV 65 IS OBSOLETE

Unclassified

SECURITY CLASSIFICATION OF THIS PAGE (When Data Entered)

20. ABSTRACT - Continued

to main and tail rotor blades of both metal and composite construction. Ratings of systems to vibrate blades are compared; electrical control diagrams for shaker mechanisms are presented; and results of a breadboard test are included. A bibliography is presented of reports pertinent to vibrational deicing of rotor blades.

SUMMARY

This study on vibrational deicing methods defines the criteria developed for five rotor blade deicing systems and contains design and analysis evaluations of pertinent parameters associated with conventional main rotor metal and composite blades. Tail rotors are also examined for feasibility for deicing by this method. Criteria are developed from U.S. Army, NASA, and Bell Helicopter Textron (BHT) sources. Application of the criteria to the evolved designs and computations of forcing functions, frequencies, and modes are included, in addition to the methodology used to perform the task.

Dual mode blade excitation was determined to be the most suitable rotor deicing system after consideration of the complexity of the system; its energy requirements; its reliability, maintainability, weight, and cost; and its applicability to the particular aircraft. Energy requirements are low (about one-third of a competing electrical blanket system) and excellent shaker frequency control and phasing was illustrated by the breadboard tests. Weight estimations of the vibrational deicing study systems indicated savings exceeding 50 percent of the electrical blanket system weight. Tail rotor deicing by this method is questionable as to its efficacy; however, composite main rotor blades are quite suitable because of their high strain capability. Applicability to various aircraft appears practical but with a detailed examination required of the vibrational characteristics of the components of the aircraft. The technical problem areas and selected or proposed solutions are discussed. Results of the study are summarized and conclusions are drawn. Recommendations for refinements of technique, criteria, and future work to permit expanding the use of vibrational deicing are made. Appendixes are included defining detailed engineering computations used in support of the study effort.

PREFACE

The work reported herein was performed by Bell Helicopter Textron (BHT) for the U. S. Army Air Mobility Research and Development Laboratory under Contract DAAJ02-76-C-0051.*

Technical program direction was provided by Mr. R. I. Adams of the Eustis Directorate, USAAMRDL. Principal Bell Helicopter personnel associated with the program were Messrs. R. Bennett, B. Hart, J. Harse, L. Hopfensperger, M. Mooney, S. Shori, G. Sparling, P. Swartz, and H. Lemont.

Data to analyze non-BHT aircraft were supplied by USAAMRDL.

*On September 1977, the name of this organization was changed from the Eustis Directorate, US Army Air Mobility Research and Development Laboratory to Applied Technology Laboratory, US Army Research and Technology Laboratories (AVRADCOM).

TABLE OF CONTENTS

TABLE OF CONTENTS - CONT

TABLE OF CONTENTS - CONC

LIST OF ILLUSTRATIONS

LIST OF ILLUSTRATIONS - CONT

LIST OF ILLUSTRATIONS - CONC

LIST OF TABLES

1. INTRODUCTION

All-weather operation of rotary-wing aircraft is a much desired military goal; however, a major deterrent has been the lack of a cost-effective and practical rotor blade deicing system. Extensive efforts have been expended to test systems for anti-icing or deicing of rotor blades; these have included, among others, chemical, electro-thermal, hot air, sonic and electrical impulses, and mechanical approaches. Cost and operational difficulties have sharply curtailed the use of these with the results that few helicopters are really protected for icing conditions.

Present practice,except in a few cases where electro-thermal systems are used, is to limit flight when the threat of icing exists. In the event that a nonprotected helicopter is caught in an icing situation, rotor rpm is usually cycled in an effort to shed ice, and the mission is generally aborted for safety reasons. Nonavailability of aircraft under this situation reduces helicopter utility in certain world areas and seasons; therefore, a means to overcome this limitation becomes critical, particularly for U.S. Army use.

In an attempt to solve this problem, various methods of vibrational deicing of main and tail rotor blades have been investigated at BHT. Basically, this involves exciting the blade through forcing function shakers mounted at various locations on the aircraft. Modal shapes are selected which cause deicing based on strain of the ice/surface bond (essentially skin strain) and produce the accelerations related to the blade higher harmonic motion. The blade modes selected for excitation of the rotor may be symmetric or asymmetric in nature. The strain on the ice/surface bond necessary for effective deicing of a metal blade was measured in ice chamber tests under a BHT Independent Research and Development (IRAD) program; strain criteria developed from these tests were used to study the effectiveness of vibrational deicing of several helicopters. While the study was limited to beamwise mode excitation for the design effort, chordwise modes were reviewed also for strain effects. Chordwise strains required for deicing were unacceptable. Torsional and coupled modes were not reviewed as computer technology does not encompass valid solutions; no reason exists for believing these modes would not be acceptable for use.

Basic criteria for the development of a suitable system were required and these were delineated on the basis of previous experience at BHT, the many NASA (NACA) and other test programs

on icing, U. S. Army studies and tests (Reference 1), and other pertinent Government and private industry sources.

During the program, emphasis was on: (a) an indepth search for the most practical means of supplying vibrational inputs to the blades, and (b) the effects of the deicing technique on helicopter and component vibration levels, fatigue life, and safety. This was because successful vibrational deicing must be based on an intimate knowledge of helicopter blade structural response and its associated stress effects. Comparative systems were evolved and evaluated for suitability for use.

As main and tail rotor blades are subject to icing effects, both types were investigated. In addition, because of the differences in characteristics between composite and metal rotor blades (particularly internal damping), a review of each was initiated. The aircraft reviewed and the mechanism approaches to vibrational deicing are shown in Table 1 as an application chart of the various vibrational deicing systems.

The operational requirements for Army helicopters were surveyed, and cycle times for the systems for various deicing rates were determined. Electronic control systems, to control the frequency, phase, and duty cycle of each of the five systems, were specified. Breadboards of two systems were constructed and tested. One breadboard represented a control for a fixed system shaker using a hydraulic actuator. The second breadboard simulated a two-bladed rotor system with a shaker on each blade. The shakers were driven by DC motors. An electronic control system was developed that controlled the frequency and relative phase of the motors. The tests demonstrated that the shakers could be controlled with the precision necessary to excite the simulated blade in both asymmetric and symmetric modes.

---

[1] J. B. Werner, THE DEVELOPMENT OF AN ADVANCED ANTI-ICING/DEICING CAPABILITY FOR U. S. ARMY HELICOPTERS, Lockheed-California Company, USAAMRDL-TR-75-34A and B, Eustis Directorate, U. S. Army Air Mobility R&D Laboratory, Fort Eustis, Virginia, November 1975, ADA019044 and ADA019049.

TABLE 1. AIRCRAFT APPLICATIONS CHART FOR VIBRATIONAL DEICING SYSTEMS

AIRCRAFT	DEICING SYSTEMS						
	T/R GEARBOX	M/R GEARBOX	BLADE TIP	ON HUB	IN BLADES	BLADE LEADING EDGE	PITCH CHANGE
UH-1	x	x	xx	x	x	x	x
AH-1	x	x	xx	x	x	x	x
AAH Hughes	x	x	xx	x	-	x	x
OH-58	x	x	--	x	-	x	x
UTTAS Sikorsky	x	*	xx	x	*	x	x
ASH	x	*	xx	x	*	x	x
CH-47	xxx	*	xx	x	*	x	x

x Probable
- Not Possible
xx Requires Blade Redesign
xxx Not Applicable
* Unknown

2. BACKGROUND

Experience at BHT with ice protection development for aircraft began in 1951 with the testing of an H-13 on Mt. Washington. In 1958, an H-13H, with electrothermal deicing blades, was thoroughly evaluated at Ottawa, Mt. Washington, and Eglin Field. Also, electrothermal and fluid ice protection systems for UH-1 rotors have been successfully tested. The fluid rotor protection system for ice protection of main and tail rotor blades of the UH-1 was found to be lighter and simpler than electrothermal concepts and performed relatively satisfactorily. BHT has, most recently, performed in-house research studies including testing of a low-cost rotor blade deicing system based on vibrational deicing of rotor blades.

Analytical tools included two computer programs (Myklestad and C81 Rotorcraft Flight Simulation) developed over the past nine years by BHT under IRAD and by several USAAMRDL contracts. This permits the employment of the best current analytical techniques to evaluate vibrational deicing systems.

Many reports on anti-icing and deicing based on numerous analyses and test data have been generated. A partial listing of deicing background data is shown in the Reference and Bibliography Sections of this report.

2.1 DEICING CRITERIA

The criteria applicable to this funded study of vibrational deicing may be delineated as the following:

- Conditions to be satisfied for successful ice removal by vibration. This may be defined as the required blade/icebond interface strain at a particular frequency.

- Operating conditions of the aircraft. This reflects Army aircraft time of operation in light, moderate, and heavy icing (Reference 1).

- General conditions for the design of mechanical/electrical components. This defines the operational capability of the shaker(s), the control system, and associated equipment and instrumentation.

The effects of these criteria on the specific designs evaluated for the study help determine system suitability while providing a standard for making comparative designs. The above general

criteria are expanded in this section of the report to reflect their usage in the study effort.

2.1.1 Conditions for Ice Removal by Vibration

Criteria for shedding ice based on a wide range of vibrational frequencies, 5 to 1000 cps, were investigated in the IR&D program first on a flat-plate model simulating blade vibration and later on a full-scale static rotor blade.

2.1.1.1 Flat-Plate Model Representing Blade Skin

Test of ice removal from the flat aluminum plate indicated that 1/8- and 1/4-inch layers of ice shed best between 20 and 50 Hz. Little deicing occurred below 20 Hz. Above 50 Hz, the accelerations required to deice markedly affected the skin fatigue life.

2.1.1.2 Blade Tests

Deicing tests (Reference 2) using a nonrotating 40-foot-diameter UH-1 rotor indicated ice did not shed until a blade natural frequency of 28 cps was reached with vibrations from 25-45 g's. When the frequency was raised to the next mode at 47 cps, the ice was shed from 25-35 g's; deicing did not occur at higher or lower frequencies. These correspond to the third and fourth out-of-plane cyclic modes as calculated by the Myklestad program for the UH-1 rotor at zero rpm. Measured accelerations at the antinodes were converted into displacements by:

$$x = (386)(\omega)^2 g \qquad (1)$$

where x is the displacement in inches; ω is the frequency in rad/sec; g is the measured acceleration in units of the acceleration of gravity. Modal participation is determined from the mode shape, and the strain level on the ice/metal bond is found by the moment distribution as calculated by the Myklestad method and the blade section properties. Strain levels at 28 cps were 0.00046 to 0.001 in./in. at the antinodes; at 47 cps, the strain levels were 0.0003 to 0.00056 in./in. Since no aerodynamic or centrifugal forces acted on the tested blade, criteria for the shakers of this study were set for exciting out-of-plane modes near 47 cps with force levels that will generate a strain of 0.0003 in./in. at the antinodes near the center of the rotor blades. Figure 1 is a summary chart of the tested antinode accelerations required to achieve surface deicing. The ice path area indicates the effect of simulated centrifugal forces on ice removal.

---

[2] H. W. Upton, MECHANICAL DEICING CONCEPT FOR HELICOPTER ROTOR BLADES, paper presented to Staying Power Symposium at Fort Rucker, Alabama, July 1975.

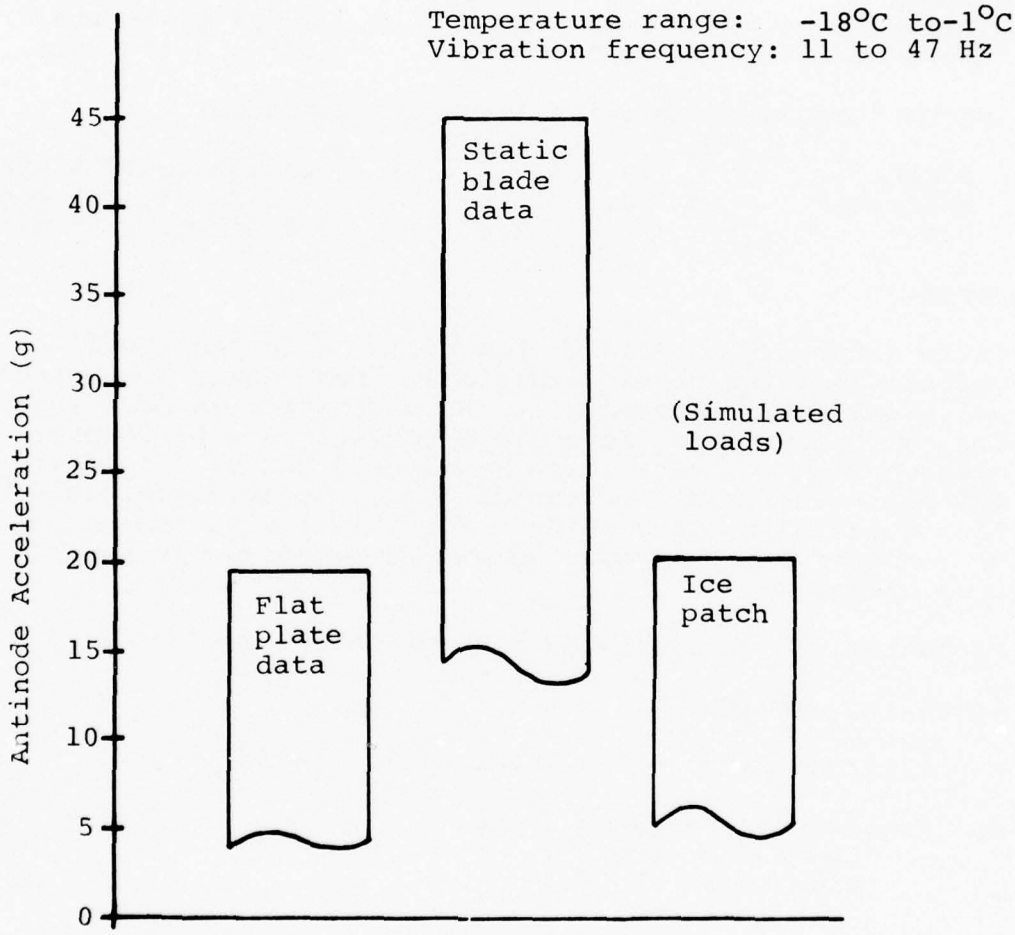

Figure 1. Range of g-levels to shed ice from metal surfaces

2.1.2 Operational Conditions of the Aircraft (Figures 2a and 2b)

1. Duty Cycle - 5 sec/shaker cycle
Continuous maximum icing (stratiform clouds)

Type of Icing	Water Content gm/m^3	Fly time .25" thick Ice*
Trace	.0 - 0.15	11 min to infinity
Light	0.15 - 0.35	5 min to 11 min
Moderate	0.35 - 1.0	1.75 min to 5 min

Intermittent maximum icing (cumuliform clouds)

Light	0.1 - 0.5	3.5 min to 17.5 min
Moderate	0.5 - 1.0	1.75 min to 3.5 min
Heavy	1.0 - 2.0	0.8 min to 1.75 min

*Reference 3

2. It is difficult to predict how often helicopters will operate in icing cloud conditions. From worldwide meteorological data, Reference 1, the assumption is made that for continuous stratiform cloud conditions a helicopter mission with moderate icing would be 3 hours. In intermittent cumuliform cloud conditions, the duration would be 15 minutes with heavy icing. For this study, fatigue life of the blades is plotted versus assumed percentage of time spent in icing conditions.

3. Mechanism TBO shall exceed that of the blade.

4. Operating Conditions:

   a. Altitude range - sea level to 10,000 ft

   b. Temperature range of icing
      Low value of -20°C
      High value of 0°C

   c. Temperature range of mechanism
      Low of -54°C
      High of +85°C

   d. Rain 6mm/hr; drop size 1.3 mm. (Ref. 1)

---

[3] R. H. Cotton, OTTAWA SPRAY RIG TESTS OF AN ICE PROTECTION SYSTEM APPLIED TO THE UH-1H HELICOPTER, Lockheed California Company, USAAMRDL TR-76-32, Eustis Directorate, U. S. Army Air Mobility R&D Laboratory, Fort Eustis, Va., November 1976, AD 034458.

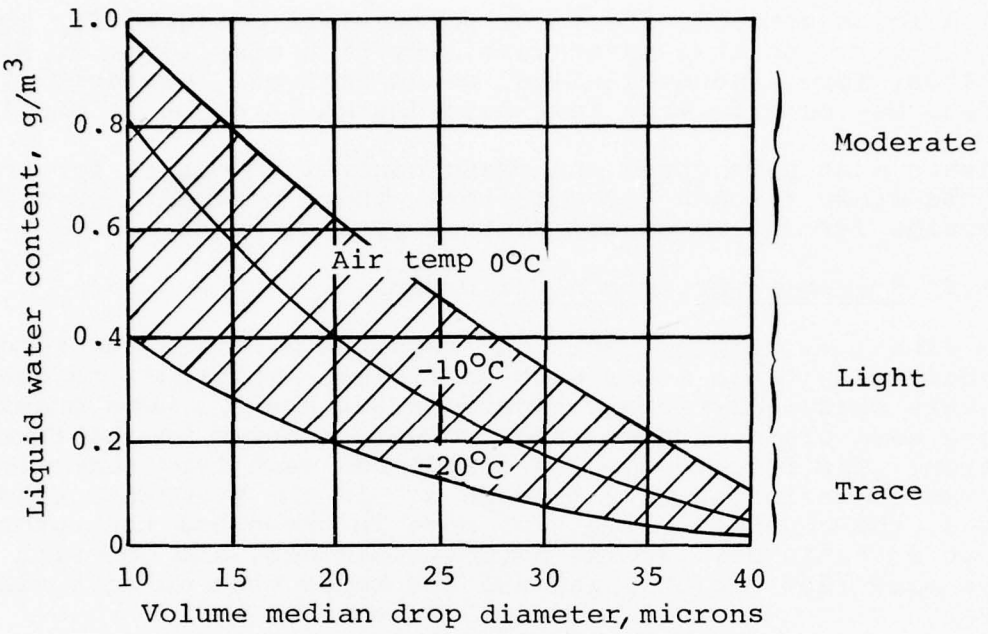

a. Continuous maximum (stratiform clouds)

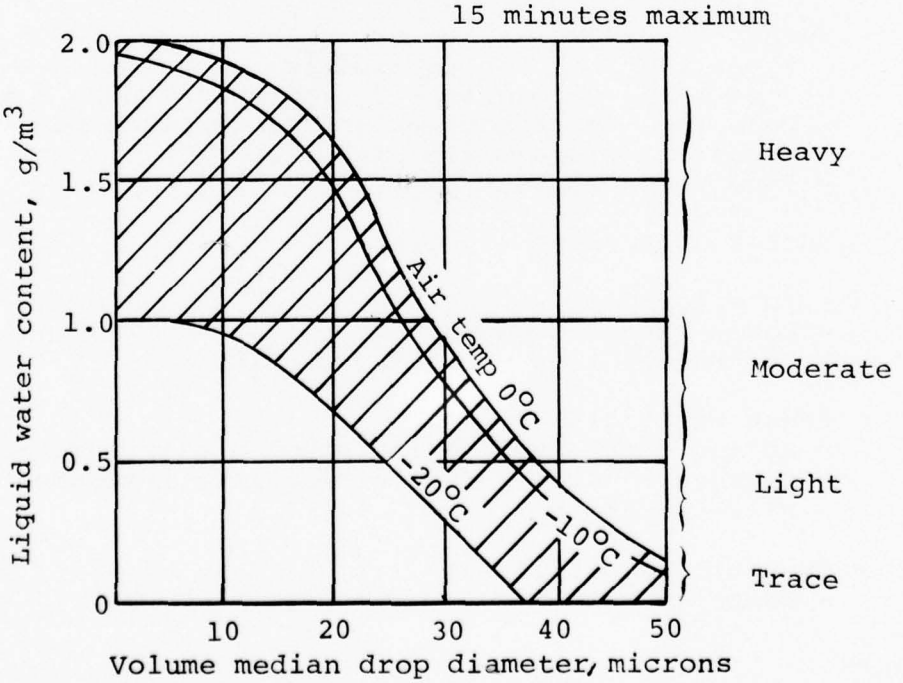

b. Intermittent maximum (cumuliform clouds)

Figure 2. Recommended atmospheric icing criteria

2.1.3 Criteria for Controller Design

All deicing controls are to be solid-state designed for good reliability and easy maintainability with compliance to MIL-E-5400E, Type 1A,and MIL-I-461 as objectives. Wherever flight safety may be effected, fail-safe design is to be accomplished.

Shakers must have speed and phase control necessary for locking on the blade resonant frequencies. There must also be a pilot override for any automatic control cycling means.

2.1.4 Criteria for Mechanical Design

The vibratory deicing technique requires exciting the rotor blades in suitable modes with sufficient amplitudes to shed ice. In this study, five basic locations for shakers were examined; three were blade mounted, and two were mounted in the fixed system. The force, power, and mode for each type were calculated and are shown in Tables 2 through 5. In the symmetric blade modes, the opposite blade tips move in phase and the rotor mast is at an antinode. In the asymmetric modes, the opposite blade tips move 180° out of phase and the rotor mast is at a vibration node.

2.1.4.1 Slip Ring Installations

- Number of rings
  - Types I and II not applicable
  - Type III - solenoids - 2 rings/blade plus 1 spare
  - Type IV - motor control - 2 rings/blade plus 1 spare; power - 2 rings/blade plus 1 spare
  - Type V - same as Type IV

- Number of brushes - 4/ring

- Ring materials
  - Power rings - copper
  - Instrumentation - silver graphite

- Brush materials
  - Spring - SAE 1095 spring steel - alternate SAE 6150
  - Brushes - power - copper/graphite; instrumentation - silver/graphite

- Operating conditions
  - Temperature
    +85°C
    -54°C

  - All weather

- Electrical capacity - power of shakers x design factor of 1.25.

2.1.4.2 Shakers

Type I - Model YAH-63 T/R Gearbox - Dual Installation

- Force and frequency per Table 2
- Power discussed in Section 3.2
- Power design installation factor = 1.25*
- Type shaker - single unbalance rotating weight (2 required)

Type II - Model AH-1G M/R Gearbox - Dual Installation

- Force and frequency per Table 3
- Power discussed in Section 3.2
- Power design installation factor = 1.25*
- Type shaker - single unbalance rotating weight (2 required)

Type III - Model UH-1 M/R Blade Aerodynamic Flap

- Force and frequency per Table 4
- Power discussed in Section 3.2
- Power design installation factor - not applicable
- Type shaker - aerodynamic flap modifying blade lift/drag characteristics

Type IV - Model UH-1 Antinodal Excitation - Single Shaker per Blade

- Force and frequency per Tables 4 & 5
- Power discussed in Section 3.2
- Power design installation factor = 1.25*
- Type shaker - single unbalance rotating weight (1 per blade)

Type V - Model UH-1 M/R Hub Excitation

- Same as Type IV

*Assumed intermittent operation (5 sec/cycle) permits three times normal motor rating to be used for design selection, i.e.,

HP_{req} = 1.25 x value of table

HP_{avail} = 3 x normal rating

TABLE 2. TAIL ROTOR GEARBOX SHAKER REQUIREMENTS ASYMMETRIC MODE*

Rotor System	Shaker Frequency (CPM)	Shaker Moment at Hub (in.-lb)	Force/Shaker 12" Spacing (lb)
UH-1	4005 (rotating)**	8150	680
	2575 (fixed)		
AH-1G	1724 (rotating)	3888	324
	294 (fixed)		
YAH-63	3688 (rotating)	900	75
	2382 (fixed)		

*Ability to excite these modes with a gearbox shaker is unknown, but they were included because they are the only modes found within frequency range.

**(rotating) induced in rotating system
(fixed) induced in fixed system

TABLE 3. MAIN ROTOR GEARBOX SHAKER REQUIREMENTS SYMMETRIC MODE

Rotor System	Shaker Frequency (CPM)	Shaker Force Total (lb)	Motion Amplitude (+in.)
UH-1	2546	840	.106
OH-58	3168	426	.0585
AH-1G	2726	3052	.015
YAH-63	2138	5148	.012

TABLE 4. MAIN ROTOR BLADE MOUNTED SHAKER REQUIREMENTS ASYMMETRIC MODE

Rotor System	Blade Station	Shaker Frequency (CPM)	Shake Force (Lb/Blade)
UH-1	28.8	2569	427
	57.6	"	338
	144.0	"	146
	288.0	"	174
AH-1	39.5	2571	757
	118.5	"	157
	264.0	"	188
CH-47	30.0	1888	394
	72.0	"	211
	180.0	"	145
	360.0	"	124
OH-58	21.2	2694	149
	42.0	"	99
	106.0	"	79
	212.0	"	51
YAH-63	42.0	2011	436
	137.0	"	245
	306.0	"	96

TABLE 5. BLADE MOUNTED SHAKER REQUIREMENTS SYMMETRIC MODES

Rotor System	Blade Station	Shaker Freq. (CPM)	Force (Lb/ Blade)	Blade Station (In)	Shaker Freq. (CPM)	Force (Lb/ Blade)
UH-1	28.8	2546	335	28.8	1752	1129
	144	"	217	100.8	"	242
	230.4	"	242	216	"	221
	288	"	222	288	"	153
OH-58	21.2	3168	180	21.2	2248	259
	53	"	99	74.2	"	66
	116.6	"	159	159	"	48
	169.6	"	149	212	"	44
	212	"	117			
AH-1	39.5	2726	474	39.5	1485	194
	118.8	"	107	184.8	"	98
	211.2	"	113	264	"	102
	264	"	142			

2.2 CONFIGURATIONS

Modal excitation of rotors for vibrational deicing may be accomplished by many approaches as shown in Figure 3. This investigation reviewed various means and selected the most promising systems for design evaluation. The aircraft of Table 1 were reviewed for applicability, and possible blade shaking systems, defined by location, are as follows:

- In the blades (cavity required)
- On the exterior of the blades
- At the hub
- In the controls (fixed or rotating systems)
- On the gearboxes

Figure 4 shows some schematic approaches to this location selection. Shakers may be of the following types as shown on the morphological chart of Figure 3.

- Mechanical
- Aerodynamic
- Hydraulic
- Electrical
- Pneumatic

Applicability of the shaker type depends upon the inherent design features of each. Shakers mounted in the rotating system required a rotary transfer valve (slip rings) between stationary structure and the rotating hub. Fluid transfer mechanisms (hydraulic, pneumatic) tend to be bulky, have reduced reliability, and require excessive maintenance. The large diameter rotating seals that would be required have indeterminate failure rates. Therefore, frequent examination and replacement might be required. Oscillating masses by electrical means (solenoids) is a heavy method for shaking blades with the frequencies and magnitudes of forcing function required. For these reasons, it was decided to investigate the mechanical and aerodynamic methods in the rotating system and the hydraulic and mechanical shakers in the fixed system.

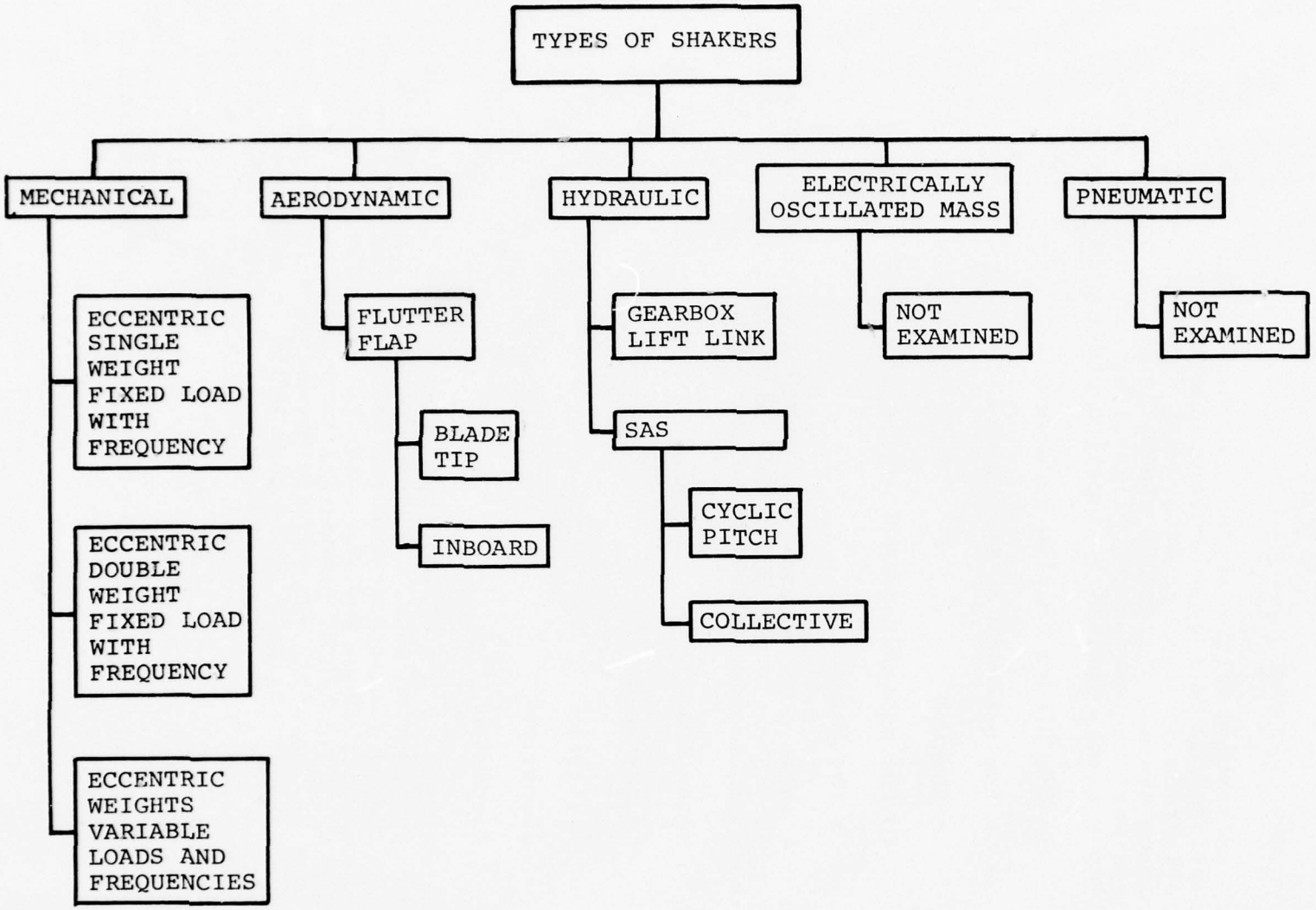

Figure 3. Types of shakers

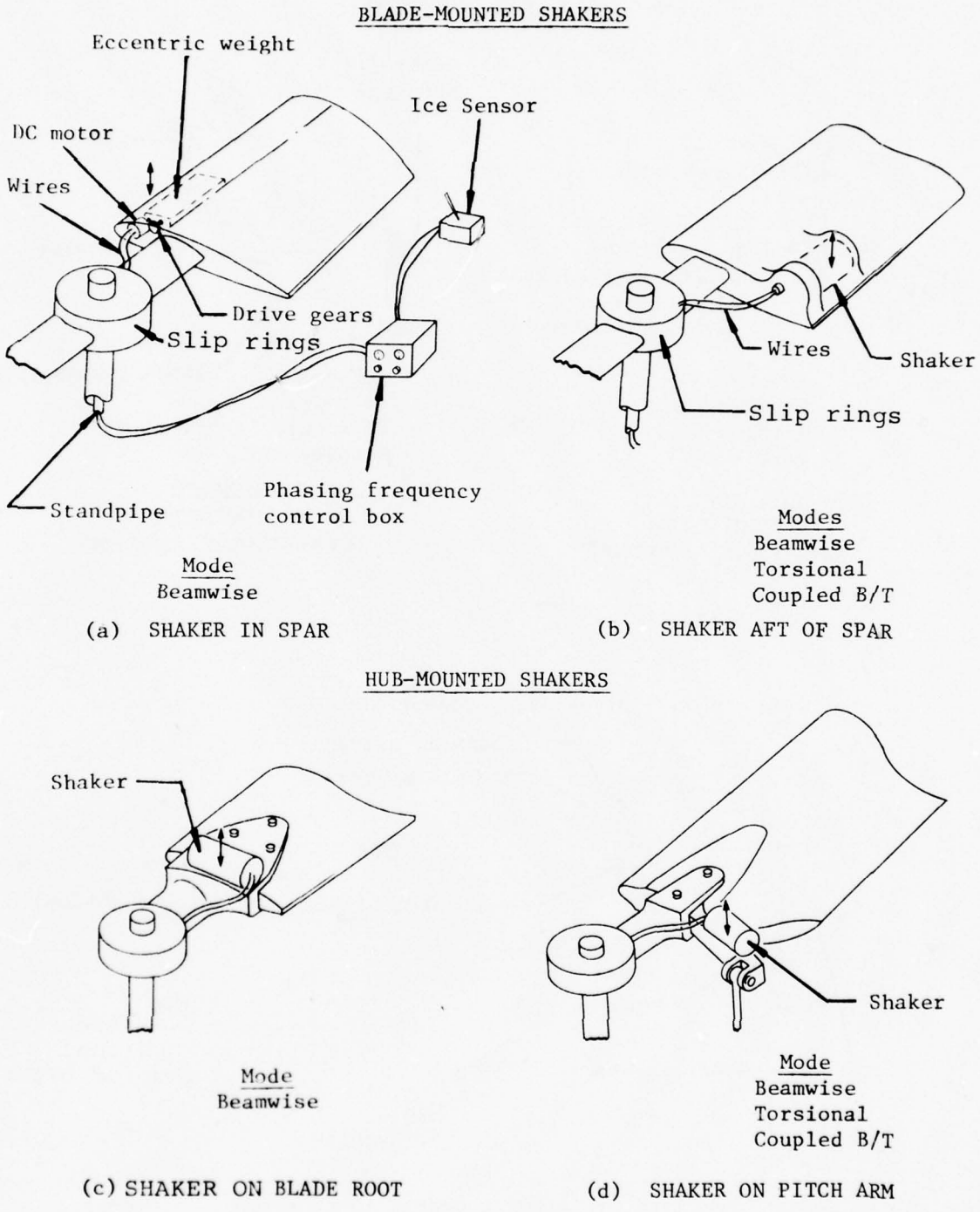

Figure 4. Examples of some possible shaker mounting locations

CONTROL SHAKERS

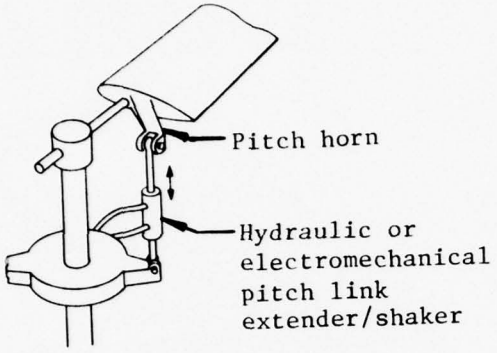

Modes
Beamwise
Torsional
Coupled B/T

(e) SHAKER IN PITCH LINK (Rotating System)

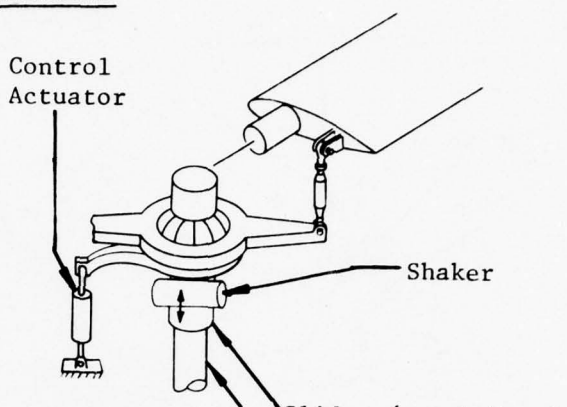

Modes
Beamwise
Torsional
Coupled B/T

(f) SHAKER ON SWASHPLATE (Stationary System)

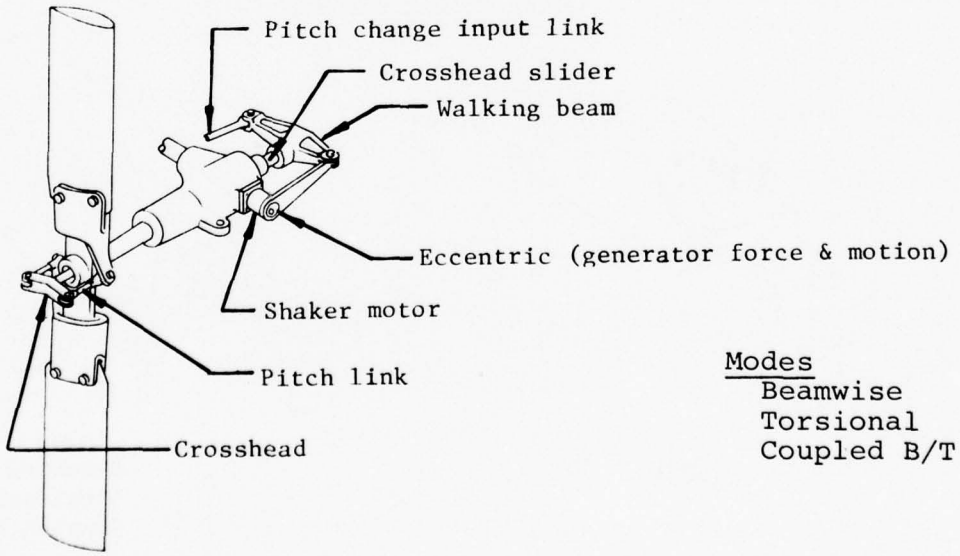

Modes
Beamwise
Torsional
Coupled B/T

(g) TAIL ROTOR SHAKER APPLICATION

Figure 4. Shaker mounting locations (Concluded)

Design of the mechanical shakers in the rotating system is markedly affected by the centrifugal force field. The closer the location of the shaker to the axis of rotation, the lower the centrifugal force applied to the mechanism. Conventional shakers have been made with two opposite rotating weights geared to give a sinusoidally varying unbalanced force. A single rotating unbalance weight will also provide a suitable forcing function. Deicing response to a forcing function occurs at the natural frequency of the blade; i.e., a single rotating weight may force only beamwise motion because of the separation between beam and chordwise frequencies. The less complex single weight design was selected because of basic simplicity for the study to avoid the on-blade problem of retention of grease in the gears and bearings in the CF environment of the rotating blade. Fretting of antifriction bearings during nonoperating conditions of the shaker in the centrifugal field requires special attention, i.e., slow rotation of bearings or the use of nonfretting types. Table 4 shows that force levels necessary to excite a particular mode are less at a midspan antinode or at the blade tip than they are at the first antinode from the hub. On the blade tip, the shaker may replace existing tip weights so the net increase in blade weight may be small or even zero.

Aerodynamic shaking may be provided either by flaps mounted on the blade at a particular spanwise location (antinode) or by cyclic or collective pitch change (dependent upon the mode excited). Flap aerodynamic forces are more effective at the dynamic pressure of the tip rather than at an inboard location, and structural modifications to a blade would probably be more easily accomplished at the blade tip (retrofit possibility); therefore, this location was selected. Oscillation of the control system to change blade pitch at a high frequency (8 per rev and higher) offers some difficulty. The control system/blade flexibility enters into the pitch response, making it difficult to control the phasing of the forcing function. The mechanism to force high-frequency pitch change (hydraulic or mechanical) is complex and heavy. Also, the modal response from control inputs would contain a torsional element with unknown effects on deicing. These considerations caused selection of the tip flap shaker as a candidate system.

Shaking of the rotor system through a flexibly mounted tail or main rotor gearbox may be accomplished either by electro-hydraulic or mechanical shakers. Tail rotor blades are usually not of sufficient size to permit the shaker to be mounted on the blade. Rotative speeds are high, and an individual shaker on each blade would require a heavy installation; normally, helicopter weight and balance considerations obviate heavy equipment located at the tail rotor station. Hydraulic shakers at the tail rotor either require a power source driven off the tail rotor drive system or suffer unacceptable line losses from main

transmission-mounted hydraulic pumps. Weight/balance considerations exist here also; therefore, the mechanical shaker was selected for this use.

From the above and for the purpose of investigating the possibly desirable systems for the basic Table 1 aircraft, the following designs were made:

Type I - Tail Rotor Excitation - Model YAH-63
Tail Rotor Gearbox with Attached Shaker(s)

Type II - Main Rotor - AH-1
Main Rotor Gearbox with Attached Shaker(s)

Type III - Main Rotor Blade Excited by Aerodynamic Tab - UH-1 Aircraft
Aerodynamic Tab and Control

Type IV - Main Rotor Blade Excited at Antinodal Point - UH-1 Aircraft

Type V - Model UH-1 Hub Excitation

2.2.1 Discussion of Designs

The study considers the relative merits of five shaker methods for force input to the blades. Each main and tail rotor of the study helicopters were analyzed to determine frequency and force requirements necessary to meet ice shedding criteria. One helicopter was then selected as an example for detailed design of each shaker type. This design was used to determine applicable size and weight for each helicopter based on the forces of Tables 2, 3, 4, and 5. A description of these designs follows:

Type I - YAH-63 Tail Rotor Excitation (Figure 5)

Excitation of the YAH-63 tail rotor mode is achieved by a gearbox dual-shaker installation of the direct-drive eccentric weight type. These are installed on a mounting bracket attached to the tail rotor gearbox on an existing bolt pattern. The center of gravity of each shaker weight is located in a plane containing the rotor axis. Shaker power is supplied by a geared 24V D.C. motor, and a forcing function of 75 pounds is available at 2382 CPM. These shakers may be operated to excite a symmetric mode of the tail rotor blade through the electrical selection of the phase location of the weights. This is basically a fixed force/frequency design. It may be noted that shaking along the rotor axis with a sinusoidally varying

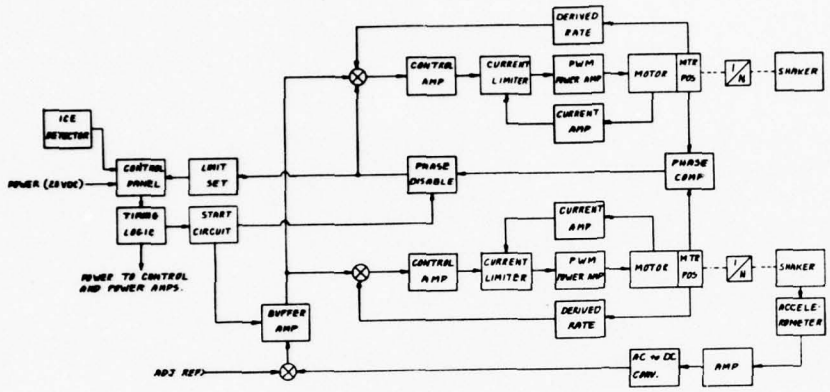

SCHEMATIC-CONTROL SYSTEM

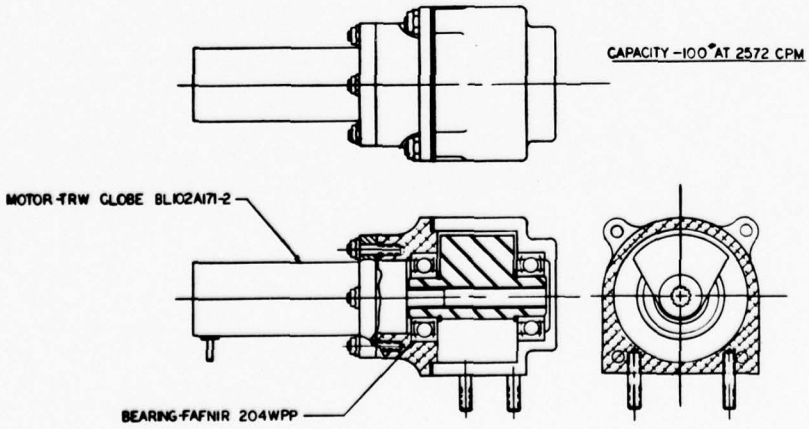

SHAKER

Figure 5. Tail rotor shaker

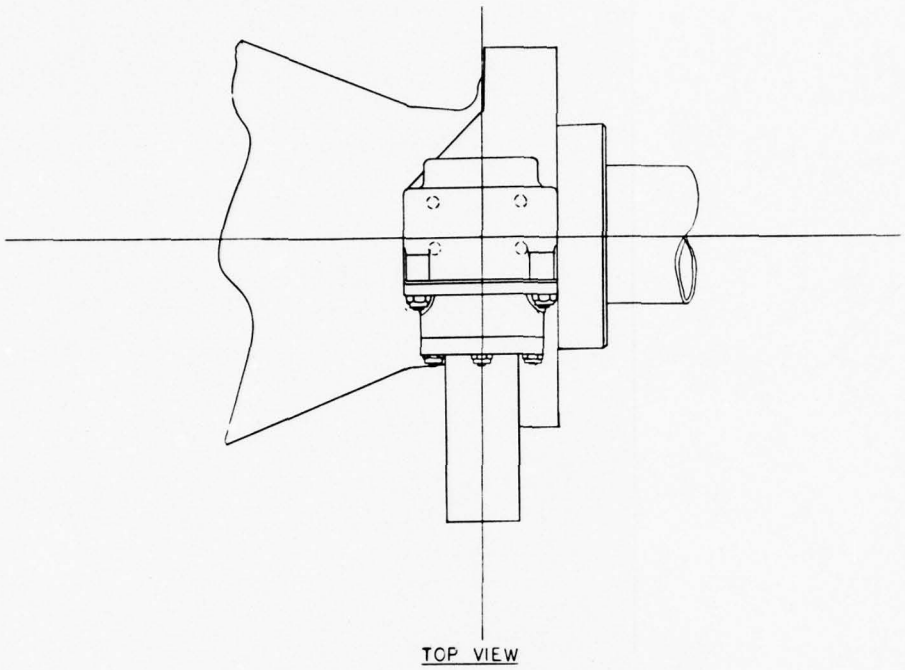

TOP VIEW

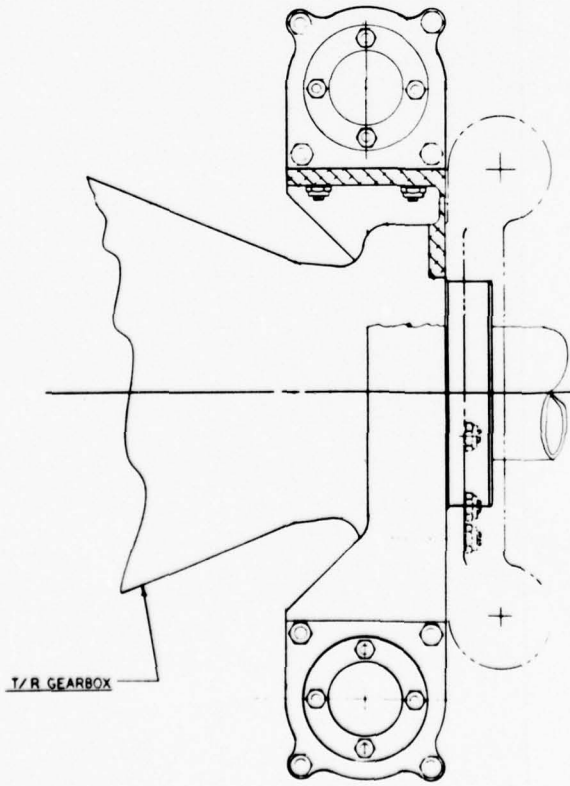

VIEW LOOKING AFT

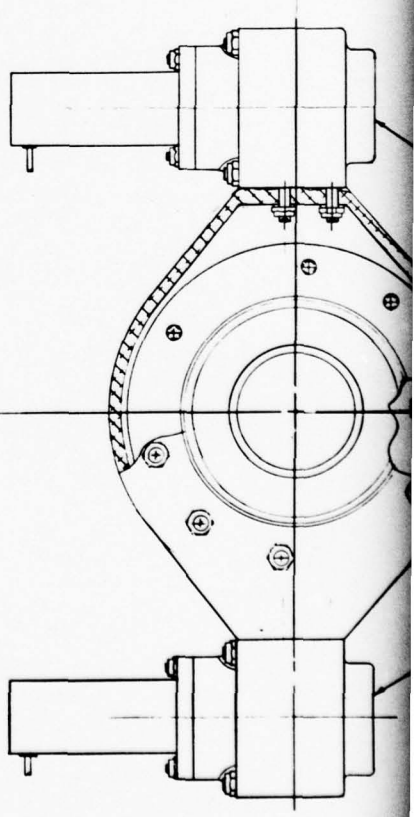

VIEW LOOKING INBOARD

SHAKER INSTALLATION

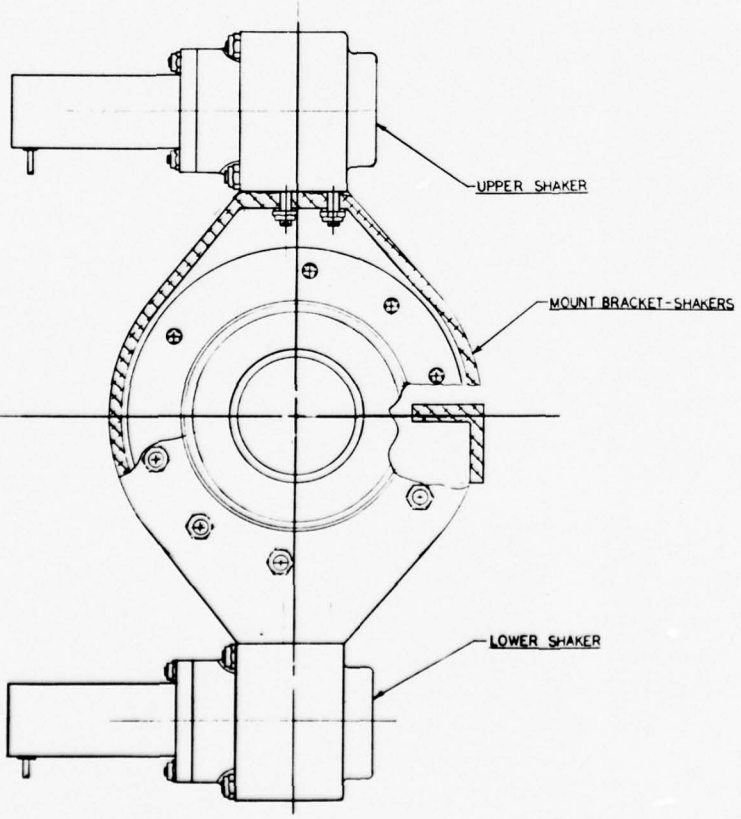

VIEW LOOKING INBOARD

AKER INSTALLATION

3

force may be accomplished as well as a sinusoidal moment input. Each shaker is self-contained with sealed, lubricated bearings. A possible schematic control system is also shown in Figure 5.

The modal excitement of the YAH-63 tail rotor is chosen for a symmetric mode. With gearbox shakers, the response of the rotor is coupled with the fuselage response because the gearbox is spring mounted to the fuselage. Therefore, it became necessary to reflect fuselage characteristics in force/frequency calculations. This was accomplished by use of the NASTRAN computer model.

Type II - AH-1G Main Rotor Gearbox Excitation (Figure 6)

Excitation of the AH-1G rotor is achieved through shaking the flexibly mounted main-rotor gearbox using a dual shaker installation of a geared single-eccentric weight type. These shakers are mounted directly to the main rotor gearbox sump with the eccentric weight centers of gravity located in a plane containing the main rotor axis of rotation. Power is supplied by a D.C. motor with a rating of about 4 Hp. The gearing has a ratio of 2:1, and the collective shaker mode has a capacity of 3052 pounds at 2502 CPM. Figure 6 shows a shaker sized for symmetric mode excitation (rotating weight equals 6.4 pounds). Figure 7 shows the blade symmetric mode shape.

Type III - UH-1 Main Rotor Blade Aerodynamic Flap (Figure 8)

The Type III aerodynamic flap exciter is tip-mounted at the trailing edge of the blade, as shown in Figure 8. It has a chord of 6 inches and a length of 18 inches. The flap is suspended on two brackets, one at the inboard end and one at the outboard end through nonlubricated radial-type woven-Teflon bearings (Faflon). The centrifugal force acting on the flap is carried to the inboard flap bracket by the internal torque rod. A split keeper and housing are used for outboard retention of the flap to the torque rod. A control system (shown in the view looking inboard) locks the flap from angle change when it is not deicing. This consists of a spring-loaded solenoid plunger (fail-safe) which pushes the linkage (via the idler arm) against an adjustable stop. Actuation of the solenoid releases the linkage, allowing the flap to flutter. The flap has a lead insert aft of the pivot axis to permit adjusting its oscillating frequency to 2569 CPM. A tip panel lift variation of 174 pounds is used for modal excitement.

The blade tip panel formed by the blade tip rib and the inboard flap bracket rib is reinforced by increased skin thickness and through corner gussets. Both flap end brackets are bolted on.

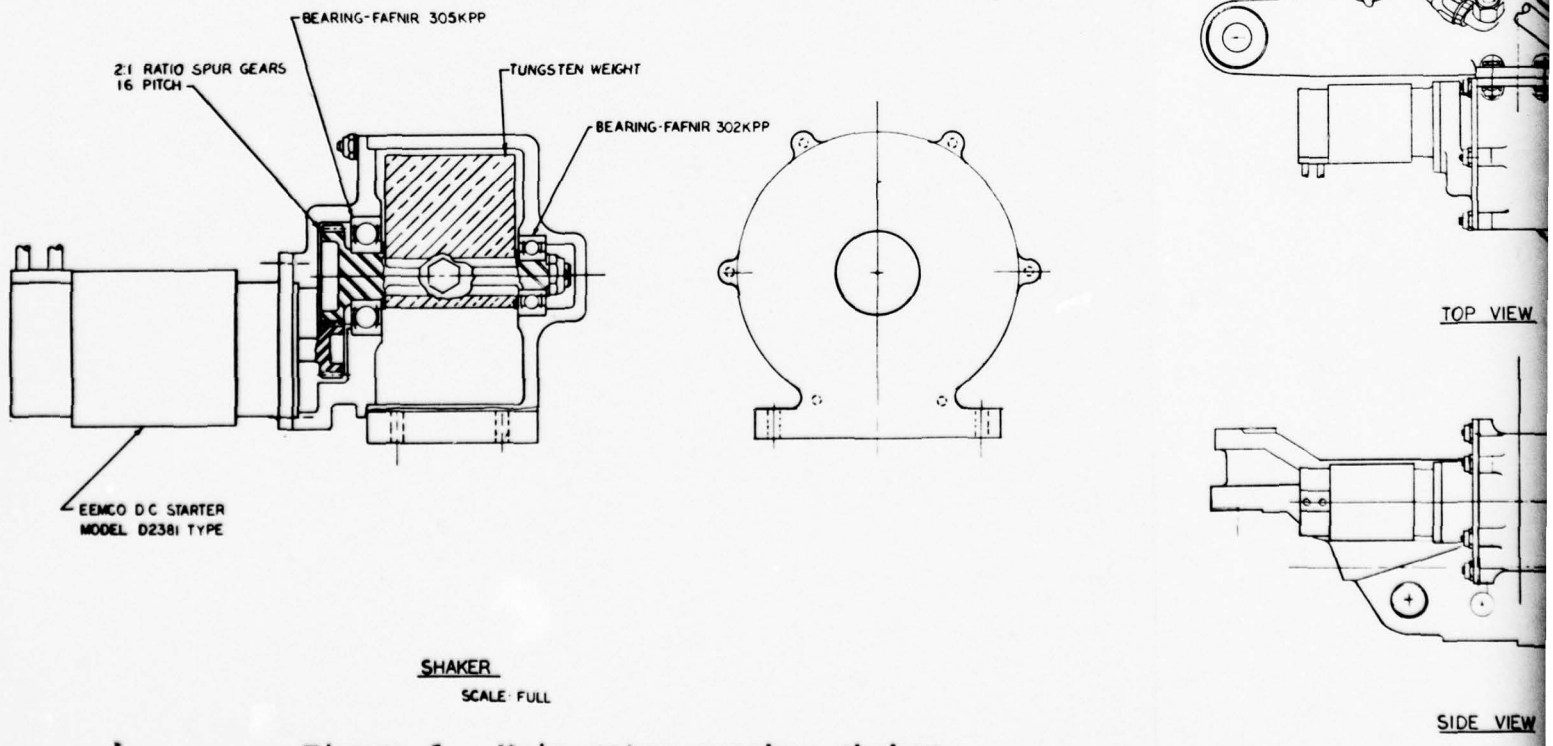

Figure 6. Main rotor gearbox shaker

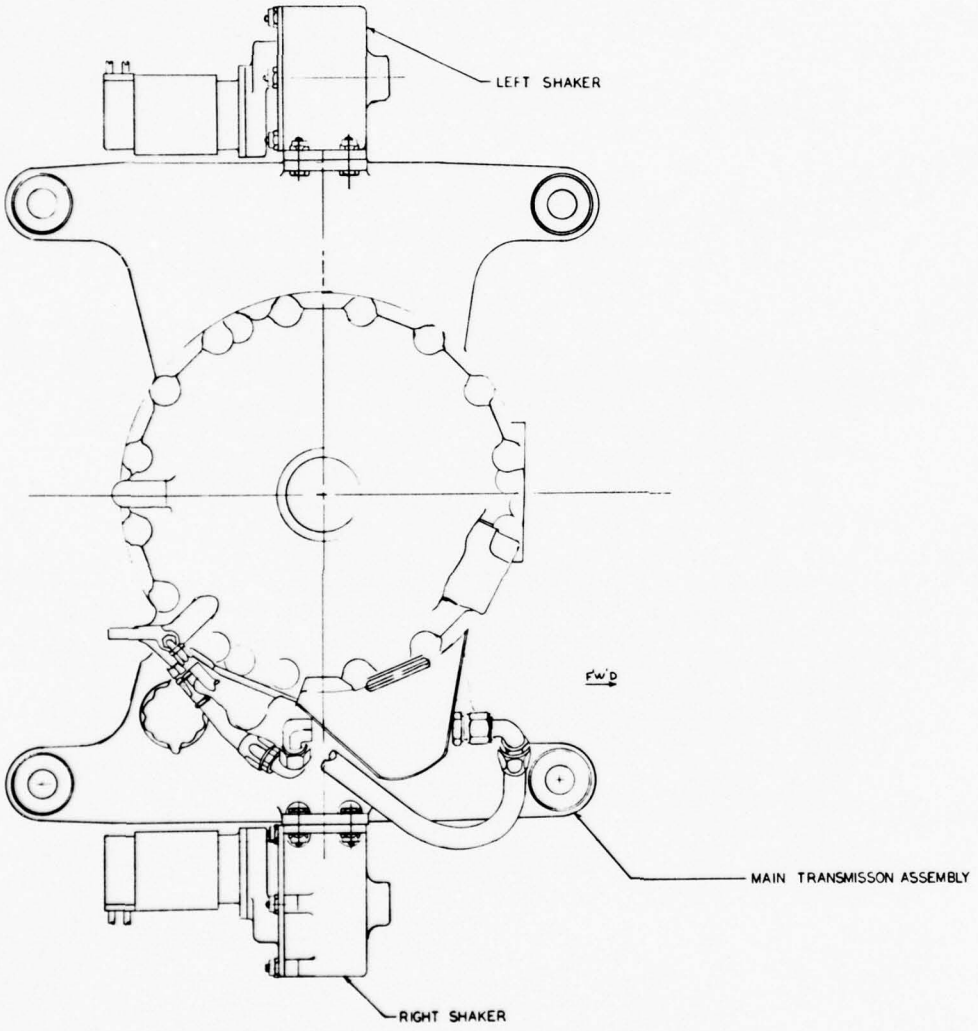

TOP VIEW

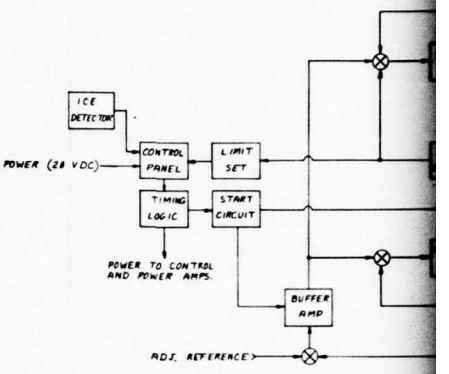

SCHEMATIC-CO

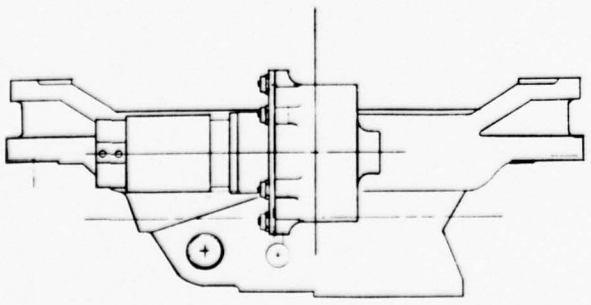

SIDE VIEW

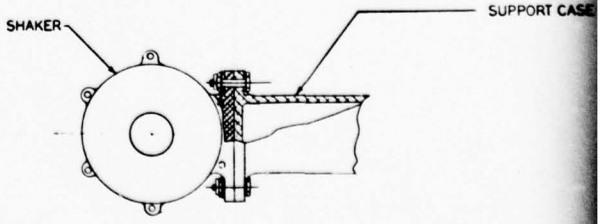

SHAKER MOUNT

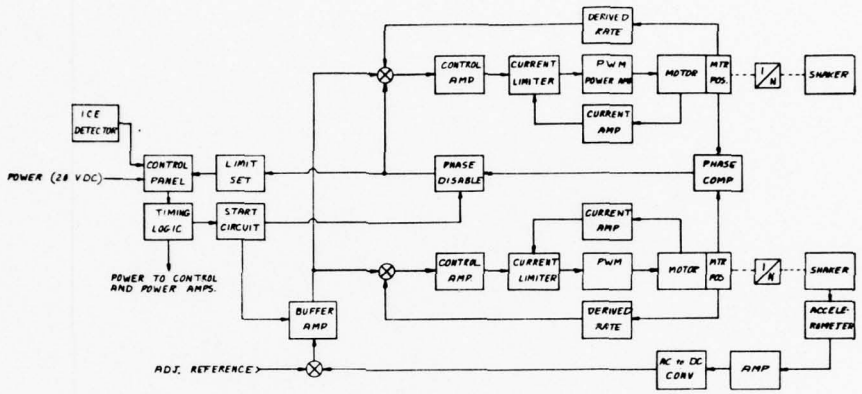

SCHEMATIC - CONTROL SYSTEM

FWD

MAIN TRANSMISSON ASSEMBLY

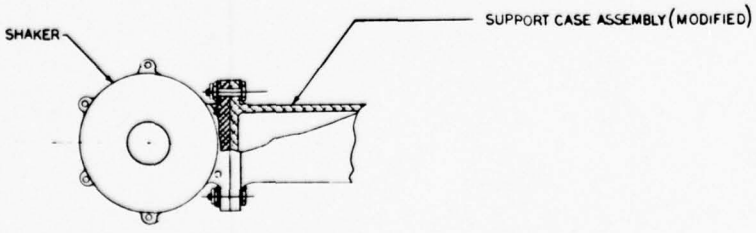

SHAKER MOUNT

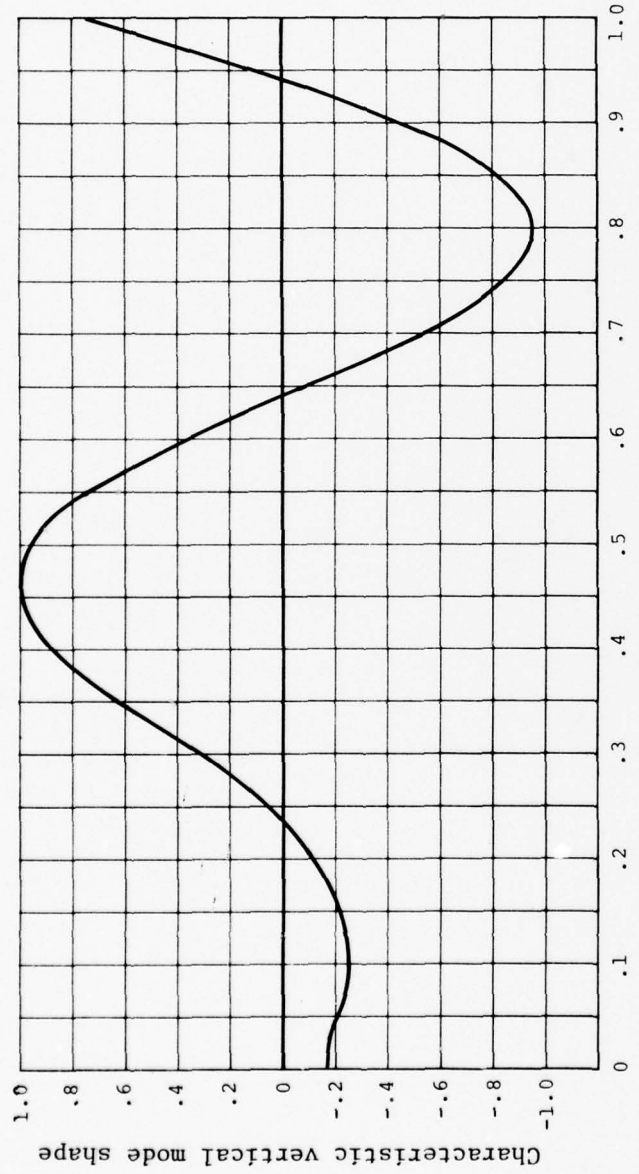

Figure 7. AH-1 symmetric mode @ 2726 CPM main rotor

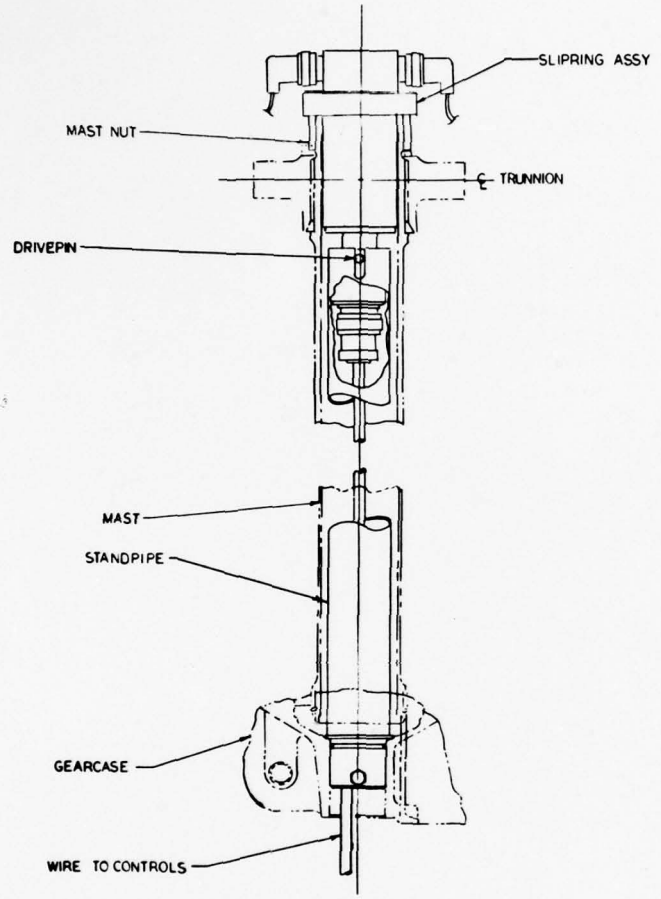

SLIP RING INSTALLATION
SCALE: 1/4

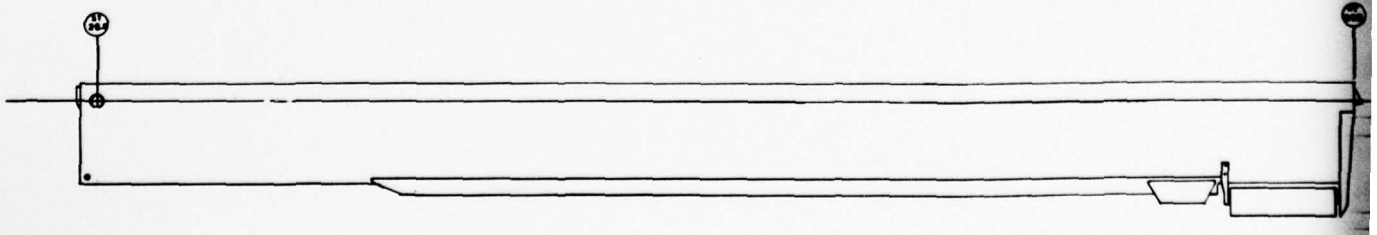

BLADE WITH FLAP
SCALE: 1/10

Figure 8. Main rotor aerodynamic flap

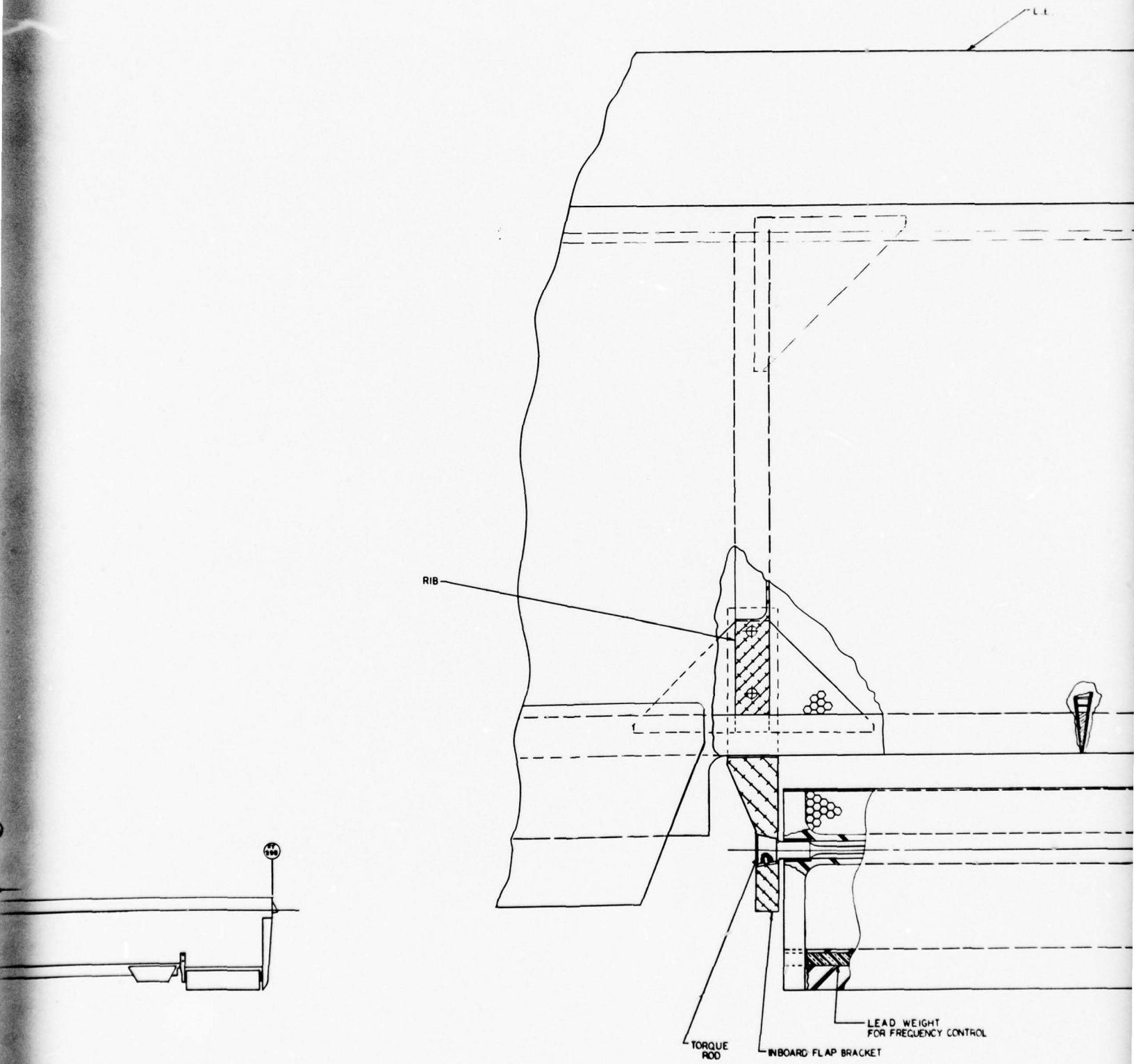
L.E.
RIB
TORQUE ROD
INBOARD FLAP BRACKET
LEAD WEIGHT FOR FREQUENCY CONTROL

BLADE TIP

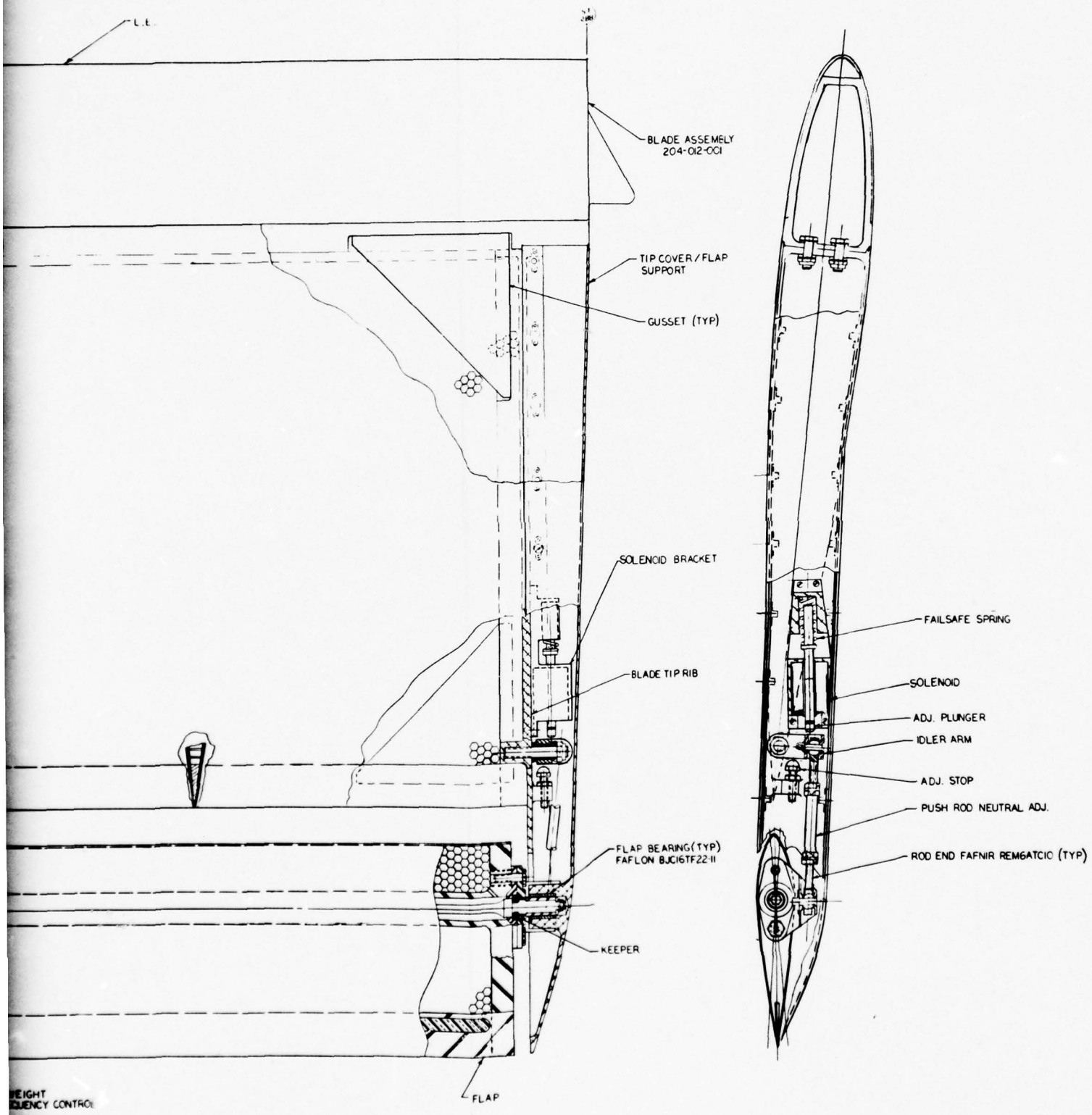

BLADE TIP

VIEW LOOKING INBOARD

3

An angular motion of between 1.5 and 2 degrees generates the tip forcing function of the criteria. A need for possible electrical flap deicing indicates that .645 Hp per blade is necessary. The mode excited by this aerodynamic flap is the symmetric mode of Figure 7.

It may be noted that no controlled phasing of flaps on opposite blades is felt necessary in that oscillations should be sympathetic and self-starting. Snubbing of the motion will occur when the solenoid current is cut off. Slip rings and a standpipe are required for solenoid power transmission. In the event flap deicing is required, of course, extra rings and circuits will be necessary.

Type IV. UH-1 Antinodal Excitation on the Blade (Figure 9)

Antinodal excitation of the UH-1, or other helicopter blades, may be accomplished at any antinode for a particular frequency. The UH-1 antinodes are at stations 57.6, 146, and 288 (at the tip). Design is easier for a shaker located at the inboard antinode because of lower centrifugal force effects. Shaker forces are generally lower at midspan and blade tip antinodes. A shaker mounted at midspan or tip locations needs to be embedded completely in the blade to prevent aerodynamic drag penalties, but it needs also to be easily accessible for inspection and overhaul. Since ice may possibly not be removed from nodal points it may become necessary to excite blades at two modes to relocate nodes and antinodes, thus permitting total deicing.

Shakers mounted in the rotating system are subject to dynamic loads caused by centrifugal, inertia, and aerodynamic forces. These loads react on the bearings of the shaker to cause so-called "false brinnelling" of the bearing races. Two possible approaches to alleviate this condition are:

- Use greatly oversized bearings
- Move the bearing races in such a manner as to distribute the loading over the complete race circumference.

The space and weight limitations of inblade mounting of shakers and weights tend to preclude using the oversize bearing approach; therefore, it becomes necessary to slowly rotate the shaker electric motor by a low current to distribute the brinnelling load.

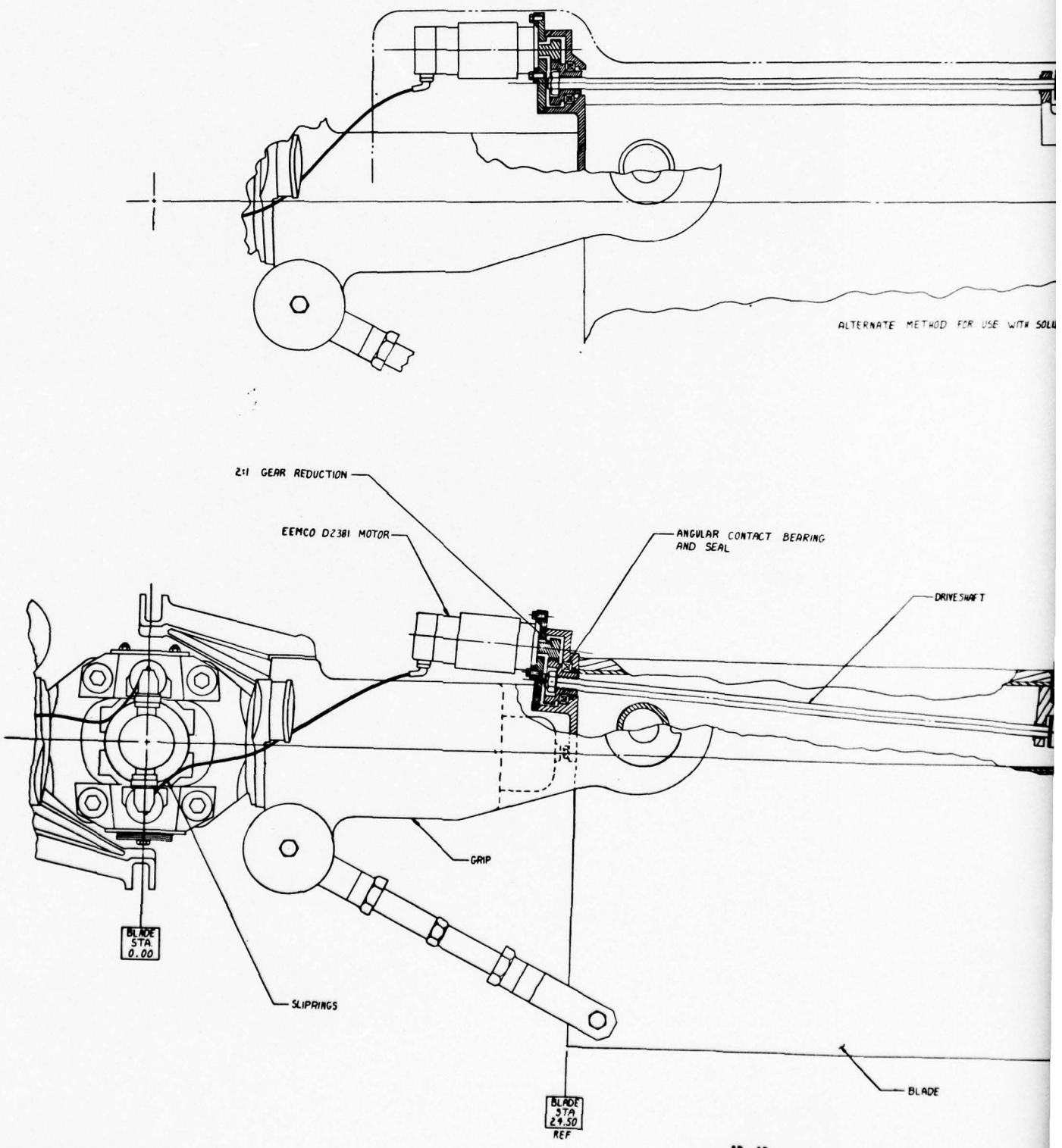

Figure 9. Main blade shakers

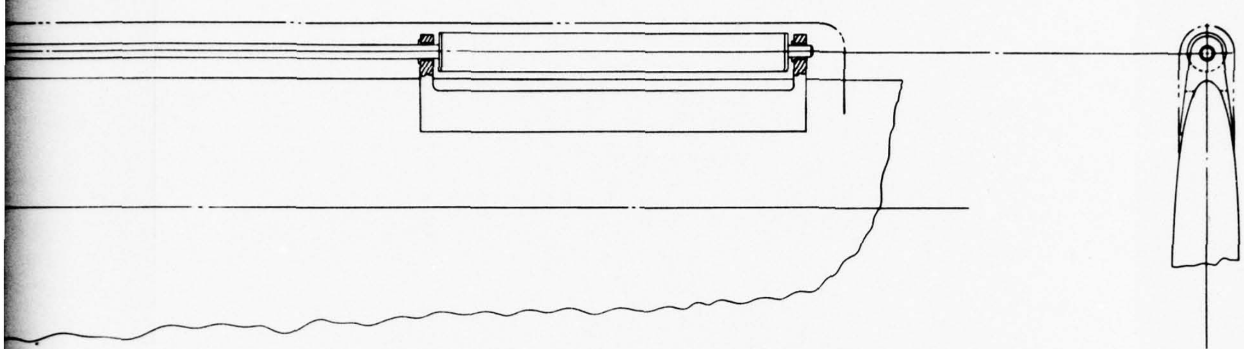

ALTERNATE METHOD FOR USE WITH SOLID BLADES

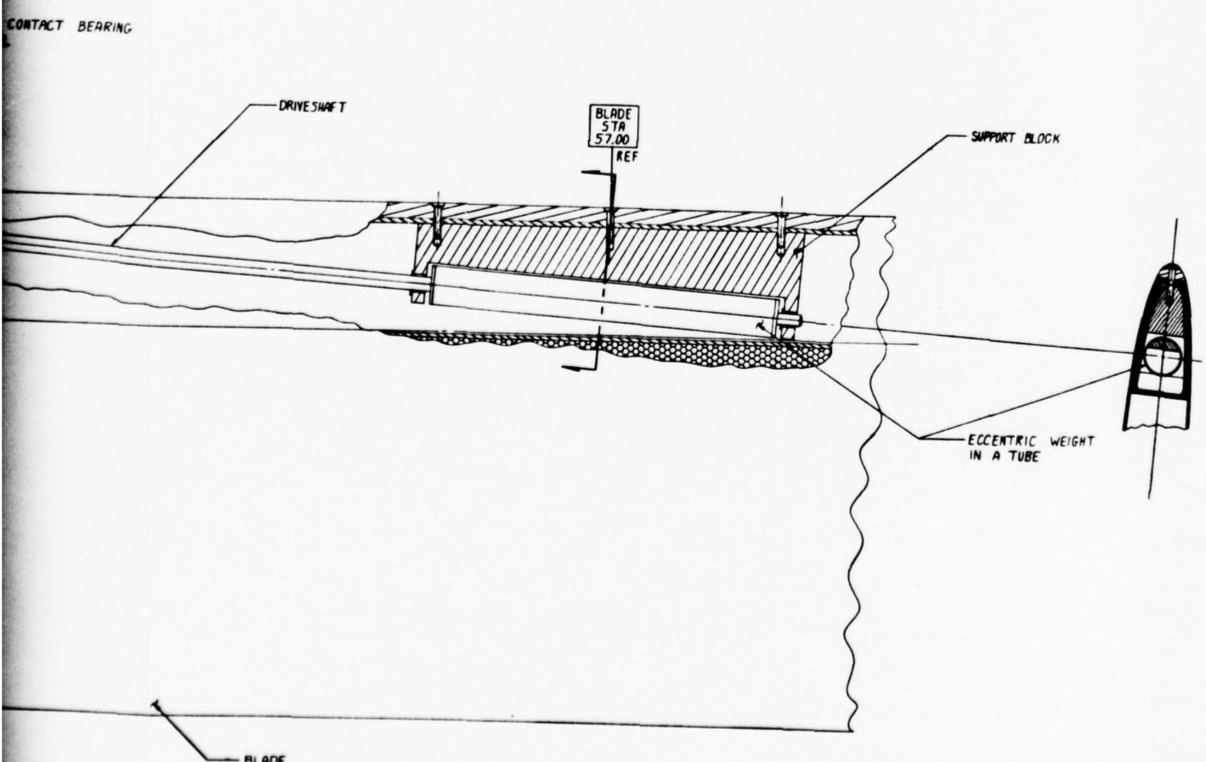

13-13
LE 1/2

2

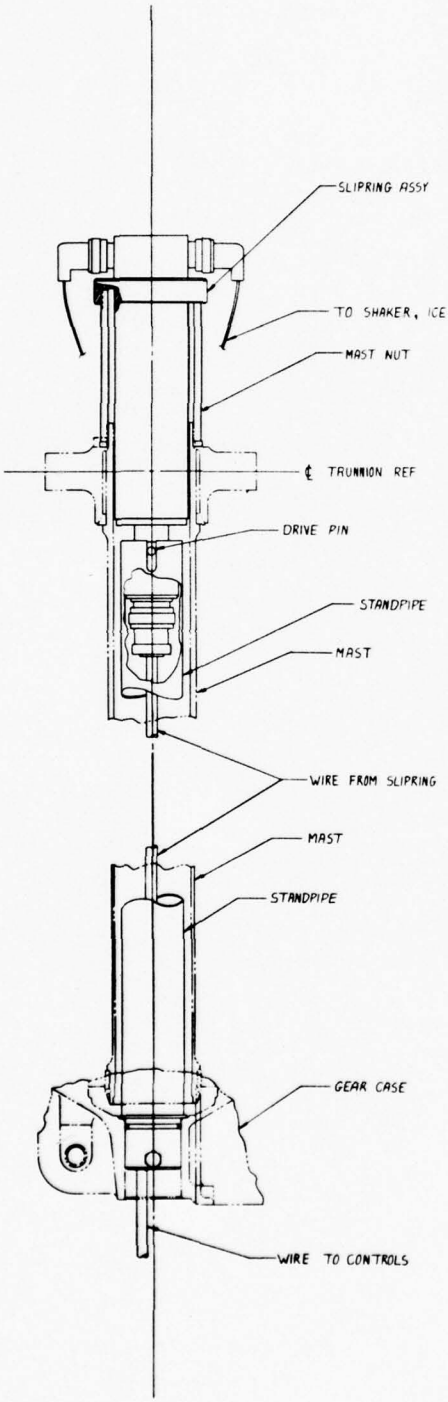

VIEW **A-A**
SCALE 1/2

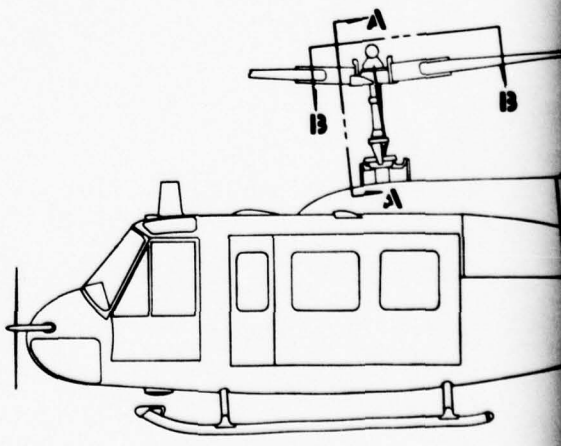

UH-1H REF

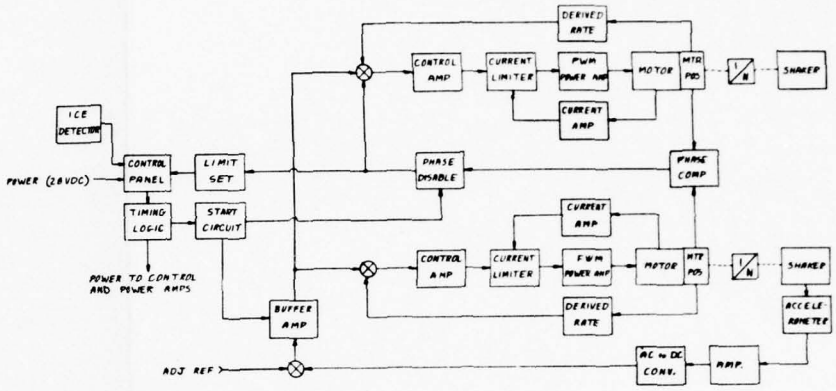
DERIVED RATE
CONTROL AMP
CURRENT LIMITER
PWM POWER AMP
MOTOR
MTR POS
1/N
SHAKER
CURRENT AMP
ICE DETECTOR
CONTROL PANEL
LIMIT SET
PHASE DISABLE
PHASE COMP
POWER (28 VDC)
TIMING LOGIC
START CIRCUIT
CURRENT AMP
CONTROL AMP
CURRENT LIMITER
PWM POWER AMP
MOTOR
MTR POS
1/N
SHAKER
POWER TO CONTROL AND POWER AMPS
BUFFER AMP
DERIVED RATE
ACCELEROMETER
ADJ REF
AC to DC CONV.
AMP.

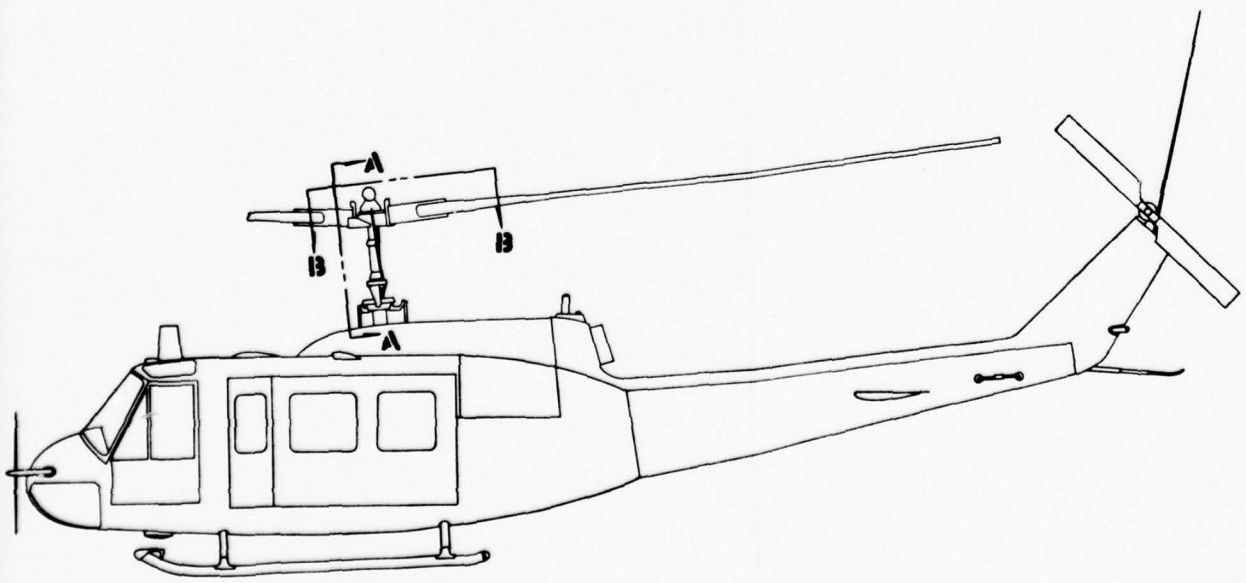
A
B
B
A

UH-1H REF

Figure 9 shows a shaker located at blade station 57.6 of the UH-1 blade.

This shaker uses a drive unit similar to the Type II shaker but with an extended hollow tube shaft to rotate the eccentric weight. The eccentric weight (off-center mass in tube) rotates on two radial woven Teflon bearings (Faflon), and its centrifugal force is carried by the shaft (beneficial stiffening effect), which is hung on a sealed angular contact bearing. The shaker is carried by a bracket bolted to existing fasteners located on the butt of the blade. Access to the internal shaker is poor in that the sleeve of the blade root attachment bolt must be removed by machining and a new one reinstalled with a temperature fit.

Some blades do not have readily accessible cavities of sufficient size in which to install the shaker. Figure 9 shows an alternate method of applying a blade shaker as an exterior installation. This requires a contour cover to fair the mechanism into the blade form.

A design sketch of a shaker mechanism for mounting in the tip of the blade is shown in Figure 10. The principal difference with this design is that it must operate in a high centrifugal force field. Tandem bearings are shown for taking the radial loads. Also, a dual weight shaker is shown so that the centrifugal force load on the eccentric weights can be borne by two sets of bearings. This design would be easily accessible from the blade tip for inspection and overhaul.

A design sketch (Figure 11) is also shown for a composite blade with a cavity and a removable cover for access to a shaker mechanism.

Both the symmetric mode (Figure 7) and the asymmetric mode (Figure 12) are excited by these shakers; however, because of the chordwise location of the shaker determined by the cavity location, torsional bending modes may be initiated also.

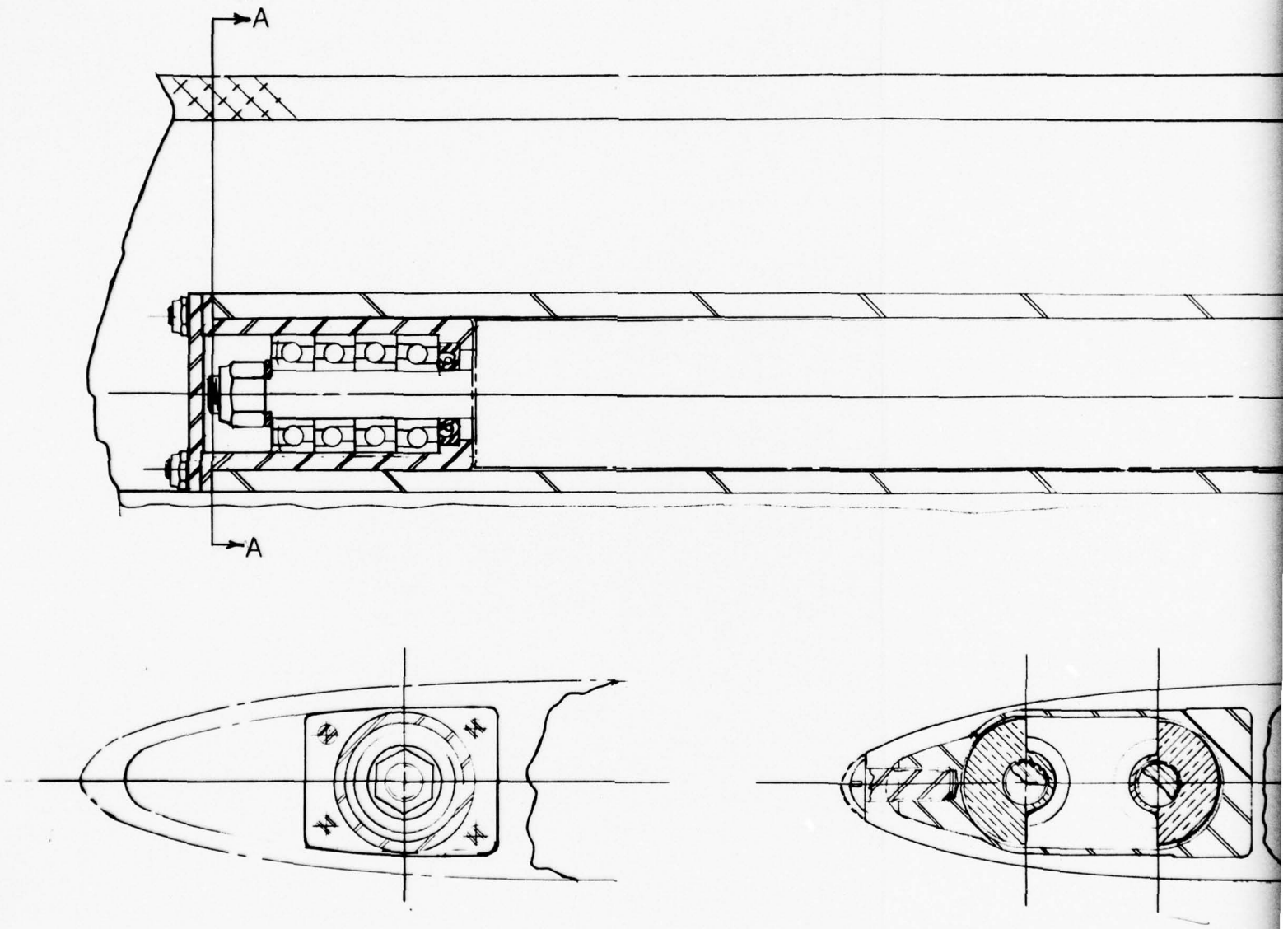

Figure 10. Blade tip shaker

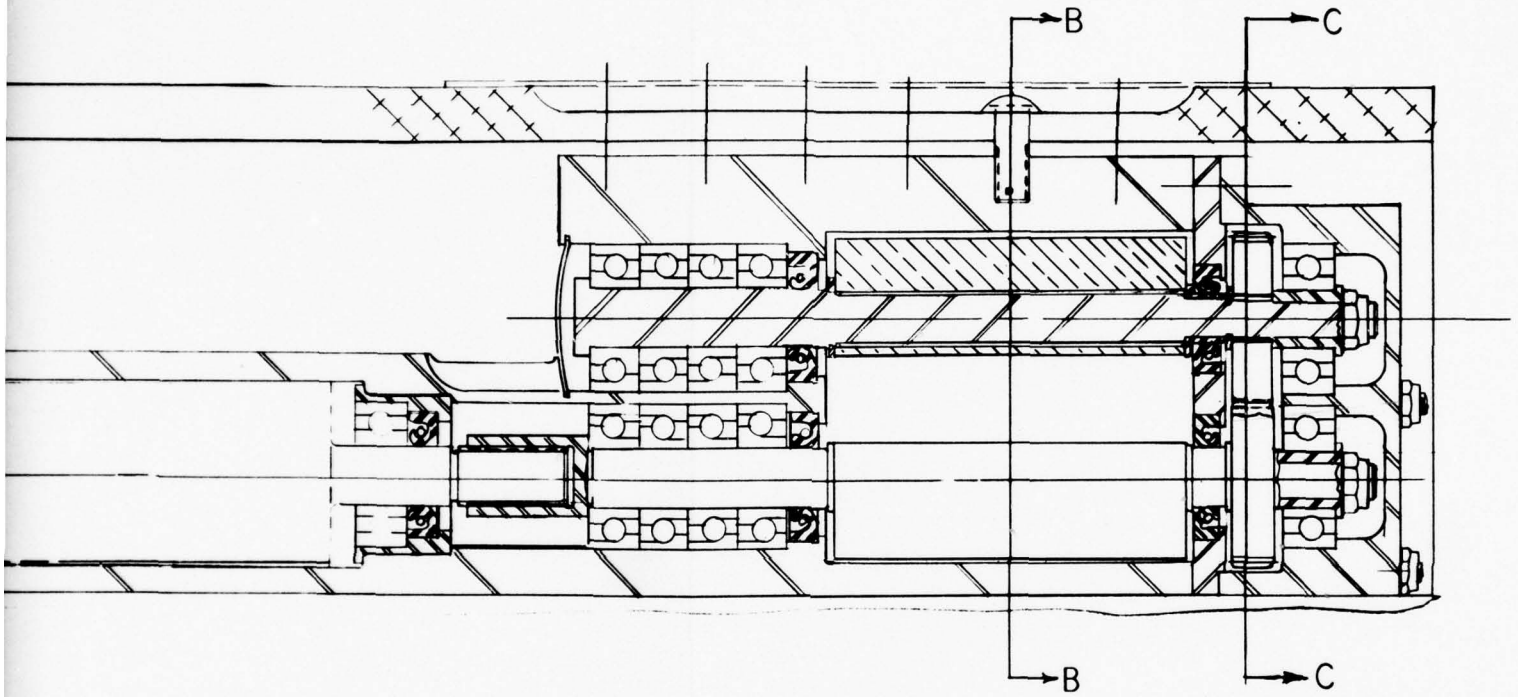

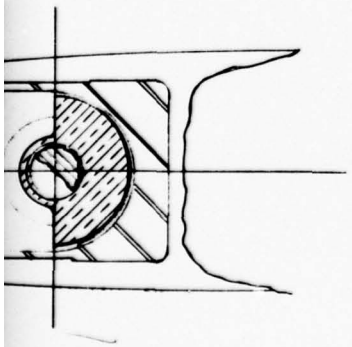

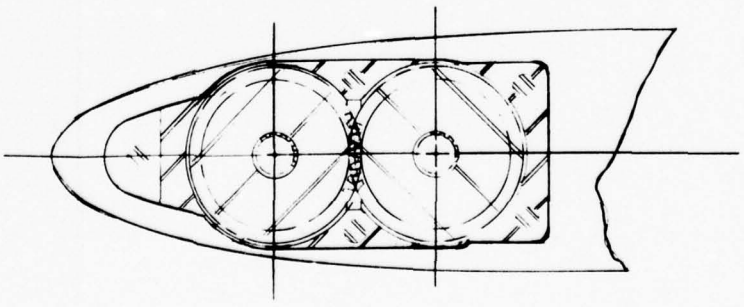

-B

SECTION C-C

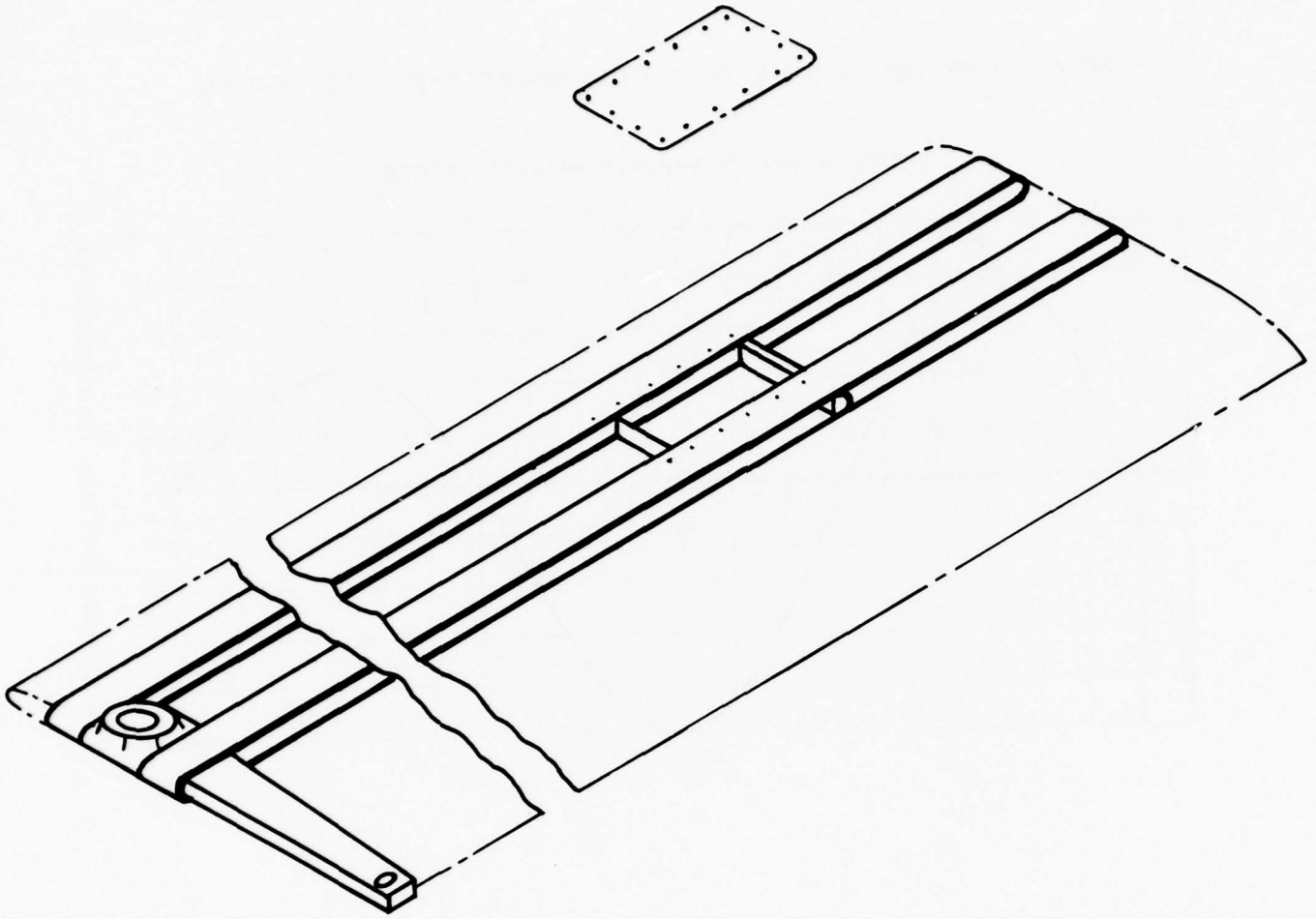

Figure 11. Composite blade with cavity

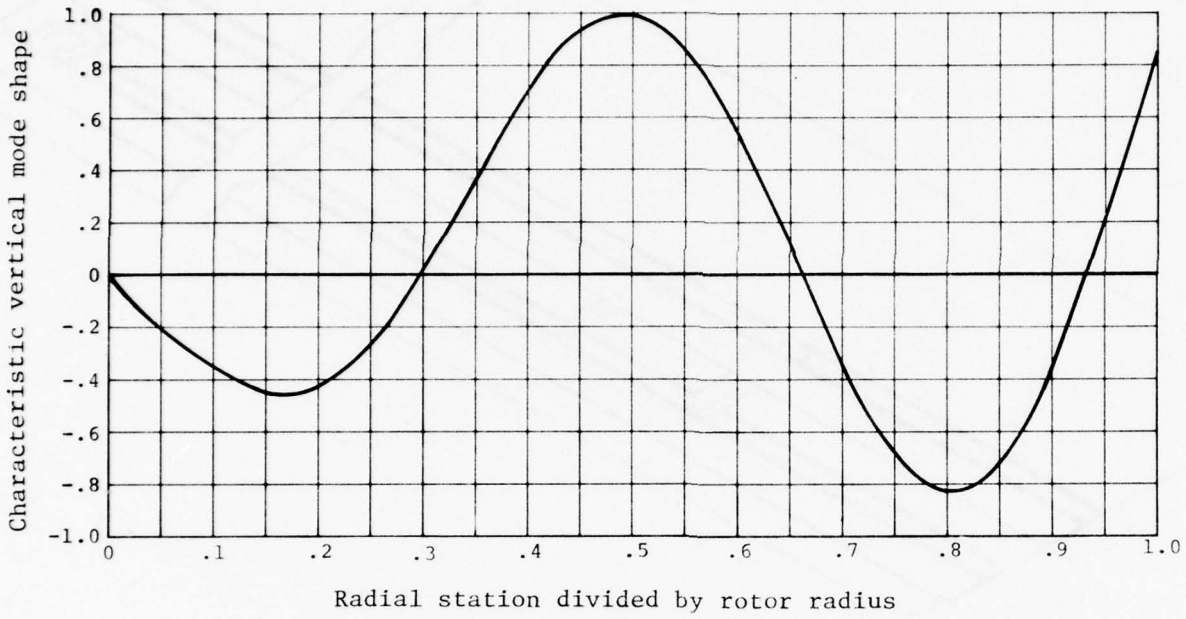

Figure 12. UH-1 asymmetric mode @ 2569 CPM main rotor

The slip ring installation, as shown for the Type III shaker, is also used in this application but more rings of a higher power capacity are required.

Type V. UH-1 Antinodal Excitation of Blade on Hub (Figure 13)

This system excites the same blade mode as Types III and IV and uses the same shaker as Type II. It is mounted on the vertical pin with suitable bracketry.

2.2.2 Variable Force/Frequency Shaker

For design comparison of the five systems (one tail rotor plus four main rotors), a simple single unbalanced weight shaker was selected for the mechanical exciter. Such an approach permits a relative comparison of the factors of the various systems for selection. Also, the single-weight type of shaker might be suitable for a single mode production system. The single-weight systems are limited for experimental use in that shakers are not capable of dual mode (in air) and on-ground deicing because of frequency/force mismatch; therefore, a controllable force/frequency/phasing shaker is required for practical use. Figure 14 shows the possible design of such a shaker as might be used on an experimental deicing flight program. Each shaker consists of two rotating unbalance weights separately powered by D.C. electric motors. The relative phasing positions of the weights are varied at a particular rotative speed (frequency) to achieve the magnitudes of unbalance required. Figure 15 shows schematically how this is accomplished. The design shown in Figure 14 is sized for the AH-1G aircraft (Type V). This shaker offers a tool for the investigation of practical deicing problems in that the magnitudes of the forcing functions are controllable to prevent overstressing of the blade; i.e., amplitudes of vibration may be readily varied while stresses are monitored. Two shakers (one per blade) are desirable to permit generation of the forces at the blade grip to permit excitation of either the symmetric or the asymmetric modes.

2.2.3 Controller Design

2.2.3.1 Dual-Motor-Driven Shaker Controller

The variable force capability of this shaker may possibly be used for the dual function of inflight or on the ground (frozen rain) deicing. No analysis was made of static blade deicing in this study although a practical demonstration was successfully achieved in the previous BHT test program. The dual-motor-driven shaker controller design concept (Figure 16) is applicable to each single-weight shaker configuration of the study. The system consists of a control panel, two D.C. motor speed control channels, designated master and slave, and a method of deriving relative frequency and phase error between the two.

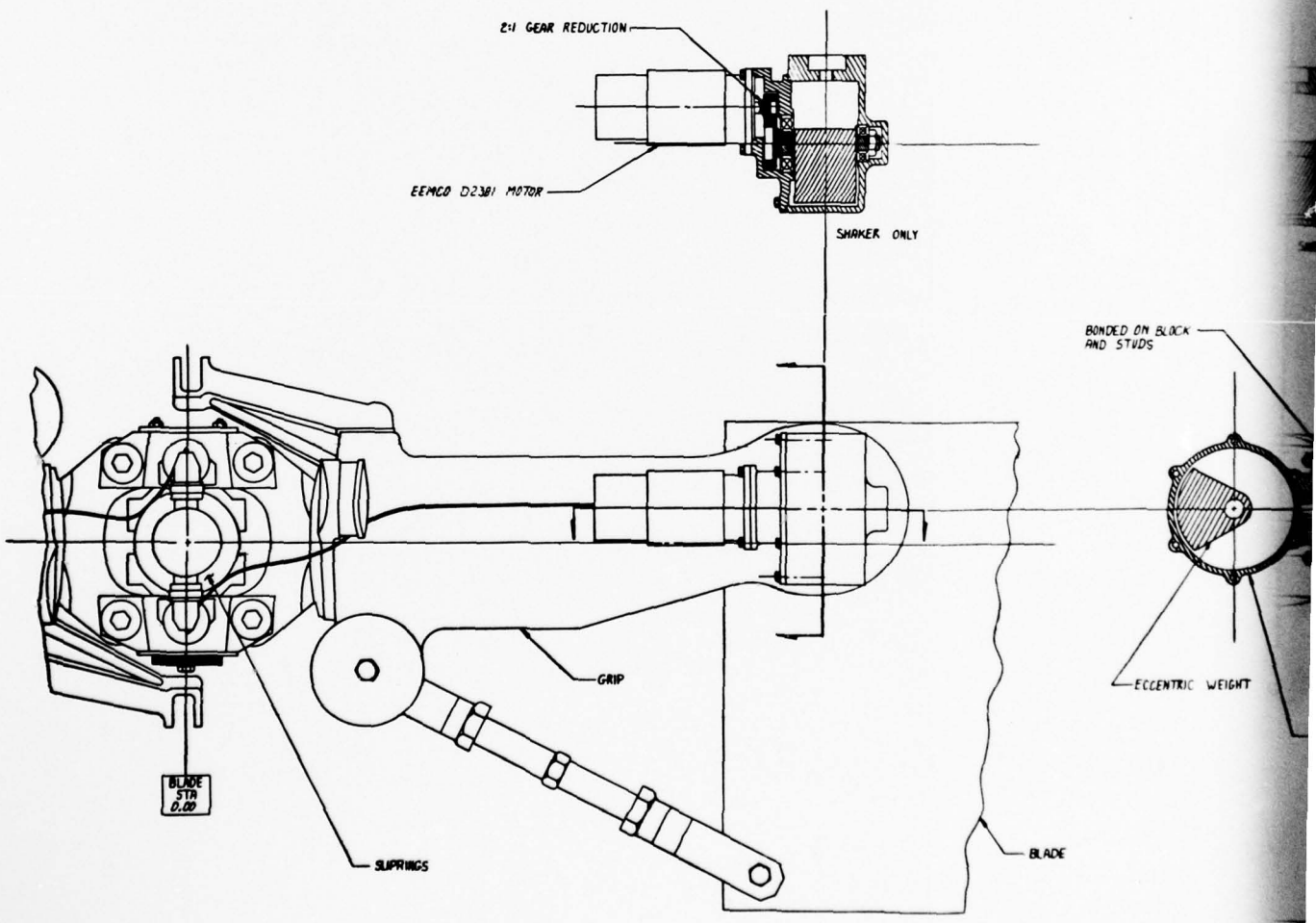

Figure 13. Hub shaker

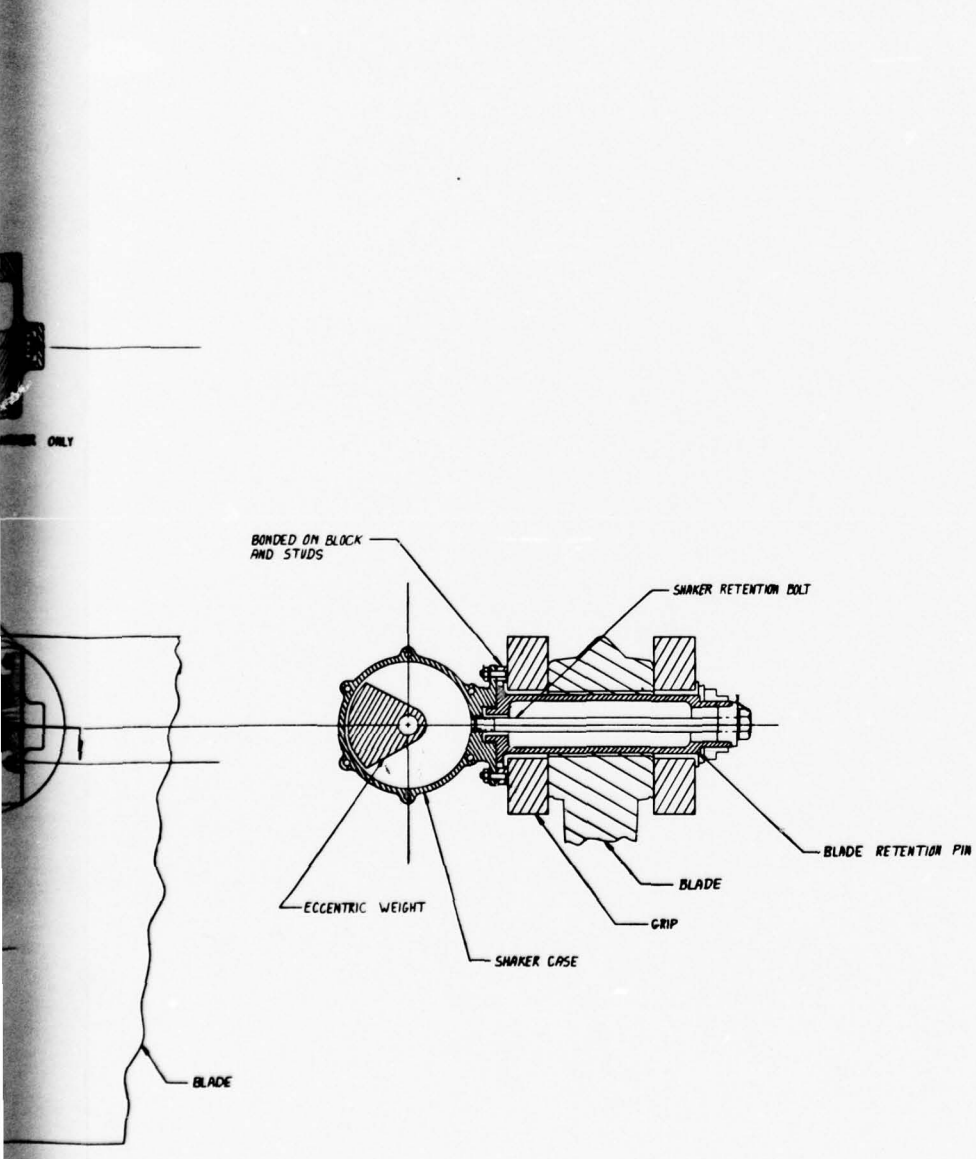

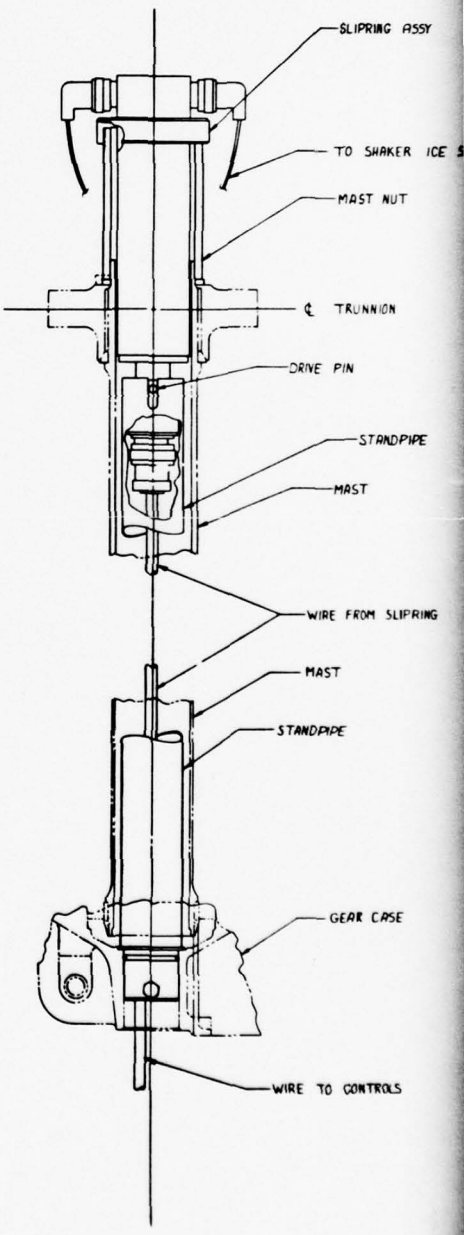

VIEW A-A
SCALE 1/2

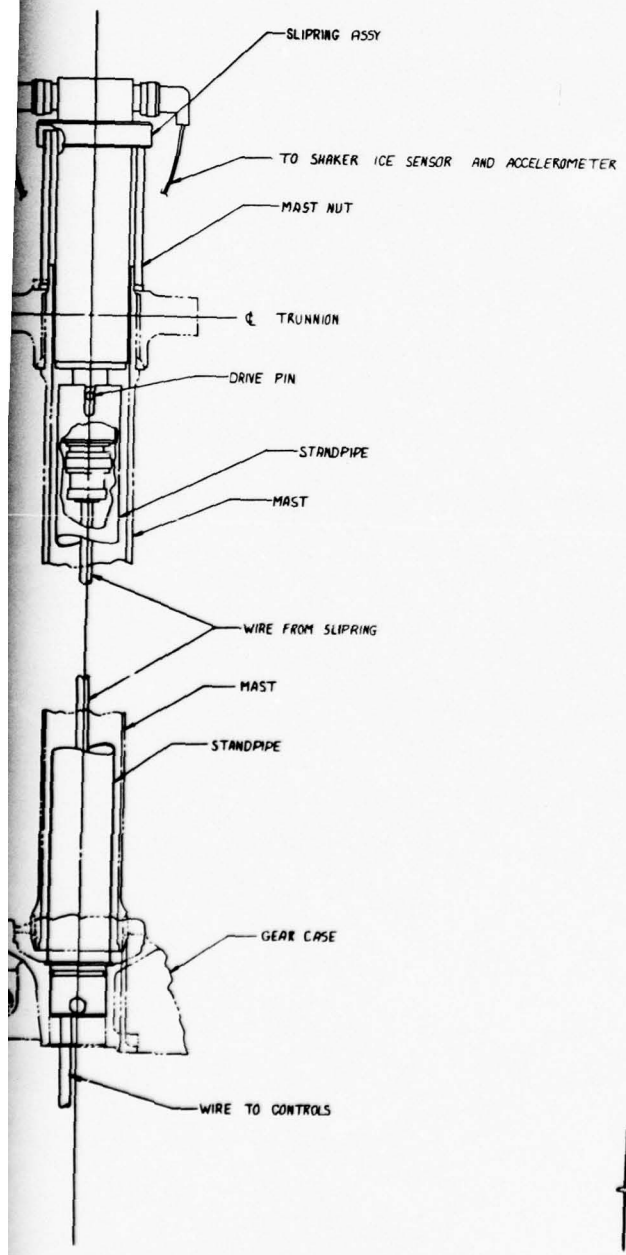
SLIPRING ASSY
TO SHAKER ICE SENSOR AND ACCELEROMETER
MAST NUT
℄ TRUNNION
DRIVE PIN
STANDPIPE
MAST
WIRE FROM SLIPRING
MAST
STANDPIPE
GEAR CASE
WIRE TO CONTROLS

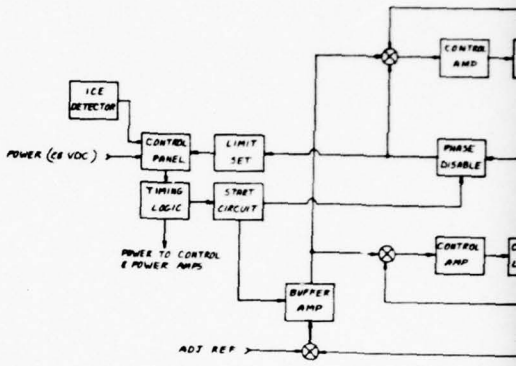
ICE DETECTOR
POWER (28 VDC)
CONTROL PANEL
LIMIT SET
TIMING LOGIC
START CIRCUIT
POWER TO CONTROL & POWER AMPS
BUFFER AMP
ADJ REF
CONTROL AMP
PHASE DISABLE
CONTROL AMP

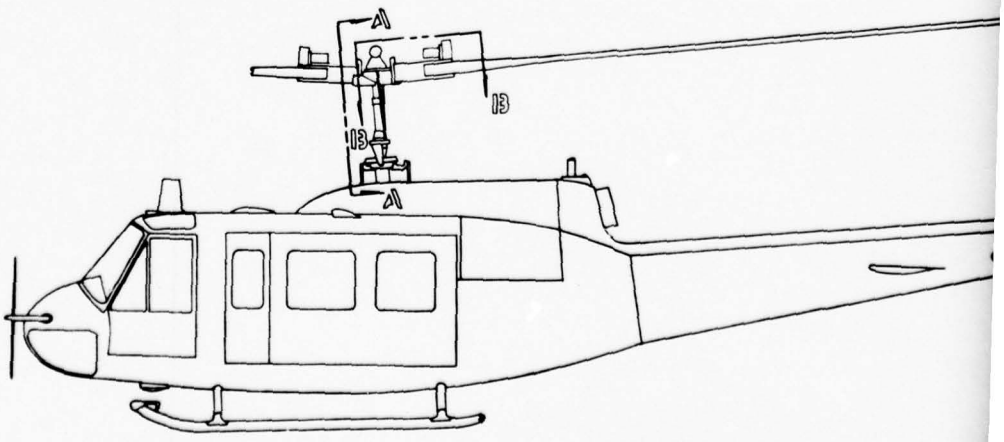
13
13

UH-1H REF

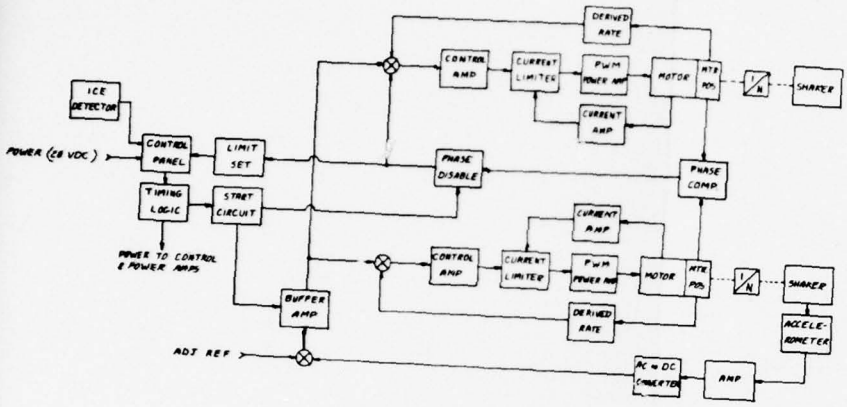
DERIVED RATE
CONTROL AMP
CURRENT LIMITER
PWM POWER AMP
MOTOR
MTR POS.
1/N
SHAKER
CURRENT AMP
ICE DETECTOR
CONTROL PANEL
LIMIT SET
POWER (28 VDC)
PHASE DISABLE
PHASE COMP
TIMING LOGIC
START CIRCUIT
POWER TO CONTROL & POWER AMPS
BUFFER AMP
ADJ REF
ACCELE-ROMETER
AC to DC CONVERTER
AMP

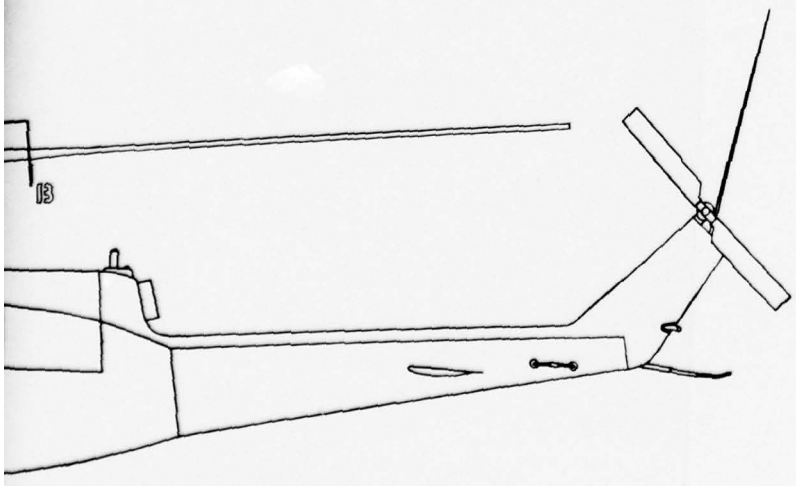

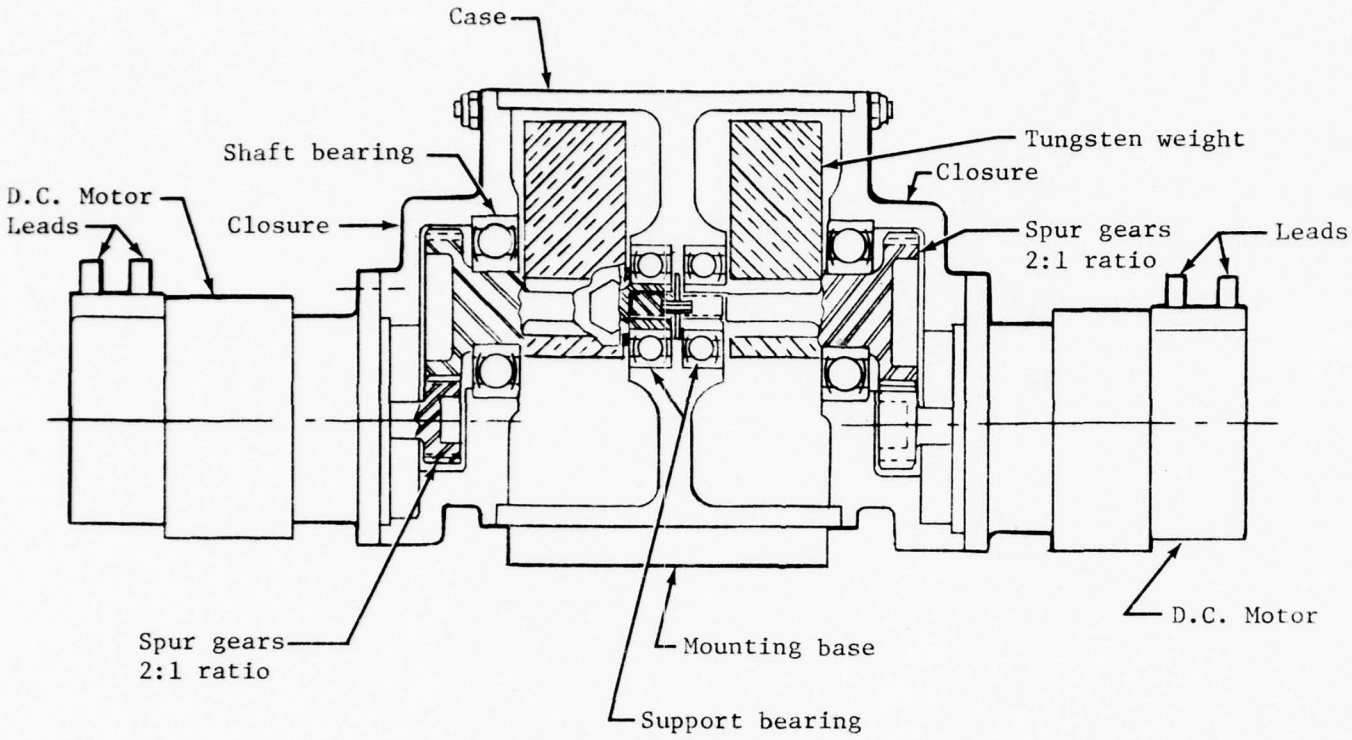

Figure 14. Variable force frequency shaker

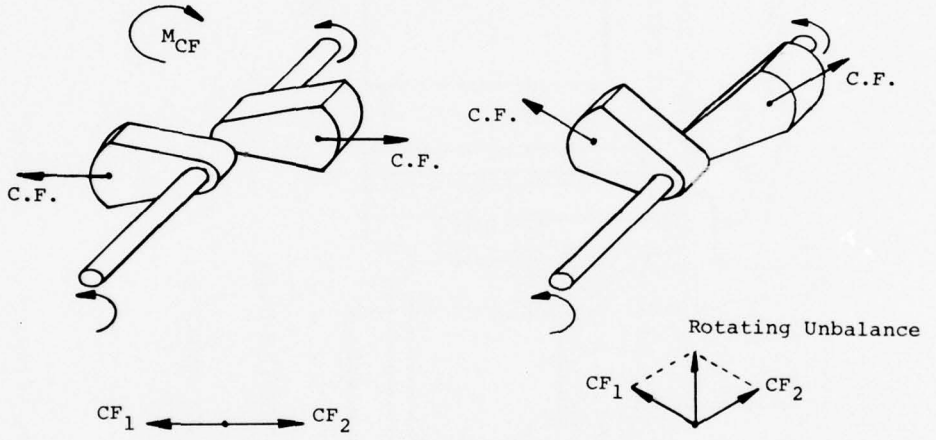

a. No Force

1. Weights Opposed
2. Rotating at desired frequency (RPM control)
3. C.F. forces of weight cancel shear but leave inplane moment
4. Inplane moment reacted by that of second shaker (not shown)

b. Force Generated

1. Weights dephased
2. Rotating at desired frequency (RPM control)
3. Unbalanced force created by Vector addition of weight C.F.

Figure 15. Variable force frequency shaker operation

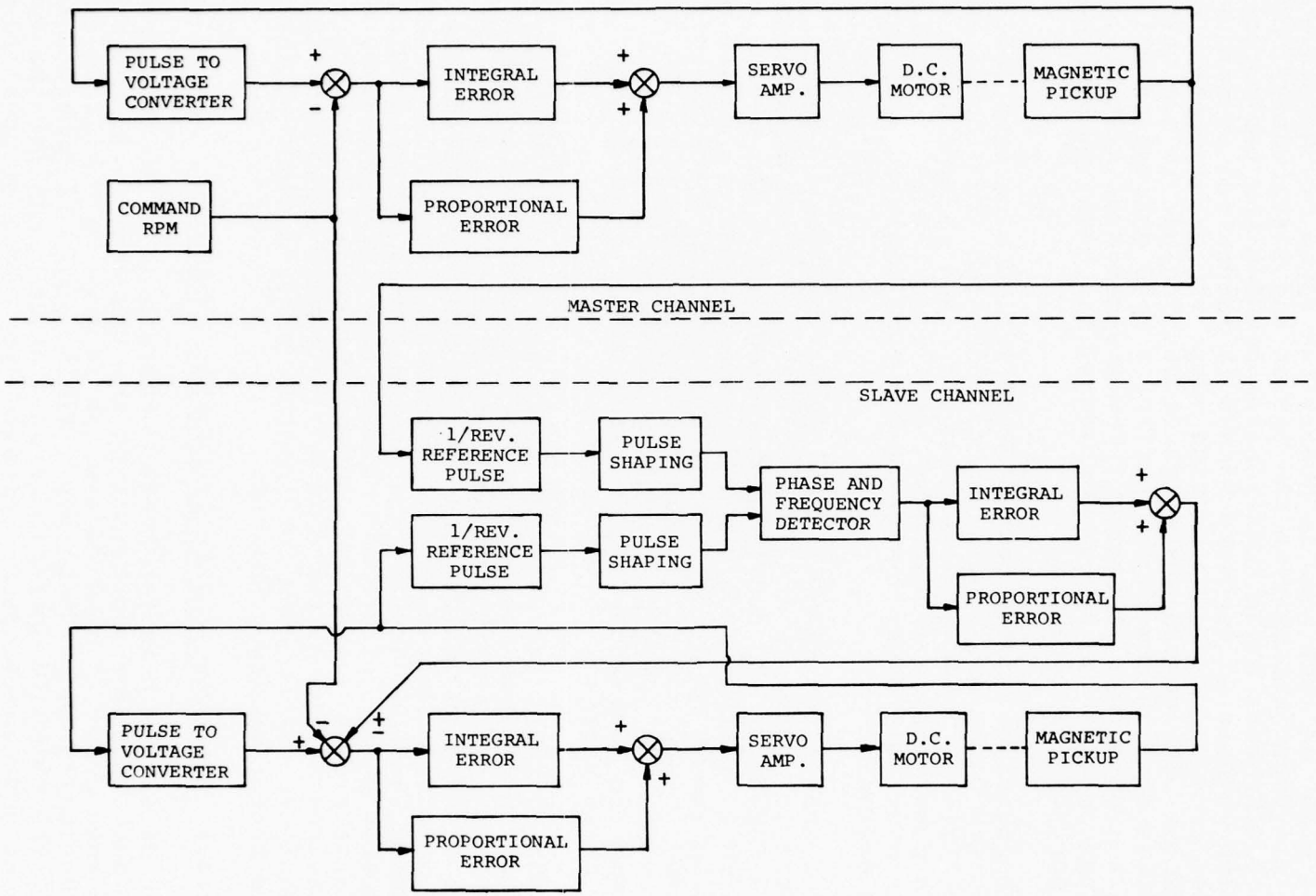

Figure 16. Master/slave motor speed and phase control

This error is then used to modify the speed of the slave motor until synchronism between the master and slave motors occurs. The synchronous phase relationship between the two motor-driven shaker weights on opposite blades is maintained at either 0 degrees or 180 degrees to provide symmetric or asymmetric mode excitation. The control panel functions include an ice warning indicator, a system engage switch, a mode excitation selector, and a system fail indicator. The ice detector systems, although part of the system configuration, have not been addressed as part of this study.

Each individual motor control loop includes current limiting, rate feedback, and a pulse width modulated (PWM) power amplifier. A relatively large amount is required and the PWM motor uses less power than a linear power amplifier. This is consistent with available power devices and a reasonable thermal packaging design.

Motor shaker position is provided by a magnetic pickup. This signal is processed and is used for both phase comparison and rate feedback. An accelerometer feedback signal may be required to further modify motor speed to insure adequate blade deflection to shed ice. To assure that the force direction is phased to apply near simultaneous maximum force in the same direction for symmetric modes or in opposite directions for the asymmetric modes, the design criterion for phase control was set at ±5 percent.

A start circuit and a timing logic are included to bring the system on line and to control the operational duty cycle. The system may be manually or automatically turned on for this period based on detecting a predetermined ice buildup by the ice detection system. The system can be turned off after an assumed 5-second duty cycle. A monitor is included which compares phase differences between the master and slave channels to a reference so that any out-of-tolerance phase difference shuts the entire system down for fail-safe operation. Similar techniques can be used for the four-motor control of the variable force/frequency shakers.

2.2.3.2 Aerodynamic Trim Tab Shaker Controller

Control of the trim tab shaker consists of solenoid snubbers for each tab; the snubbers lock the tab when it is not activated, and when power is applied the tab is free to oscillate at the mechanically tuned frequency. Timing logic is provided to control the solenoid operational duty cycle times for the same values and conditions described above. Control panel functions are essentially the same as the dual-motor-driven shakers except there is no mode excitation selector. Failure monitoring of solenoid operation is required for automatic snubbing of both tabs.

2.3 METHODOLOGY

2.3.1 Analytical Techniques for Evaluating Deicing Concepts

A major problem in determining the effectiveness of the various vibrational deicing concepts is the lack of a precise mathematical model describing how ice is shed by fatigue-like failure from metal and composite surfaces. A limited model developed from BHT's work (Reference 2) and others indicates the relative blade deflections caused by the shakers are an important measure of deicing effectiveness.

Among the analytical factors considered are the effects of the ice as it builds up and is shed from the blades. The mass of the ice changes the natural frequencies and mode shapes, resulting in increased blade loads or increased fuselage vibration. The stiffness of the ice, especially in compression, also affects the natural frequencies. The analytical technique also considers the effects of the centrifugal force field and aerodynamic loads.

Two computer programs were used to evaluate the rotor blade deicing systems.

2.3.1.1 C81 Program

The Rotorcraft Flight Simulation Program, C81, was modified so that a shaker force could be applied at a specified radial location, frequency, and magnitude. The responses of the deicing modes that were calculated by C81 were considerably smaller than the responses calculated by the Myklestad method with the same force levels and locations. This was due to the high-frequency aerodynamic damping that C81 calculated by the change in angle of attack due to the elastic characteristics of the blade. Current state-of-the-art methods do not predict high-frequency aerodynamic damping or the effects of unsteady aerodynamics to any degree of confidence. Since the Myklestad computer program calculates the same aerodynamic damping for each mode that C81 calculates, the use of C81 was discontinued.

2.3.1.2 Myklestad Program

This program calculates the fully coupled (beam, chord, torsion) natural frequencies and mode shapes for the rotor blade (see Appendix H). Knowing the natural frequencies and mode shapes makes possible the design of a shaker system for a given level

of blade excitation. The Myklestad program was also used to define the effect of the ice and shaker masses on the blade's natural frequencies and mode shapes.

2.3.2 Main Rotor Blade-Mounted Shaker Requirements

To determine the requirements for a main rotor blade-mounted shaker, a blade mode near the desired frequency range with a significant amount of out-of-plane motion must be selected; the modal participation to obtain the strain level at the antinode is determined from the moment distribution calculated by Myklestad for the given mode. The forcing function that will drive the mode shape to the desired amplitude must overcome the associated structural and aerodynamic damping. The magnitude of the force, F, determined from the modal equation at the natural frequency for the given mode is

$$F = \frac{2\zeta\omega_n{}^2\delta(GI)}{MS} \qquad (2)$$

where ζ is the damping factor, ω_n is the natural frequency, δ is the modal participation factor, MS is the shape where the force is to be applied, and GI is the generalized inertia for the mode.

The structural damping factor for a BHT rotor blade lies between 0.005 and 0.01, and the aerodynamic damping factors in the frequency range of interest are estimated to be between 0.005 and 0.015. Therefore, a total damping factor of 0.02 was assumed for all force calculations on the basis of Appendix A.

For a blade-mounted shaker, cyclic modes near seven-per-rev appear most desirable to excite; this is related to the out-of-plane antinode locations near the hub (advantageous for shaker location) and near the midspan of the blade. Table 4 presents the computed shaker frequencies and force levels per blade for the main rotor systems of the selected aircraft. The values given are for shaker locations at the main retention bolt hole (inboard) and at midspan antinodes and the blade tip.

These frequencies and force levels vary slightly when the weight of the shaker components and the accumulated ice are taken into consideration in the natural frequencies and mode shapes. For example, one computer run was made on a UH-1 blade with an ice accumulation of 27 pounds per blade (0.25 inch thick and covering 6 inches from the leading edge on the upper and lower surfaces). This ice lowered the natural frequency selected for deicing by 3 percent (1.33 hertz). The changes to the mode

shape and force requirements were insignificant. The weight of a midspan blade-mounted shaker showed an even smaller effect on the natural frequency and mode shape. The computed force level is considered to be a maximum because the rotor blade responses to higher harmonic aerodynamic excitations that exist in forward flight were not included in the force calculations.

As fuselage characteristics in this frequency range are not known precisely, the coupled rotor blade modes need to be verified by flight testing.

2.3.3 Main Rotor Gearbox Shaker Requirements

Vertical excitation of the main rotor gearbox will force the symmetric out-of-plane modes. To determine the shaker frequency and force level, the responses of the fuselage, pylon, and rotor must be known. The vertical deflection, z, at the hub for these modes is given by:

$$z = \frac{\text{Vertical shear}}{k} \tag{3}$$

where k is the vertical impedance of the fuselage-pylon combination. Although k is typically assumed to be independent of frequency, for this study the Myklestad program was modified to express the vertical impedance as a function of frequency using the fixed system natural frequencies and mode shapes as calculated by the finite element computer program NASTRAN.

For each fixed system mode shape it is possible to write

$$\ddot{\varepsilon}_n + 2\zeta\omega_n\dot{\varepsilon}_n + \omega_n^2\varepsilon_n = \frac{B(P\sin qt)z_n(0)}{GI_n} \tag{4}$$

where Psin qt is the externally applied vertical force at the top of the mast, $z_n(0)$ is the vertical mode shape at the top of the mast for the nth mode, GI is the generalized inertia for the nth mode, ω_n is the natural frequency for the nth mode, ε_n is the generalized coordinate of the nth mode,and B is the number of blades.

Equation (4) can be solved to give the inphase component

$$\varepsilon_n = \frac{B(P\sin qt)z_n(0)}{GI_n\left\{(\omega_n^2-q^2)^2 + 4\omega_n^2\zeta^2\right\}^{1/2}} \tag{5}$$

The total displacement at the top of the mast for the nth mode is:

$$z_n(0,t) = z_n(0)\varepsilon_n(t) = \frac{B(P\sin qt)z_n^2(0)}{GI_n\left\{(\omega_n^2-q^2)^2 + 4\omega_n^2\zeta^2\right\}^{1/2}}$$

If N fuselage modes are used,

$$z(0,t) = (B)P\sin qt \sum_{n=1}^{n} \frac{z_n^2(0)}{GI_n\left\{(\omega_n^2-q^2)^2 + 4\omega_n^2\zeta^2\right\}^{1/2}} \quad (6)$$

which can be rearranged to give the impedance k as a function of the frequency q to be

$$k(q) = \frac{(B)P}{z(0,t)} = \sum_{n=1}^{n} \frac{GI_n\left\{(\omega_n^2-q^2)^2 + 4\omega_n^2\zeta^2\right\}^{1/2}B}{z_n^2(0)} \quad (7)$$

Using the vertical impedance k(q) as given by equation (7), the Myklestad program calculates the rotor blade natural frequencies using the boundary condition given by equation (3). An out-of-plane collective mode near the desired frequency is now selected. The modal participation factor is determined in the same way as for the main rotor blade mounted shaker; the force level is equal to the number of blades times the value calculated by using equation (2). Table 3 presents the calculated main rotor gearbox shaker frequencies and force levels for the helicopters where fuselage and rotor data are available. Again, the rotor blade responses to higher harmonic aerodynamic excitations that exist in forward flight were not included, so the calculated force levels are considered to be a maximum. NASTRAN predictions of high-frequency modes and vibration levels are not reliable; therefore, coupled fuselage/pylon/rotor modes need to be verified by flight testing.

2.3.4 Tail Rotor Shaker Requirements

The only tail rotor modes with a significant amount of bending within the frequency range (where ice shedding occurred during the static deicing test) are asymmetric out-of-plane modes that can be best excited by mounting a shaker on the tail rotor hub or blades. The size of the tail rotor hubs and blades makes this impractical. The symmetric out-of-plane modes with a sufficient amount of bending occur at higher frequencies (where ice did not shed during the static deicing test). Since tail rotors experience much higher centrifugal forces and a different aerodynamic environment than main rotors, the criteria set for main rotors may not apply to tail rotors. These high

frequency symmetric out-of-plane modes (which can be excited by a gearbox shaker) may be acceptable for deicing. However, the proper force levels for vibratory deicing can only be determined experimentally.

2.3.5 RPM Effects on Shaker Requirements

Shaker computations were based on an assumed amount of total damping and no contribution of higher harmonic airloads. At normal operating rotor angular velocities, the effects of higher harmonic airloads on the excitation of modes selected for deicing are at a minimum. A possible procedure to reduce the required shaker force would be to shift rotor RPM to an integer per rotor revolution. An even harmonic would be required for symmetric modes and an odd harmonic for asymmetric modes. The shaker force would then be the value required to add to the mode shape excited by the airloads.

2.3.6 High-Frequency Cyclic Pitch Requirements

Another possible means of vibratory ice shedding is to change the cyclic pitch at a frequency that will excite a main rotor blade out-of-plane mode. The change in the lift, due to the cyclic pitch changes, drives the mode to the amplitude necessary to deice the rotor blade. This change in lift, ΔL, is analogous to the force that is applied to the rotor

$$F = \int_o^R \Delta L dr = \int_o^R \frac{\rho c a_o (\Delta\theta)\ \Omega^2 r^2 dr}{2} \tag{8}$$

where ρ is the density of air; c is the rotor chord; a_o is the slope of the lift curve; Ω is the rotor angular velocity; and $\Delta\theta$ is the change in angle of attack. The work done by this force on a given mode at its natural frequency is

$$\frac{\rho c a_o (\Delta\theta) \Omega^2 \int_o^R r^2 MS dr}{2} = 2\zeta\omega_n{}^2 \delta\, GI \tag{9}$$

Rearranging the terms gives

$$\Delta\theta = \frac{4\zeta\omega_n{}^2\ \delta\ GI}{\rho c a_o \Omega^2 \int_o^R r^2 MS dr} \tag{10}$$

For a given rotor, all of the terms in equation (1) are known or determined by the Myklestad program for a given mode. Tables 4 and 5 present the frequency and force levels of two modes for three main rotor blade systems.

3. COMPARISONS

3.1 EFFECTIVENESS FOR ICE PROTECTION

The effectiveness of a system in deicing rotor blades depends upon its characteristics in relation to functionability; i.e., for optimum parameters for each system, the detail comparison of specific features is necessary. The vibrational deicing systems of this study are compared for the following general characteristics: acceptable functioning, use factors, and costing.

Acceptable functioning is related to satisfactory deicing for flight operation of the aircraft as defined by the criteria of Section 2.1 of this report and Reference 2. The most important consideration is, of course, deicing capability. A system must effectively induce shedding of ice from the entire surface in order to be considered a viable candidate. Under the section on energy requirements, it is shown that excitation of the blades at a second mode is considered to be necessary in order to clear ice from the nodal points of the first mode used. Based on work done on the static blade it is indicated that two frequencies are necessary to assure ice shedding from all nodal points. In actual operation the airloads and force field may, in fact, cause shedding from nodal points and one-frequency operation may be possible. This must be determined by field testing. The blade shakers can be operated in phase for symmetric shedding or out of phase for asymmetric shedding. Although theoretical indications are that the Type II gearbox shaker can excite the symmetric mode but not the asymmetric mode, BHT model tests have shown a capability to excite the asymmetric mode. In this report that capability is not assumed and the Type II gearbox shaker is penalized for single mode operation. The other important factors considered for system effectiveness are:

- System capability
- Complexity
- Power
- Weight
- Reliability
- Maintainability
- Noise
- Safety
- Acceptability
- Controllability
- Cost

Complexity is evaluated by a comparison of the various subsystems necessary to make the total system, the complexity of these, and the quality of the parts necessary to achieve functionality. Table 6 defines the systems from the design sketches and Table 7 is a comparison table of the complexity of the typical systems investigated in this report. A rating scale of 1 to 10 is used, with the lowest value being the most desirable system.

TABLE 6. SYSTEM COMPLEXITY

Type	No. of Shakers	Slip Rings	Stand-pipe	Mounting Means	Control System	Shaker Size	Power Source	Drive Shafts	CF Effects	Critical Bearings
I	2	-	-	Bracket	Complex	Small	Gen	-	-	-
II	2	-	-	Trans. Sump	Complex	Large	Gen	-	-	-
III	1/blade	3/blade	Yes	Bracket to Blade	Simple	Large	Gen/ Air	-	High	Flap Motion and Linkage
IV	1/blade	6/blade (3 light 3 heavy)	Yes	Two Fittings per Blade	Complex	Medium	Gen	Tension 1/Blade	High	Shaft Thrust and Shakers
V	1/blade	6/blade (3 light 3 heavy)	Yes	1 Bracket 1 Bolt per Blade	Complex	Medium	Gen	-	Mod.	Shaker

Note: Refer to page 30 for type descriptions.

TABLE 7. SYSTEM COMPLEXITY COMPARISON

DESIGN	SHAKER DESIGN	SLIP RINGS	STANDPIPE	MOUNTING MEANS	CONTROL SYSTEM	SHAKER SIZE	POWER SOURCE	DRIVE SHAFT	CENTRIFUGAL FORCE EFFECT	CRITICAL BEARING	SUMMARY	RATING ORDER
TYPE I												
2 Blade	2	-	-	2	5	1	1	-	-	-	11	2
4 Blade	2	-	-	2	5	1	1	-	-	-	11	
TYPE II												
2 Blade	4	-	-	1	6	4	2	-	-	-	17	1
4 Blade	4	-	-	1	6	4	2	-	-	-	17	
TYPE III												
2 Blade	5	2	1	10	1	5	10	-	10	6	50	3
4 Blade	6	2	1	10	2	5	10	-	10	6	51	
TYPE IV												
2 Blade	8	3	1	8	6	3	2	3	8	8	50	4
4 Blade	10	4	1	8	10	3	2	3	8	8	57	
TYPE V												
2 Blade	4	3	1	3	6	3	2	-	6	3	31	2
4 Blade	6	4	1	3	10	3	2	-	6	3	38	

(1) May be deficient operationally because of single mode excitation limitation.

(2) T/R installation not comparative with main rotor systems.

TABLE 8. RATING OF SYSTEMS FOR M/R USE

	COMPLEXITY	POWER REQUIRED	WEIGHT	RELIABILITY	MAINTAINABILITY	NOISE	SAFETY	ACCEPTABILITY	CONTROLLABILITY	COST	RATING NO.	RATING ORDER
TYPE I												
TYPE II △1	1	1	1	2	1	1	1	1	1	1	11	1
TYPE III △1	2	3	2	1	3	3	4	2	2	2	24	3
TYPE IV	4	2	4	4	4	2	3	3	3	4	33	4
TYPE V	3	2	3	3	2	2	2	3	3	3	26	2

△1 May be deficient in operation because of single mode excitation limitation.

Power, weight, reliability, and maintainability are evaluated in the following sections of this report for inclusion in the system rating (Table 8). Although the tabular rankings for the various system types indicate Types I and II to be lighter and simpler, the performance of Types I and II is limited because the analysis used shows only single mode operation. Type III is also limited to a single mode because of the resonant-type control system.

Type V is shown to be the most desirable system of the various approaches. It should also be understood that detailed characteristics of a particular aircraft may modify the rating somewhat. For instance, if a particular helicopter blade should have existing blade balance weights that could be replaced by shaker and motor assembly weight, then the weight factor for system IV, the blade shaker, would be improved.

3.2 ENERGY REQUIREMENTS

Among the basic considerations in evaluating the types of vibrational deicing systems for their power required are the following.

- The energy to force the blade to vibrate is based on the structural and aerodynamic damping forces that must be overcome at a particular vibration amplitude. This was computed with an assumption of 2 percent of critical damping. A discussion of this assumption and the results of a literature search on the subject may be found in Appendix A. Table 9 presents a summary of the power required for the various blade modes and for the noted aircraft.

TABLE 9. POWER REQUIRED (HP)

	UH-1	AH-1	OH-58	AAH	CH-47
Main Rotor					
Blade-mounted shaker (per blade)	1.34	1.38	0.49	1.07	1.03
Gearbox force shaker	3.6	2.03	1.25	3.41	-
Tail Rotor					
Gearbox shaker	3.66	0.16	-	0.58	-

- The efficiency of the D.C. electric motors operating in the cool temperatures and load conditions of this system can be expected to be on the order of 75 percent. In the event that electrical ice protection is required for the blade tip flap, a value of the estimated power for a surface heater covering the lower surface and the forward 25 percent of the flap chord is .645 Hp (Reference Appendix B). As this is assumed to be a resistance heater with an efficiency of 50 percent, the power required per blade would be:

$$Hp = \frac{.645}{\text{Resistance Eff} \times \text{Gen Eff}}$$

$$= \frac{.645}{.50 \times .75}$$

$$Hp = 1.72 \text{ per blade}$$

- Aerodynamic losses occur by increased drag of flaps, exposed shakers and structure, or nondeiced areas of the blade. Appendix B contains an estimate of flap HP due to the increase in tip section drag. This indicates about 6 percent of the basic blade power. If the rotor is operating at a mean level of 400 hp per blade during normal flight, this is a 24 hp loss per blade over the life of the aircraft.

  The exposed shakers and the slip ring assembly on the hub for inblade and hub use generally lie within the projected frontal area of the rotor head; therefore, it could be expected that any drag increase would be negligible.

  The aerodynamic power penalty estimated for single mode deicing on the UH-1, because of ice on nodal points, is presented in Appendix B and appears as 4.5 percent of the blade operating horsepower (400 hp), which is 18 horsepower per blade (during icing conditions only). For a comparison, a badly iced-up blade could be expected to have a drag increase of about 50 percent for a delta horsepower increase of 200 hp. Total blade horsepower required in this case would be expected to exceed 600 hp.

- NACA icing reports (References 4 through 10) indicate small loss of airfoil section lift values and increase of moment coefficients for as much as six inches of ice protruding ahead of the blade leading edge,but a more significant effect occurs in the drag data. Dual mode deicing could be expected to minimize the effect of residual ice in that changing nodal points during the deicing cycle should clean the blade major surfaces completely.

- Penalties result from increased aircraft weights, i.e., mechanism, fuel supply and delta tankage, etc. It is expected that the effect of these penalties on basic aircraft weights would not be significant for extended flight in icing conditions if dual mode deicing is used except in the case of the tip flap. Assuming a 40-pound installed system weight and a 10 lb/hp lifting system gives 4 hp to lift the system. This is 4/800 or a .5 percent penalty. In the case of the tip flap, a continuous 6 percent power loss plus the weight of the

---

[4] V. H. Gray and U. H. von Glahn, *EFFECT OF ICE AND FROST* FORMATIONS ON DRAG OF NACA 651-212 AIRFOIL FOR VARIOUS MODES OF THERMAL ICE PROTECTION, NACA TN-2962, 1953.

[5] G. M. Preston and C. C. Clackman, EFFECTS OF ICE FORMATIONS ON AIRPLANE PERFORMANCE IN LEVEL CRUISING FLIGHT, NACA TN-1598, 1948.

[6] T. F. Gelder, J. P. Lewis, and S. L. Loutz, ICING PROTECTION FOR A TURBOJET TRANSPORT AIRPLANE: HEATING REQUIREMENTS, METHODS OF PROTECTION, AND PERFORMANCE PENALTIES, NACA TN-2866, 1953.

[7] D. T. Bowden, EFFECT OF PNEUMATIC DE-ICERS AND ICE FORMATIONS ON AERODYNAMIC CHARACTERISTICS OF AN AIRFOIL, NACA TN-3564, 1956.

[8] V. H. Gray, CORRELATIONS AMONG ICE MEASUREMENTS, IMPINGEMENT RATES, ICING CONDITIONS, AND DRAG OF A 64A004 AIRFOIL, NACA TN-4151, 1958.

[9] V. H. Gray and U. H. von Glahn, AERODYNAMIC EFFECTS CAUSED BY ICING OF AN UNSWEPT NACA 65A004 AIRFOIL, NACA TN-4155, 1958.

[10] V. H. Gray, PREDICTION OF AERODYNAMIC PENALTIES CAUSED BY ICE FORMATIONS ON VARIOUS AIRFOILS, NASA TN-D-2166, 1964.

mechanism occurs,which indicates a fuel/tankage penalty exceeds 7 percent (6 percent plus extra fuel for loss, .5 percent fuel for system weight, and a tank weight of .5 percent).

- The criterion for ice shedding for this study was based on the BHT tests of ice frozen on stainless steel blades. It appears that the energy to separate the ice would be reduced significantly if the adhesion shear value was reduced. The adhesion shear value is 300 psi for stainless steel, 80 to 90 psi for rubber or polyurethane, and 60 to 70 psi for Teflon. If a polyurethane leading edge covering was used instead of the stainless steel used in the lab tests, the blade deflections to shed ice should be reduced to approximately 25 percent of the criteria values with a consequent reduction in the power required. It is also expected that ice phobic materials can be developed to further reduce the force required to shed ice. For this study the high values of shear of stainless steel were used; however, data should be gathered for other surfaces,particularly for composite blades to insure optimization of a particular system.

Applying the above to the estimation of the energy requirements for a particular system indicates the following. Weight calculations are provided in Appendix F.

For the Type I installation on tail rotor (the only mode found in frequency range for deicing):

AIRCRAFT	POWER TO VIBRATE (HP)	POWER FACTOR	HP REQD
UH-1	3.66	.75	4.88
AH-1	.16	.75	.213
AAH	.58	.75	.77

Electrical heating tail rotor protection from Reference 1 indicates a weight requirement of 17 pounds using a 20 watt/sq-in. power density. If 100 sq in. of blade area are heated, 2000 watts are required or 2.68 hp. Seventeen pounds of weight at 10 lb/hp lift is the equivalent of 1.7 hp; therefore, for the UH-1 tail rotor, an electrical deicing system equivalent (neglecting the delta generator weight) power would be:

$$\text{Equivalent power} = \frac{2.68}{.75} + 1.7$$

$$= 5.27 \text{ Hp}$$

This may be compared to the .77 Hp value of the above table plus a 1.48 weight equivalent of horsepower or 1.556 Hp for vibrational deicing.

For the Type II installation on the main rotor gearbox:

AIRCRAFT	POWER TO VIBRATE	POWER FACTOR	HORSEPOWER REQUIRED
UH-1	3.6	.75	4.8
AH-1	2.03	.75	2.7
OH-58	1.25	.75	1.66
AAH	3.41	.75	4.55

Reference 1 indicates the use of 6900 watts per blade or a total of 13,800 watts for the electrical deicing system; this is the equivalent of 18 hp and the system weighs 133 pounds or the equivalent of 13.3 hp at a 10 lb/hp lifting ratio. The total power thus becomes:

$$HP_T = \frac{18}{.75} + 13.3$$

$$= 37.3$$

Power for single mode vibrational deicing for the AH-1 may be estimated as follows:

From the above	2.7
Single mode deicing	36
Wt of 37 lb @ 10 lb/hp	3.7
Total	42.4

Double mode vibrational deicing with this system is not considered.

For the Type III (flap installation on the blade tip) the following would appear assuming a 400 hp level of blade operation (800 rotor hp):

ITEM	HP LOSS
Basic power loss @ 6 percent	48.00
Single mode deicing loss @ 4.5 percent	36.00
Flap deicing	1.72
Total	85.72 Hp

Double mode deicing is difficult to apply with this system and is therefore not considered.

For the Type IV blade modal vibration system the following appears:

AIRCRAFT	POWER TO VIBRATE	POWER FACTOR	HORSEPOWER REQUIRED
UH-1	2.68	.75	3.57
AH-1G	2.76	.75	3.68

Power for UH-1 blade shaker

	Single Mode	Double Mode
From the above	3.57	3.57
Single mode deicing loss	36.00	---
Wt @ 10 lb/hp for 71 lb	7.10	7.10
Total	46.67	10.67

Power for AH-1G tip shaker

	Single Mode	Double Mode
From the above	3.68	3.68
Single mode deicing loss	36.00	---
Wt @ 10 lb/hp for 37.9 lb	3.79	3.79
Total	43.47	7.47

For the Type V system the required power to vibrate is the same as for Type IV. For the UH-1

	Single Mode	Double Mode
From the above	3.68	3.68
Single mode deicing loss	36.00	
Wt @ 10 lb/hp for 59.8 lbs	6.00	6.00
Total	45.68	9.68

In summary of the above, the following appears:

ITEM	HORSEPOWER SINGLE MODE	HORSEPOWER DOUBLE MODE
Type I	.77	-
Type II	42.4	-
Type III	85.72	-
Type IV (UH-1)	46.67	10.67
(AH-1G)	43.47	7.47
Type V	45.68	9.68

The power required for vibratory deicing indicates that a double-mode system of Type IV or V requires only 7.47 to 10.67 horsepower. A comparable electrothermal system will require 37.3 horsepower. If it should be found from tests that ice is shed completely with single mode excitation, then the Type II vibratory system would require only 6.4 horsepower.

3.3 RELIABILITY OF DEICING SYSTEMS

Reliability for the system designs has been assessed with relation to the criteria of Section 2.1. These criteria include component selection and rating criteria for the phase control, frequency control, and timing elements; redundancy requirements for any slip ring connection between the mast and the rotor; and positive checkout capability for shaker-motor elements, if installed in each blade.

An assessment of the probable changes in reliability of the rotor from deicing system incorporation was made.

Reliability is expressed in terms of mean-time-between-failures (MTBF) based on failure modes, effects, and criticality analysis, and the possible/probable failure modes are identified. The effects of each failure mode are evaluated and a criticality is assigned to each failure mode. Results are documented in the following section.

3.3.1 Type I and Type II - Tail Rotor Gearbox With Attached Shakers and Main Rotor Gearbox With Attached Shakers

The failure rates were determined by similarity using failure data from the Navy 3-M program for the UH-1N and the Government Industry Data Exchange Program (GIDEP).

The shaker installation on these systems should not present any unusual problems.

A detailed analysis was not performed but cursory examinations reveal that the deicing excitations should not reduce the reliability of the gearboxes, suspension, and rotating controls system.

References 11 and 12 give a view of the detailed operating frequencies of the transmission system for the UH-1 series and the YAH-63 helicopters.

Table 10 is a summary of the MTBF values of the systems. It may be noted that these values correspond to many hours of aircraft operation in that the system operates only 5 seconds for each deicing cycle. Appendix D shows the breakdown of these computations.

TABLE 10. MTBF SUMMARY

Item	MTBF (hr) Continuous Operation	MTBF (hr) Continuous Moderate Icing *
TYPE I	77.2	3860
TYPE II	72.5	3625
TYPE III	100.1	5005
TYPE IV	59.9	2995
TYPE V	69.9	3495

*With duty cycle of 5 seconds each 4 minutes.

It would appear that operational reliability would be adequate for all of the studied systems.

3.3.2 Type III - Main Rotor Blade Excited by Aerodynamic Tab

The failure rates were determined by the same sources as described in 3.3.1. The failure data assume that the mechanism will work; also, no derating was applied to account for the centrifugal force to which the system is subjected.

This centrifugal force is significant. As an example, the plunger in the solenoid which weighed approximately .05 pound would have a 38-pound g response at 300 rotor rpm. All components in this system would be subjected to forces in excess of 700 times their weight.

---

[11] R. B. Patten, B. Hart, and J. F. Bartholomew, ENGINEERING STUDY FOR ADVANCED ATTACK HELICOPTER (AAH) AUTOMATIC INSPECTION DIAGNOSTIC AND PROGNOSTIC SYSTEM (AIDAPS), Bell Helicopter Textron Report 299-949-007, October 1976.

[12] Bell Helicopter Textron Report 299-099-521, AUTOMATIC INSPECTION DIAGNOSTIC AND PROGNOSTIC SYSTEM (AIDAPS) TESTBED PROGRAM - TASK II.

3.3.3 Type IV - Main Rotor Blade Excited at Antinodal Point

The failure rate data were determined by the same sources as described in 3.3.1. The failure data assume that the mechanism will work; also, no derating was applied to account for the centrifugal force on the system.

The thrust force on the bearing at blade station 57 is approximately 628 pounds; at station 146 it is 2873 pounds; and at station 288 it is in excess of 11,000 pounds. At station 57, the thrust force is considered low enough to be accommodated by a reasonably sized bearing configuration.

The oil seal arrangement should be changed to a face-type seal or a double-lip seal with an overboard drain to prevent an unbalance condition on the blade. Also, consideration should be given to operating the motor at low speed, when not deicing, to prevent the bearing from brinnelling.

Analysis indicates it would be possible to operate the shaker at station 146 by changing the gearbox to incorporate a tandem pair of angular contact bearings. The bearings should be made from M-50 steel. A Fafnir 7270W 30° tandem pair will have a B_{10} life of 112 hours; using the life improvement for M-50 steel, an anticipated life of twice this is conservative.

3.3.4 Type V - Hub Excited by Shaker

The failure rate data were determined by the same sources as described in 3.3.1. No derating factor has been applied to account for the centrifugal force of the system.

This system requires grease-lubricated sealed bearings. A problem with sealed bearings is the tendency of the lubricant to migrate out of the bearing. In this application, this will be compounded by centrifugal force. A study to determine if the gears could be manufactured from a moly-filled plastic such as Teflon or nylon might eliminate the need for oil in the gear section.

Although the tendency of centrifugal force to brinnel the bearings is far lower than for the Type III and IV systems, it might still be prudent to operate this sytem at low rotational speed when not in the deicing mode.

3.4 MAINTENANCE TECHNOLOGY

The MMH/FH required for corrective and preventive maintenance of the ice protection equipment at the required levels of maintenance were assessed. The on-aircraft analysis included a study of accessibility. Changes in MMH/FH of the dynamic components were directly related to the changes in failure rates that may be caused by additional vibration patterns due to the integration of the shaking equipment.

The additional MMH/FH required to maintain the aircraft as a result of adding the ice protection equipment and estimates of variations of MMH/FH on the different aircraft by considering accessibility and varying sizes of ice protection equipment required were factored into the study.

The analysis of the five systems indicates the following:

I.	Tail Rotor Gearbox with Attached Shakers	.000456 MMH/FH
II.	Main Rotor Gearbox with Attached Shakers	.000848 MMH/FH
III.	Main Rotor Blade Excited by Aerodynamic Tab	.002919 MMH/FH
IV.	Main Rotor Blade Excited at Antinodal Point	.018143 MMH/FH *
V.	Main Rotor Hub Excited by Shaker	.001776 MMH/FH

The values above are predicted unscheduled maintenance. Appendix E shows the breakdown of these computations.

*Type IV tip shaker maintenance will be less due to easy access.

3.5 WEIGHTS

The weights of the various types of installed vibrational deicing system mechanisms are estimated to be as shown in Appendix F. The sketches of the various schemes are viewed as general in nature, i.e., to indicate location requirement effects on the systems. Adjustments to the schematic designs of the basic shakers as to the magnitude of the rotating unbalance weight were made to conform to the load/frequency requirements of the relevant deicing criteria. Shaker case lengths and rotor weights were modified to correspond to the needs of each design.

Data from Reference 1 were modified and added to Table 11 for comparative purposes to indicate possible weight differences between vibrational and electrical deicing.

TABLE 11. COMPARISON TABLE OF SYSTEM WEIGHTS

Item	System Weight, Lb
Type I - Model 409 Tail Rotor	14.92
Type II- AH-1G Gearbox-Symmetric Mode	37.65
Type III - Aerodynamic Flap - UH-1	38.71
Type IV - Inblade Shaker - UH-1	67.16
Exterior Shaker - UH-1	71.16
AH-1G Tip Shaker	37.9
Type V - Hub Modal Excitation	59.88

From Reference 1, basic main rotor electrothermal production deicing system weight = 176 lb.

Less:

Item	Wt, Lb	
Glass Windshield Controls	-34	
Ice Detector and OAT System	- 4	
Balance Blankets	- 5	
	-43	- 43
Comparative electrothermal UH-1 main blade deicing system weight =		133 lb

3.6 COST

One of the important considerations in the selection of a rotor blade deicing system is system cost. Although at present vibratory deicing is only a concept, an attempt has been made to "ballpark" the nonrecurring development and recurring production costs for quantities of 100, 500, and 1000 systems. The normal costs to research, develop, and produce a new system are divided into:

1. Cost to prove feasibility
2. Cost to develop production system
3. Cost to qualify
4. Cost to produce

Since the object is to compare relative costs of producing the systems, only items 2 and 4 are included in this estimate.

The following assumptions were used in making the estimates.

- A feasibility model has been designed, and feasibility of the concept has been proven.
- The production design will use components that have been proven technically feasible, but some design and material changes will be made to improve producibility and decrease costs.
- The nonrecurring design costs would include:
  - Design of detailed parts
  - System design
  - Bench test
  - Operational test
  - Debugging and safety of flight test

The nonrecurring development costs for the five systems are (no prototype system included):

System I	$342,375
System II	367,400
System III	260,850
System IV	391,025
System IV (Alternate)	391,025
System V	350,000

The per unit production costs for the five systems are:

	100 Systems	500 Systems	1000 Systems
System I	$ 8,200	$ 6,500	$ 5,725
System II	8,650	6,950	6,125
System III	18,300	13,100	11,100
System IV	20,300	16,175	14,175
System IV (Alt)	20,700	16,500	14,450
System V	11,525	9,250	8,125

3.7 AIRCRAFT PENALTIES

Possible penalties exist that might limit performance of aircraft equipped with vibrational deicing systems. These penalties are as follows:

- Those associated with aerodynamics degradation, i.e., drag, lift, control loads, and pitching moments.
- Power losses due to equipment consumption.

- Power losses associated with incomplete deicing of the rotor(s).

- Limitations imposed by sympathetic aircraft component vibrations possibly induced by forcing blade motion.

- Fatigue effects on blades and other components.

The first three of the above items have been discussed in the section on Energy Requirements of this report. A possible increase in control loads due to single-mode deicing is an important consideration also.

Ice build-up over a portion of the blade has the following effect on the section aerodynamics (References 4 through 10).

- Lift and pitching moment are practically unchanged.

- Drag may increase up to 50 percent of the basic drag at a particular angle of attack.

Ice at the nodes builds up lumps extending ahead of the blade leading edge. Such a lump could exist at each of the two nodal points of the selected mode. If this lump became large enough, its location at the leading edge of the blade could cause a significant increase in the blade centrifugal restoring moment and thus affect control loads. The reason for vibratory deicing in two modes is to assure that no ice will remain on the blade to cause control load problems. It should be recognized, however, that flight test may show that single mode excitation may completely clear the blade.

Shaking the blade at a particular high frequency (8 plus per rev) could possibly have a deleterious effect on other components of the vehicle in the event these could respond sympathetically at the same frequency. Any aircraft with vibrational deicing must be investigated for this situation. References 11 and 12 show a review of the drive system of the UH-1D aircraft. Examination of these reports indicates the possibility that some transmission components operate at frequencies close to the blade resonance excitation for deicing; however, response in this 40 to 50 hertz range is minimal. Other components were not reviewed for sympathetic vibrational response for this study; however, for a practical aircraft installation, analysis and test of this factor is in order to prevent limitations to performance that might exist such as a necessary off-optimum engine rpm operation (reduced power) to permit avoiding a vibratory flight condition.

Fatigue effects may reduce aircraft performance by a reduction of service life of critical parts; therefore, a part of the vibrational examination is the review of part stress under oscillatory loading conditions. Section 3.9 shows the possible effect of increasing the fatigue loads from vibrational deicing on rotor blades.

3.8 COUNTERMEASURE EFFECTS

It would appear that vibrational deicing techniques would cause no appreciable change in the normal helicopter requirements for countermeasures. Increased sonic effects from higher frequency blade vibrations are attenuated quite rapidly in air and could be expected to be masked by the overall sound level of the aircraft. Radar reflectivity of the vehicle is unchanged by the added vibrational mechanisms. The change in the heat level of the aircraft from mechanism energy input is minimal, and no high temperature point source exists. In the event that flap deicing (Type III) should be required, the heat signature is quite low and should be insignificant compared to the engine plume/exhaust pipe temperatures.

From the above, the countermeasure effects of vibrational systems are negligible.

3.9 BLADE VIBRATION EFFECT

A study of the fatigue life of main and tail rotor blades with a mechanical deicing system was made; the results are presented in the form of a graph relating fatigue life versus shaker operating time. In order to determine the effect of the shaker, the following conservative assumptions were made:

- Deicing will be accomplished during V_{NE} level flight; therefore, the oscillatory loads due to the deicer are added to those measured in V_{NE} level flight.
- The maximum load occurs at the operating frequency of the deicer.
- There is no gross weight reduction. (It is assumed that deicing must be accomplished to maximum load.)
- The deicer will be operated for functional test, ground deicing, and inflight deicing. Functional tests and ground deicing endure for only a few seconds before each flight. Operation in flight is shown as blade fatigue life versus percent time in icing conditions.

Two blade modes were studied: the asymmetric and the symmetric. Blade loadings in the form of beam and chord induced vibratory moments at various stations were calculated and added to level flight loads. These were then used to determine the loads and the critical blade station. The operating time of the shaker was determined, using the assumptions above. Using this information, together with the blade endurance limit and the shaker operating frequency, damage fractions and blade life were calculated using Miner's rule.

Figure 17 shows the fatigue life versus deicer operation for the existing metal AH-1G main rotor blade. The assumption was made that the blade is excited alternately in the asymmetric and symmetric modes in order to completely clear ice from the nodal points. The normal fatigue life of the blade is 1150 hours. The curve shows that with 2 percent of the time spent in icing conditions the blade life is reduced to 950 hours. If icing conditions should be five times worse than expected or 10 percent of the time, then blade life would be reduced to approximately 650 hours. It is obvious that for the present metal blades on the AH-1G, it will be necessary to include a timer to record the number of deicing cycles accumulated on the blades. The implications of using fiberglass blades are discussed in paragraph 3.10.

The fatigue life versus deicer operation for the AH-1G main rotor blade, excited in the asymmetric mode, is shown in Figure 18. Note that there is no damage, in addition to normal flight fatigue, in using the deicer in the symmetric mode of operation. This is so because the limiting fatigue point on this blade is at trailing edge station 192. Figure 7 shows that this is near a node point for beam bending at the frequency used; therefore, there is no additional damaging stress caused by deicer action. Figure 18 shows that in normal icing conditions, using a blade shaker which had alternate asymmetric and symmetric mode cycles, the metal blade life would be reduced from 3000 to 2000 hours.

The Model YAH-63 main rotor blade fatigue life versus deicer operation is shown in Figure 19. Both asymmetric and symmetric excitation of this blade causes a slight increase in fatigue and decrease in blade life due to the deicer operation. Alternate excitation of the two modes would give a result midway between the two curves shown. Helicopter operation in icing during 2 percent of its expected life would decrease blade life from 4000 to 2500 hours. Undoubtedly, fiberglass blades would

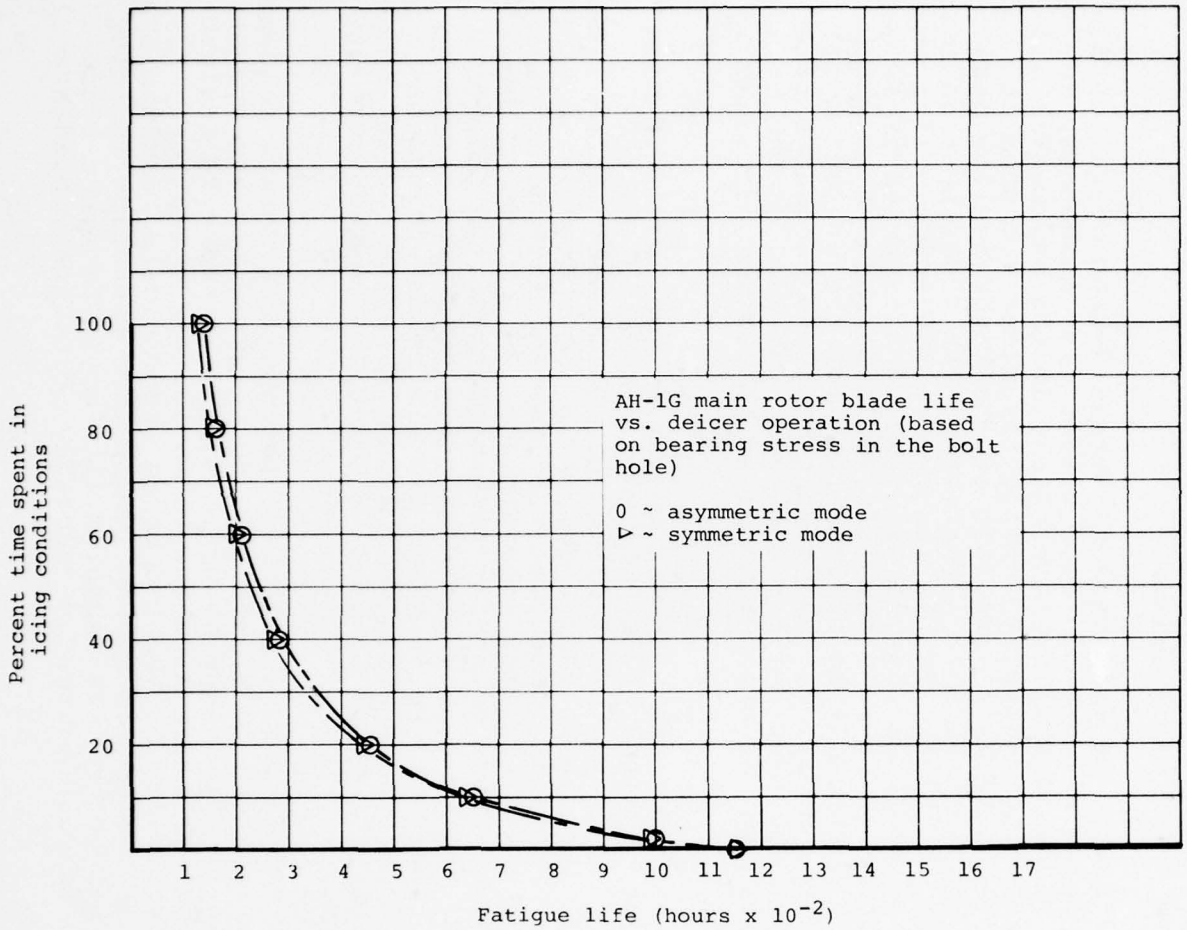

Figure 17. AH-1G main rotor blade life vs deicer operation

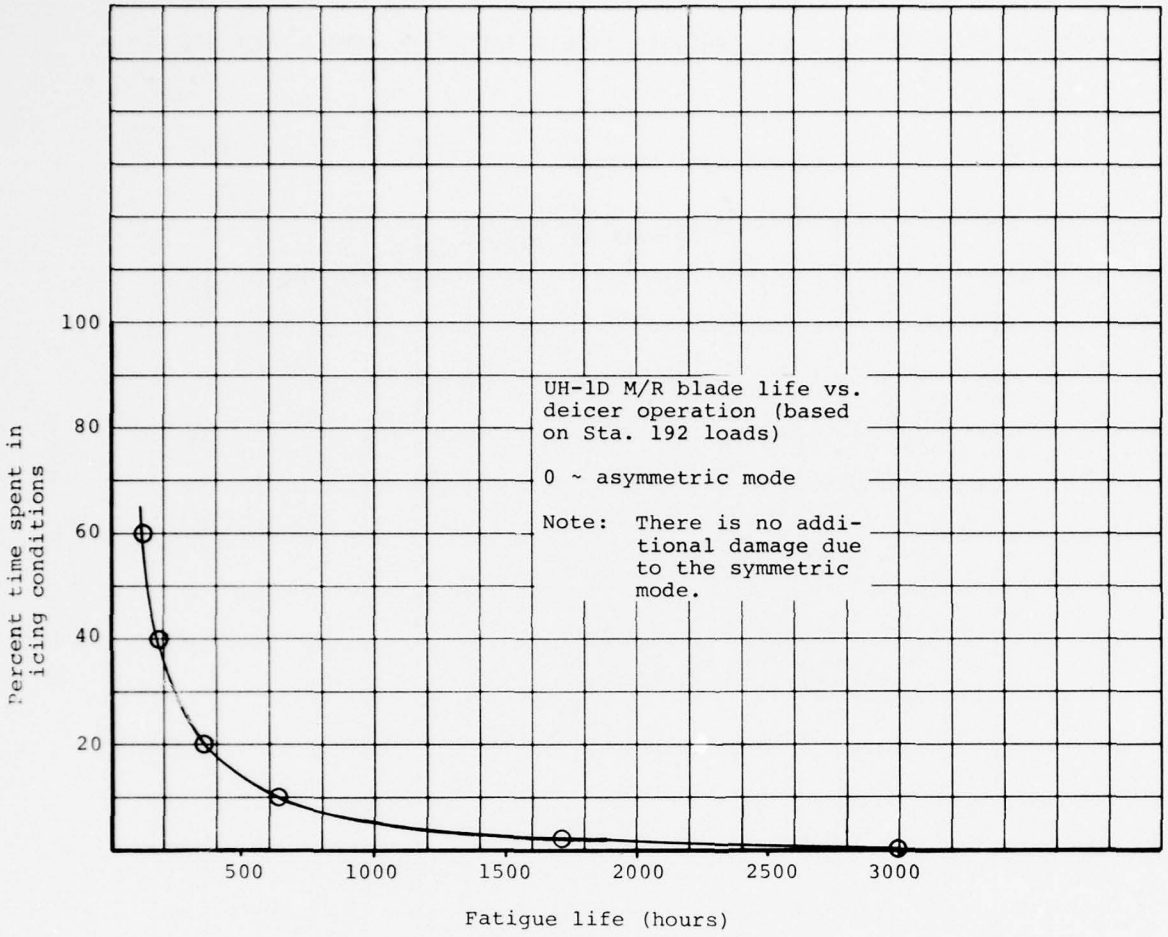

Figure 18. UH-1D main rotor blade life vs deicer operation

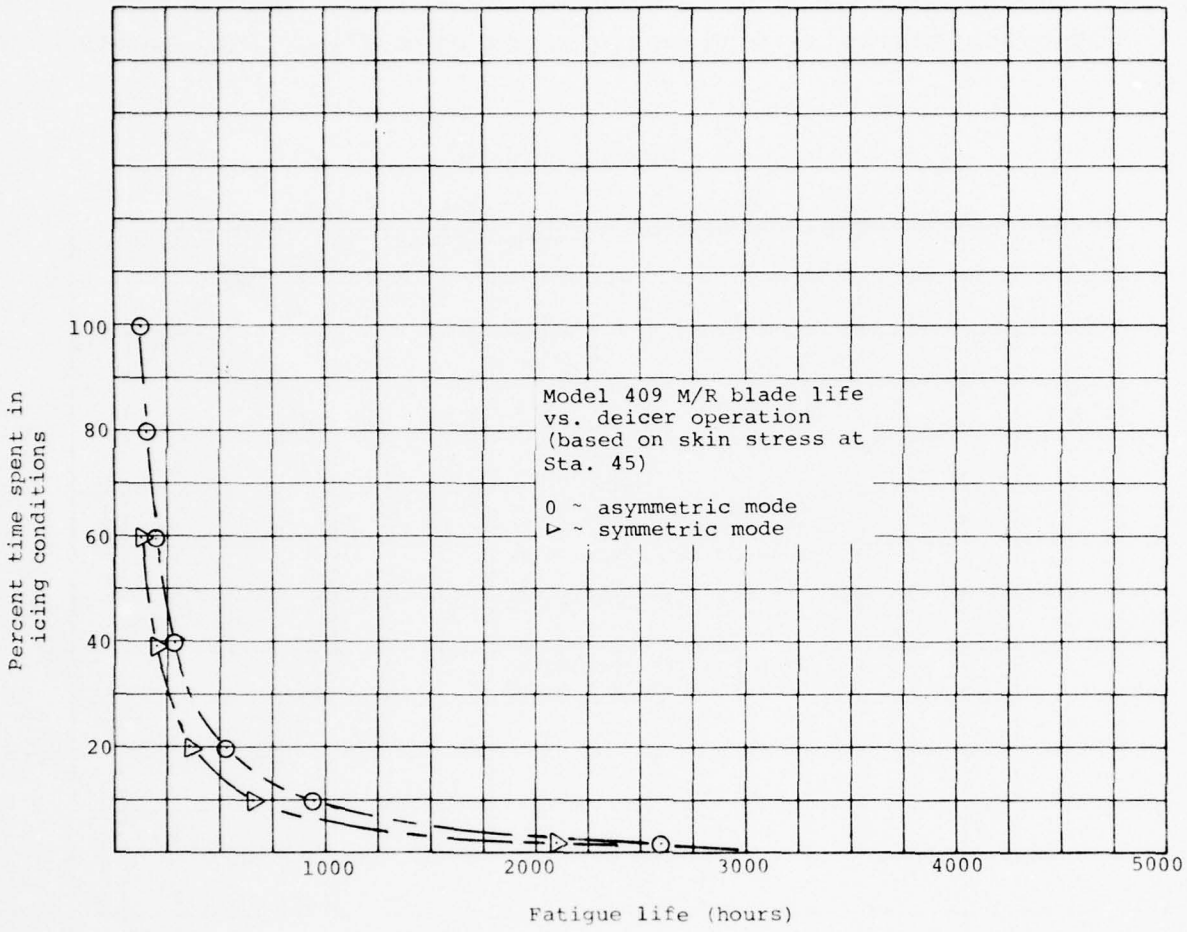

Figure 19. YAH-63 main rotor blade life vs deicer operation

be much better. The fatigue life of the tail rotor blades was not analyzed in detail, because suitable modes that could be excited with a gearbox shaker were not found in the frequency range for vibratory deicing. Data were furnished by the contracting agency so that computer analysis of CH-47 main rotor resonant frequencies could be made. A typical resonant mode is shown in Appendix H. Unfortunately, the fatigue report necessary to perform a fatigue analysis of the blade was not available.

It is obvious that each blade must be examined for fatigue effects with vibrational deicing. The above analysis was made with the most conservative assumptions. All calculations were made assuming V_{NE} flight. Actually, flight in icing conditions would normally be performed at moderate speeds and thus, the base stress level to which the shaker induced stress is added would be much lower than that encountered at V_{NE}. In addition, all flight time was considered to occur at the heaviest gross weight (i.e., no gross weight reduction) which is extremely conservative. The 5-second shaker duty cycle is also considered to be conservative in that during the ice chamber feasibility tests, when the vibration levels used for the deicing criteria were reached, the ice was shed immediately (within a fraction of a second). It is assumed that an operational system would be turned off when the ice is shed. This may result in less than 5 seconds of operation.

3.10 COMPOSITE BLADE CONSIDERATIONS

The helicopter industry is rapidly converting from metal to composite material main rotor blades. One of the reasons for this is composite blades have a typically noncatastrophic failure mode which allows a failsafe design.

The criterion used for deicing is blade beam bending causing a strain of 300 μ in./in. in the skin. Glass materials normally used in composite blades have a capability of 1500 μ in./in. strain without fatigue damage. This means that composite blades could be vibrated to several times the amplitudes used in this study without fatigue damage. The study results indicate the vibratory system is feasible with existing metal blades. In some cases, there might be a reduction in fatigue life of metal blades. With composite blades on these same helicopters it is estimated that there would be no reduction even if blade bending amplitudes were increased.

3.11 APPLICABILITY TO AIRCRAFT

In applying vibrational deicing to any particular aircraft some basic rules of application are:

- Select modes of operation to permit dual mode deicing. Blade bending and torsional/bending modes are of most interest.

- Check practical blade structural and aerodynamic damping values for these modes and select initial forcing function levels to avoid compromising blade life.

- The range of frequency variation about a mean resonance value which will cause deicing is important in establishing forcing function magnitudes.

- For gearbox shaker deicing, the coupled fuselage/gearbox/blade motions are vital to the concept. Aircraft with flexibly mounted main rotor gearboxes (UH-1, OH-58, YAH-63, and AH-1G) appear to be natural designs for this deicing purpose. Certain amplitudes of motion for a particular spring mounting of these gearboxes are developed from the forcing function magnitude based on the damping. Typical of these are the displacements noted in Table 12.

TABLE 12. GEARBOX AMPLITUDES OF MOTION

Aircraft	Motion, ± In.	Frequency (CPM)
UH-1	.106	2546
OH-58	.0585	3168
AH-1G	.015	2726
YAH-63	.012	2138

Design flexibility of this type of gearbox/rotor installation permits variations of spring rates (fuselage/gearbox coupling) to achieve desirable deicing parameters. It may be seen that the magnitudes of the motion amplitudes are relatively small for the required deicing frequencies; therefore, the addition of slight flexibility at the gearbox mounting points (elastomeric pads or washers) for so-called solid-mounted rotor systems should permit a ready achievement of similar magnitude amplitudes. Changes required would be the installation bracketry to mount the shakers on the gearboxes, and location of the deicing control system, and the space requirements of the system. In light of the increasingly stringent fuselage vibration standards, the full impact of the installation on the non-BHT ships requires further investigation.

The hydraulic actuator shaker configuration described in Appendix G 1.2 also affected the coupled fuselage/gearbox/blade motions. Since the hydraulic actuator is mounted in the lift link between the gearbox and fuselage, the fuselage will be excited to a greater extent than by the Type II gearbox shaker. For this reason this system is given little consideration.

Application of vibrational deicing to the tail rotors of the BHT aircraft is less clear in that modes for proper icebond breakage at a reasonable stress level do not exist in most cases; however, this does not necessarily indicate that such deicing may not be accomplished. Rather, it indicates the lack of knowledge of all of the facets of the system, i.e., modal use other than bending, icebond shear allowables, etc.

In addition, there is some question as to the need for tail rotor deicing on some aircraft (Reference 1) such as the UH-1H. The engine exhaust plume apparently keeps this ice free. For the AAH and UTTAS aircraft the need for tail rotor deicing is predicated on the nature of any possible IR suppression device and its effect on the tail rotor. Because of insufficient information on structural/dynamic parameters on these aircraft no effort to evaluate vibration deicing for these tail rotor systems was made in this study; however, blade symmetrical beamwise modes and/or coupled torsion modes capable of deicing may exist. It should be possible by changing stiffness values of tail rotor gearbox mountings (elastomeric mounts) that appropriate modes could be created, as desired, if none exist, i.e., make the proper mode for deicing. Feasibility of tail rotor deicing may thus become possible; however, individual review of each aircraft is again a necessity.

Control of a deicing system for production aircraft should be as automatic as possible, i.e., the system should be activated based on ice build-up. A dual mode duty cycle should be automatic with on-off timing related to the severity of icing conditions; safety limits by monitoring of critical accelerations should provide a shutoff capability. Phasing of the shaker weights, frequency selection, synchronization of motors, etc., constitute the capability of the dual automatic control unit. This unit, plus the appropriate dual mode shaker (Reference Section 2.2.2), may be readily installed in its entirety in the aircraft of this study. Provisions for installation of ice accretion instrumentation for system control will be necessary. Duty cycles will vary between aircraft.

Operation of the controls would be automatic but with an override capability for the pilot. Visual signaling of the imminent operation of the system to the pilot will be made.

4. SUMMARY OF TECHNICAL PROBLEM AREAS

The study to assess the feasibility of vibrational deicing has defined the gearbox shaker system as being a most suitable type. Inherent in any such evaluation is the assumption of various parameters to conduct the study; normally, best engineering judgement is used in making selections. Testing then follows as a method of confirming such judgements for parameter selection. The vibrational deicing investigation has, of course, required such assumptions, one of which involves the vibrational damping of rotor blades.

When operating a blade at resonance, its amplitude of motion is determined by the associated damping, i.e., the energy input to keep a constant vibration amplitude must equal the damping energy. Therefore, the selection of structural and aerodynamic damping values for analysis purposes defines the size of the required shakers and their force magnitude. The proper deicing frequency is selected from previous tests. It then becomes necessary to select a blade modal shape in the frequency range with correspondingly appropriate ice bond/surface strains.

Structural damping, in general, depends upon material characteristics, joining methods, and the vibration frequency. Higher harmonic aerodynamic damping values are related to unsteady aerodynamics; these may vary from near zero at an even harmonic integer of the rotor RPM to about 1 percent of critical damping. As structural damping may be from .1 percent of critical for metal blades and .9 percent of critical for cross-ply composite blades, a wide range of damping values is possible.

For this study, 2 percent of critical damping was used for shaker sizing in that this was felt to be a conservative value for both metal and composite blades. Assumed comparative values for both metal and composite blades permit related information to be evolved. However, for a flight program, more flexibility in the approach is required. As an example, if the combined damping is 1 percent, then the shaker force magnitude would be one-half of the 2 percent critical damping forcing function. Overstressing of the blade might occur if there was a mismatch of the shaker and blade characteristics. For this reason, it is necessary to vary the force by shaker weight selection or by use of the variable frequency/force shaker previously described. The flexibility of this force/shaker approach permits testing with a conservative build-up of resonance amplitude until a proper value is achieved; blade overstressing is thus avoided. The variable frequency feature also permits accurate adjustment of the forcing function to the resonance point.

Bending (out-of-plane) modes instead of torsional modes were selected for deicing because the limited vibratory deicing test data which dictated the shaker criteria were for out-of-plane modes. Also, the cross-coupling terms for the torsion modes in the frequency range of interest are not precisely known.

5. RESULTS OF STUDY

The results of the study may be summarized as follows:

- The Type IV blade and Type V hub shaker systems appear to have design and operational advantages over the other examined candidates.

- Dual mode operation appears desirable for continuous heavy icing use of helicopters for safety and energy reasons.

- Flight tests may show that single mode deicing is feasible.

- Energy requirements are low for the dual mode vibrational deicing even with conservative selections of structural and aerodynamic damping. The Type IV and V dual mode deicing shows a 10.75 hp requirement versus 37.3 hp for an electrical blanket system (Reference 1). The Type IV tip shaker shows 7.18 hp; therefore, energy requirements appear to be minimal.

- Control of shakers as to frequency and phasing may be readily accomplished as illustrated by the breadboard testing of the program.

- Reliability appears to be adequate for all of the examined systems.

- Maintainability of all of the systems is within the requirements for maintainability of Army aircraft.

- Weight of the Type V system appears to be less than one-third of an equivalent electrothermal type system (Reference 1). Type IV, with the shaker placed at the blade tip, can be much less than the weight of the electrothermal system,particularly when it replaces blade tip weights.

- Penalties to the aircraft from vibrational deicing indicate minor decreases in the fatigue life of metal blades may result. Composite blades could be designed with no decrease in the fatigue life.

- Vibrational deicing has no significant effect on the normal helicopter requirements for countermeasures.

- Applicability of vibrational deicing to a specific aircraft appears to present no problem; however, individual aircraft parametric examination and blade/fuselage modal selection are critical.

AD-A057 329 BELL HELICOPTER TEXTRON FORT WORTH TEX F/G 1/3
VIBRATORY ICE PROTECTION FOR HELICOPTER ROTOR BLADES.(U)
JUN 78 H E LEMONT, H UPTON DAAJ02-76-C-0051
UNCLASSIFIED USAAMRDL-TR-77-29 NL

2 OF 2
AD
A057329

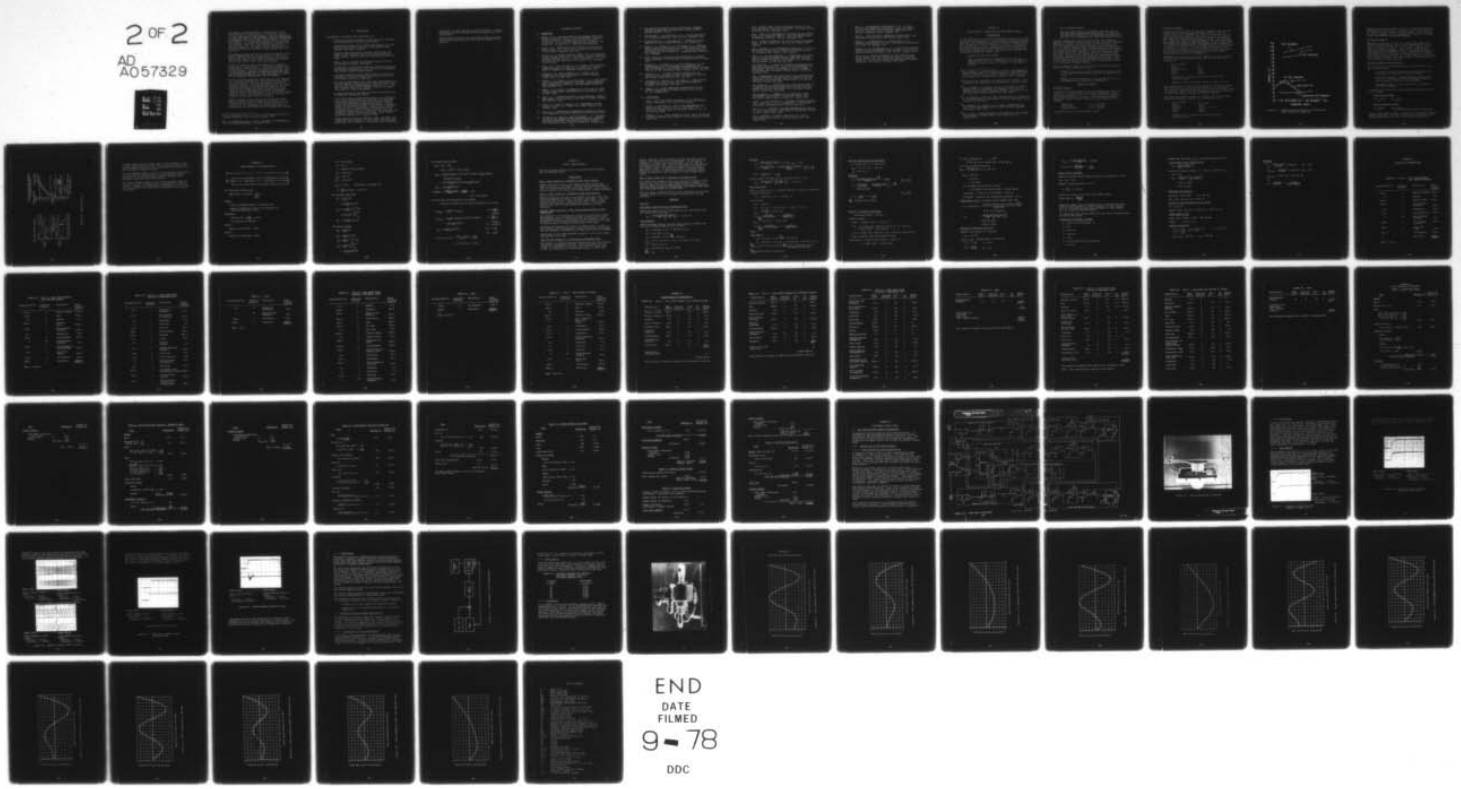

END
DATE
FILMED
9-78
DDC

- The analysis and design study of deicing tail rotors indicates that the feasibility of vibrational deicing of tail rotors is very questionable. The only beam bending mode calculated in the frequency range for deicing was an asymmetric mode which might require shakers on the tail rotor blades. It is considered impractical to implement the shakers, slip rings, and controllers on present tail rotor designs. New tail rotors may be designed for vibratory concepts. The small surface area of tail rotor blades makes the electrothermal system competitive for this use.

- The symmetric modes that can be excited by the tail rotor gearbox shakers used in the study are at a higher frequency than existing data shows can be used for deicing. The fatigue effects of all modes examined cause limitations on the life of metal tail rotor blades.

- Deicing of composite main rotor blades with vibratory techniques is very practical. The higher allowable skin strain should separate the ice surface bond better than on metal blades. If other than metallic materials, such as polyurethane, neoprene or rubberized types are used, the ice bond strength will be less (References 13 and 14) and the necessary shaker force will be reduced.

- Current available analytical techniques are not adequate for a precise description of the aeroelastic behavior of the rotor blades at the high frequencies required for vibratory deicing. Particularly difficult are (1) determining the structural and aerodynamic damping, and (2) including the effects of elastic torsion on the high-frequency blade mode shapes and natural frequencies. Although further research efforts could be directed toward these two topics, the likelihood of useful relevant information in the near future is doubtful.

- Basic knowledge of the strains and accelerations necessary to deice a blade is based on two tests: one on a flat plate and one on a UH-1D nonrotating blade. An expansion of this knowledge is a prime necessity for optimization of vibrational deicing equipment and systems.

---

[13] J. R. Stallabrass and R. D. Price, ON THE ADHESION OF ICE TO VARIOUS MATERIALS, CAAS Journal, September 1963.

[14] D. L. Loughborough and E. G. Haas, REDUCTION OF THE ADHESION OF ICE TO DEICER SURFACES, JAS, March 1946.

6. CONCLUSIONS

Conclusions to be drawn from this study are:

- Vibrational deicing appears to offer excellent potential for ice protection for main rotor blades.

- Vibrational deicing has a limited applicability for present-day tail rotors. New tail rotor designs might include vibrational deicing.

- Analysis techniques do not reliably predict what will happen to the ice metal bond in the high centrifugal force fields. There is need for more basic data in this area.

- Shaker control systems for accurate frequency control and phasing are readily achievable.

- Development and production costs for vibrational deicing systems are estimated to be cost effective in comparison with present electrothermal systems.

- A program including flight tests should be conducted to practically prove the concept and to obtain data to refine present analytical techniques.

- The test program should be a full-scale investigation on an instrumented aircraft using the dual mode deicing concept of main rotor mounted shakers (Type IV or V). The Type V system (hub mounted shaker) would be the lowest cost means of testing the concept.

- A shaker mounted in the blade tip might hold promise for an effective operational system.

- A portion of the program should consist of ground operation of the deicing system to ascertain the blade/gearbox/fuselage response to the various forcing function levels and frequencies suitable for deicing. Strain levels for nonrotating blades (ground deicing) necessary to deice would be investigated. Monitoring of fatigue stress levels to restrict forcing function values to reasonable levels should be conducted; the structural and aerodynamic damping should be measured. This program should be repeated for a rotating blade.

- Flight testing should be conducted under simulated icing conditions (spray tanker or Ottawa spray rig) using the ground data for selection of vibrational system operating

conditions for both dual and single mode deicing. Deicing effectivity of the vibrational deicing concept would thus be evaluated.

- System control operation and components should be tested and refined during both the ground and air phases of the program.

7. REFERENCE MATERIAL

7.1 REFERENCES

1. Werner, J. B., THE DEVELOPMENT OF AN ADVANCED ANTI-ICING/DEICING CAPABILITY FOR U. S. ARMY HELICOPTERS, Lockheed-California Company, USAMRDL-TR-75-34A and B, Eustis Directorate, U. S. Army Air Mobility R&D Laboratory, Fort Eustis, Va., November 1975, ADA019044 and ADA019049.

2. Upton, H. W., MECHANICAL DEICING CONCEPT FOR HELICOPTER ROTOR BLADES, paper presented to Staying Power Symposium at Fort Rucker, Alabama, July 1975.

3. Cotton, R. H., OTTAWA SPRAY RIG TESTS OF AN ICE PROTECTION SYSTEM APPLIED TO THE UH-1H HELICOPTER, Lockheed California Company, USAAMRDL TR-76-32, Eustis Directorate, U. S. Army Air Mobility R&D Laboratory, Fort Eustis, Va., November 1976, AD 034458.

4. Gray, V. H., and von Glahn, U. H., EFFECT OF ICE AND FROST FORMATIONS ON DRAG OF NACA 651-212 AIRFOIL FOR VARIOUS MODES OF THERMAL ICE PROTECTION, NACA TN-2962, 1953.

5. Preston, G. M., and Clackman, C. C., EFFECTS OF ICE FORMATIONS ON AIRPLANE PERFORMANCE IN LEVEL CRUISING FLIGHT, NACA TN-1598, 1948.

6. Gelder, T. F., Lewis, J. P., and Loutz, S. L., ICING PROTECTION FOR A TURBOJET TRANSPORT AIRPLANE: HEATING REQUIREMENTS, METHODS OF PROTECTION, AND PERFORMANCE PENALTIES, NACA TN-2866, 1953.

7. Bowden, D. T., EFFECT OF PNEUMATIC DE-ICERS AND ICE FORMATIONS ON AERODYNAMIC CHARACTERISTICS OF AN AIRFOIL, NACA TN-3564, 1956.

8. Gray, V. H., CORRELATIONS AMONG ICE MEASUREMENTS, IMPINGEMENT RATES, ICING CONDITIONS, AND DRAG OF A 64A004 AIRFOIL, NACA TN-4151, 1958.

9. Gray, V. H., and von Glahn, U. H., AERODYNAMIC EFFECTS CAUSED BY ICING OF AN UNSWEPT NACA 65A004 AIRFOIL, NACA TN-4155, 1958.

10. Gray, V. H., PREDICTION OF AERODYNAMIC PENALTIES CAUSED BY ICE FORMATIONS ON VARIOUS AIRFOILS, NASA TN-D-2166, 1964.

11. Patten, R. B., Hart, B., and Bartholomew, J. F., ENGINEERING STUDY FOR ADVANCED ATTACK HELICOPTER (AAH) AUTOMATIC INSPECTION DIAGNOSTIC AND PROGNOSTIC SYSTEM (AIDAPS), Bell Helicopter Textron Report 299-949-007, October 1976.

12. Bell Helicopter Textron Report 299-099-521, AUTOMATIC INSPECTION DIAGNOSTIC AND PROGNOSTIC SYSTEM (AIDAPS) TESTBED PROGRAM - TASK II.

13. Stallabrass, J. R., and Price, R. D., ON THE ADHESION OF ICE TO VARIOUS MATERIALS, CAAS Journal, September 1963.

14. Loughborough, D. L., and Haas, E. B., REDUCTION OF THE ADHESION OF ICE TO DEICER SURFACES, JAS, March 1946.

15. Mazza, L. T., Paxson, E. B., and Rogers, R. L., MEASUREMENT OF DAMPING COEFFICIENTS AND DYNAMIC MODULUS OF FIBER COMPOSITES, Eustis Directorate, U. S. Army Air Mobility R&D Laboratory, Fort Eustis, Va , USAAVLABS TN-2, February 1970, AD869025.

16. Zenev, Clarence, ELASTICITY AND ANELASTICITY OF METALS, Fifth Impression, The University of Chicago Press, Chicago, 1965.

17. Bousman, W. G., Sharpe, D. L., and Ormiston, R. A., AN EXPERIMENTAL STUDY OF TECHNIQUES FOR INCREASING THE LEAD LAG DAMPING OF SOFT INPLANE HINGELESS ROTORS, Proceedings of the AHS 32nd Annual Forum, Preprint 1035, May 1976.

18. Ormiston, R. A., A STUDY OF STALL INDUCED FLAP LAG INSTABILITY OF HINGELESS ROTORS, Proceedings of the AHS 29th Annual Forum, Preprint 730, May 1973.

19. Daughaday, H., DuWaldt, F., and Gates, C., INVESTIGATION OF HELICOPTER BLADE FLUTTER AND LOAD AMPLIFICATION PROBLEMS, AHS Journal, July 1957.

20. Loewy, R. G., A TWO-DIMENSIONAL APPROXIMATION TO THE UNSTEADY AERODYNAMICS OF ROTARY WINGS, C.A.L. Report No. 75, October 1955.

7.2 BIBLIOGRAPHY

- Anon., YH-13 HELICOPTER, EVALUATION AT LOW TEMPERATURE, Project NRAVN 1655, AD 113141, date unknown.

- Burpo, F., and Kawa, M., TEST OF AN EXPERIMENTAL HELICOPTER DEICING SYSTEM ON AN H-13 HELICOPTER, Bell Helicopter Company Report 502-099-002, Parts I, II, III, and IV, July 1958.

- Campbell, C. W., (DATA TABULATION) UH-40 (HU-1) HELICOPTER CLIMATIC LABORATORY TEST, WADC TN 58-357, ASTIA No. 207165, June 1959.

- Anon., SERVICE TEST OF UH-1 HELICOPTER, Report of the U.S. Army Arctic Test Board US ConArC, Ft. Greely, Alaska, ASTIA AD 299-187, September 1959.

- Anon., TEST OF AN EXPERIMENTAL HELICOPTER DEICING SYSTEM ON AN H-13 HELICOPTER, PART IV , Bell Helicopter Report 502-099-002, ASTIA No. 242-233, September 1959.

- Anon., CLIMATIC LABORATORY TEST OF THE YHU-1D HELICOPTER, Report of Test Project No. AVN 1562 (CL) 294337, date unknown.

- Anon., CATEGORY II LOW TEMPERATURE EVALUATION OF A YUH-1D HELICOPTER IN THE ARCTIC, Technical Documentary Report No. ASD-TDR-63-564, 422643, date unknown.

- Burpo, F., and Van Wyckhouse, J., DEVELOPMENT AND GROUND TEST OF AN ELECTROTHERMAL DEICING SYSTEM FOR THE MAIN AND TAIL ROTORS OF THE UH-1 HELICOPTER, Bell Helicopter Company Report 512-099-002, May 1960.

- Van Wyckhouse, J., LIQUID ICE PROTECTION SYSTEM DEVELOPMENT AND FLIGHT TEST OF A LIQUID AND ELECTROTHERMAL ICE PROTECTION SYSTEM FOR THE ROTORS OF THE UH-1 SERIES HELICOPTER, Bell Helicopter Company Report 518-099-001, November 1960.

- Anon., DEVELOPMENT AND GROUND TEST OF AN ELECTRO-THERMAL DEICING SYSTEM FOR THE MAIN AND TAIL ROTORS OF THE UH-1 HELICOPTER, Bell Helicopter Company Report 512-099-002, ASTIA No. 241-166, May 1960.

- Van Wyckhouse, J., DEVELOPMENT AND ICING FLIGHT TESTS OF A CHEMICAL ICE PROTECTION SYSTEM FOR THE MAIN AND TAIL ROTORS OF THE UH-1 HELICOPTER, Bell Helicopter Company Report 518-099-002, June 1961.

- Van Wyckhouse, J., SUMMARY OF ICE PROTECTION SYSTEM DEVELOPMENT AND TESTING FOR HELICOPTER ROTORS, Bell Helicopter Company Report 529-099-001, August 1961.

- Coombs, P., and Stanford, E., CATEGORY II EXTREME TEMPERATURE EVALUATION OF A YHC-1B HELICOPTER IN THE CLIMATIC LABORATORY, ASD-TDR-62-1076, 404725, March 1963.

- White, B. L., CATEGORY II EXTREME TEMPERATURE EVALUATION OF A UH-1D HELICOPTER IN THE CLIMATIC LABORATORY, ASD-TDR-62-1066, 405922, April 1963.

- Anon., CATEGORY II CLIMATIC EVALUATION OF A UH-1F HELICOPTER, ASD-TR-66-15, Wright-Patterson AFB, Ohio, January 1967.

- Kawa, M., ENVIRONMENTAL DEVELOPMENT OF THE U.S. ARMY OH-58A LIGHT OBSERVATION HELICOPTER, paper presented at the joint Symposium on Environmental Effects on VTOL Designs, Arlington, Texas, November 1970.

- Burpo, F., HELICOPTER ICE PROTECTION INVESTIGATION, Bell Helicopter Company Report 299-099-487, March 1971.

- Eskin, S. G., Fontaine, W. E., and Witzell, O. W., STRENGTH CHARACTERISTICS OF ICE, Refrigeration Engineering, pp. 33-38, 52, December 1957.

- Graham, G. L., and McGuigan, M. J., A SIMPLIFIED EMPIRICAL METHOD FOR ROTOR COMPONENT FATIGUE DESIGN, Journal of the American Helicopter Society, Vol. 15, No. 2, April 1970.

- Upton, H. W., PLANNING DOCUMENT FOR MAIN ROTOR DEICING ON THE MODEL UH-1H, Bell Helicopter Company report submitted to U.S. Army Air Mobility Research and Development Laboratory, Fort Eustis, Virginia, July 1975.

APPENDIX A

BLADE DEICING - STRUCTURAL AND AERODYNAMIC DAMPING

INTRODUCTION

In the computation of the forcing functions necessary to vibrate helicopter rotor blades for deicing purposes, an assumption was made that the combined blade structural and aerodynamic damping was two percent of critical damping. In order to investigate this assumption, a cursory investigation of the literature on the subject (References 15 through 20) was made covering both metal and composite structures. Two general test methods used to determine structural damping are:

- Logarithmic Decrement Method

  This is computed from an exponential decay record (amplitude vs time) of a vibration, i.e., the amplitude reduction between cycles is a measure of the damping present.

---

[15] L. T. Mazza, E. B. Paxson, and R. L. Rogers, MEASUREMENT OF DAMPING COEFFICIENTS AND DYNAMIC MODULUS OF FIBER COMPOSITES, Eustis Directorate, U. S. Army Air Mobility R&D Laboratory, Fort Eustis, Va., USAAVLABS TN-2, February 1970, AD869025.

[16] Clarence Zenev, ELASTICITY AND ANELASTICITY OF METALS, Fifth Impression, The University of Chicago Press, Chicago, 1965.

[17] W. G. Bousman, D. L. Sharpe, and R. A. Ormiston, AN EXPERIMENTAL STUDY OF TECHNIQUES FOR INCREASING THE LEAD LAG DAMPING OF SOFT INPLANE HINGELESS ROTORS, Proceedings of the AHS 32nd Annual Forum, Preprint 1035, May 1976.

[18] R. A. Ormiston, A STUDY OF STALL INDUCED FLAP LAG INSTABILITY OF HINGELESS ROTORS, Proceedings of the AHS 29th Annual Forum, Preprint 730, May 1973.

[19] H. Daughaday, F. DuWaldt, and C. Gates, INVESTIGATION OF HELICOPTER BLADE FLUTTER AND LOAD AMPLIFICATION PROBLEMS, AHS Journal, July 1957.

[20] R. G. Loewy, A TWO-DIMENSIONAL APPROXIMATION TO THE UNSTEADY AERODYNAMICS OF ROTARY WINGS, C.A.L. Report No. 75, October 1975.

- Forced Response Method

  Data are taken exactly at resonance where the inertia and the spring forces cancel each other. At this point, one-half the reciprocal of the amplification factor is the sum of the aerodynamic and structural damping factors.

Practical separation of the structural from the aerodynamic damping is difficult without vacuum testing; structural damping additionally depends upon the nature of the structure, i.e., riveted, bonded, type of metal, hardness, type of composite, etc. It could be expected that a homogeneous structure (bonded or molded) rather than one made up from riveted bits and pieces (an airplane wing has 2 percent to 8 percent structural damping) would have structural damping similar to one-piece test specimens. Working of the joints with its additional damping effects is eliminated with the bonded/molded structure. Damping coefficients of blades are presented herein as the ratio of the observed damping (structural and/or aerodynamic) to the critical damping (deadbeat damping).

Data on damping of materials are presented as damping capacity defined by either method as follows:

- Damping is the ratio of plastic strain to elastic strain in the Hookes Law deflection range of the stress/strain curve.

- Damping of the stress/strain curve is the ratio of the hysteresis area to the area of deformation.

RESULTS OF SURVEY

Material Damping

In general, materials tend to have less damping the harder the material; i.e., hardened steel has about one-quarter to one-eighth the damping of soft iron. Basic steels and aluminums have damping of about .1 percent. Unidirectional filament beams have damping factors (damping/critical damping ratio) as follows:

Glass epoxy	.1 to .9 percent
Boron epoxy	.4 to .6 percent
Graphite epoxy	.5 to .9 percent

Crossplies have 3 to 6 times these values.

Structural Damping

Damping values were found for metal and composite beam specimen tested both with and without aerodynamic damping (air and vacuum testing) per Reference 15. Both the logarithmic decrement and the forced response methods were used in this testing and results are presented as Figure A-1 (Figure 7 in Reference 15). This is a plot of damping constant versus frequency with data taken in a vacuum of .2mm of mercury. It may be noted that at 40 hertz the unidirectional (0^{o}) composite has a damping of .1 percent of critical while the 2024-T4 aluminum specimen shows .22 percent of critical. Crossply composites indicate about ten times the aluminum values. Correlation between these tests and an analytical prediction method for structural damping estimations may be found in Reference 16.

Reference 17 presents the uncoupled flapping and lead lag damping of a flex-retention model rotor with the following characteristics:

No. of blades	2
Twist	0^{o}
Lock No. *	7.99
Solidity ratio	.033
Radius	.811m
Chord	.0419m

Construction - PRD49 composite with uniaxial and cross-ply layers.

*Ratio of rotor aerodynamic forces to inertia forces.

Data were taken for lead-lag decay motion of the blade by locking the hub after a cyclic mode of vibration was established. This damping includes profile drag and structural damping; values of structural damping with the aerodynamic drag value removed at 50 hertz were about .4 percent of critical damping.

Reference 18 presents a value of .1 percent of critical damping as the structural damping for the following rotor:

No. of blades	2
Twist	-11.94^{o}/m
Solidity	.0601
Lock No.	2.84 (a = 5.73)
Radius	.907m
Chord	.0856m

Construction - aluminum spar, balsa aft blade, fiberglass wrap

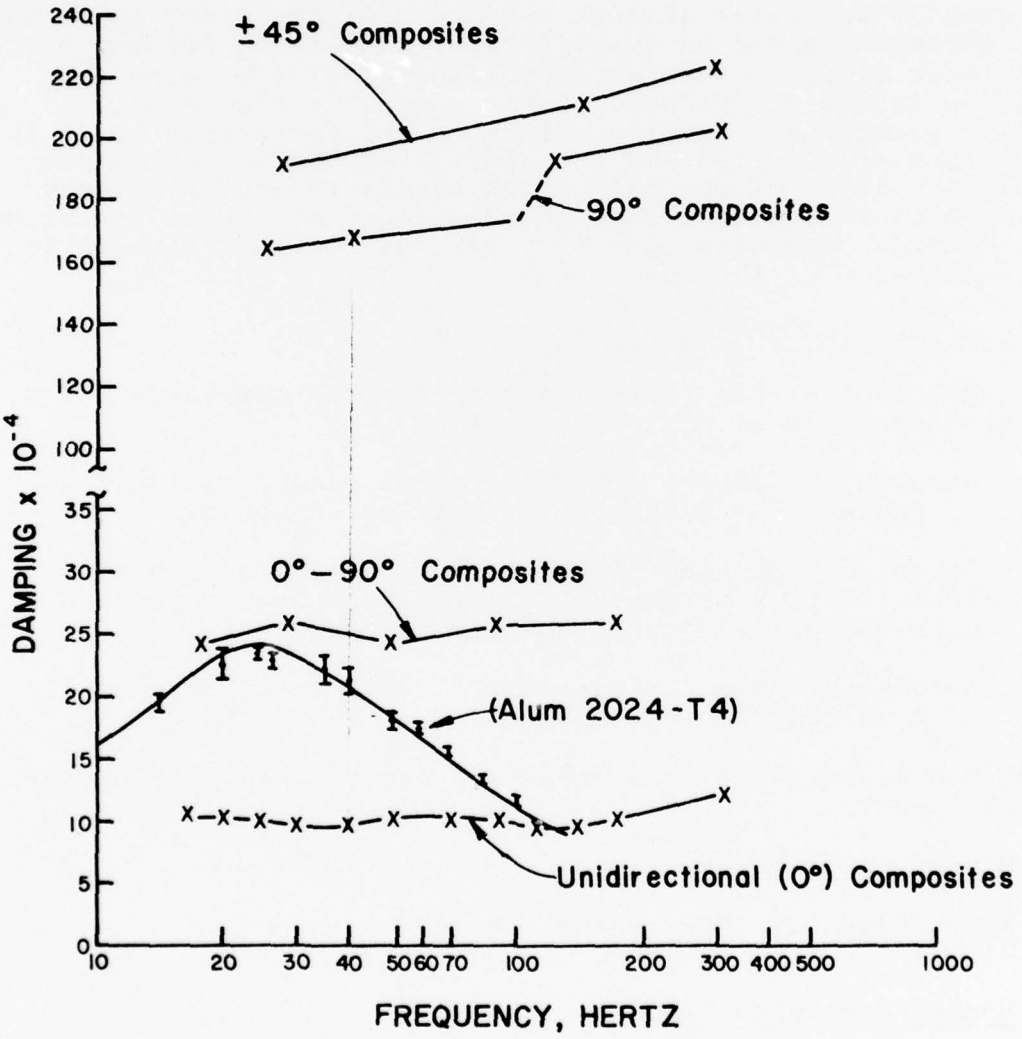

Figure A-1. Damping versus frequency for aluminum and fiber-reinforced composites

Reference 19 uses data based on the forced response method for a model rotor, and Figure A-2 (Figures 5 and 6 from Reference 19) shows structural damping varying between .3 and 1 percent of critical damping for first bending mode damping and between .7 and 1 percent for second mode damping.

Aerodynamic Damping

Reference 19 indicates (Figure A-2) that higher order aerodynamic damping based on Loewy's paper (Reference 20) may be equal to or close to zero at even integers of the rotor rpm under low inflow conditions. Other sources indicate that negative aerodynamic damping exists on the retreating blade in the regions of $\psi = 225^{o}$ and $\psi = 315^{o}$. Because of the as yet uncodified nature of unsteady aerodynamics theory it appears that damping values from zero to .7 percent may exist for higher order damping depending upon the nearness of the frequency to an even integer of the rotor rpm.

Resultant Damping Characteristics

In recapitulation, the following appears from the above and the attached figures:

- Structural damping of bonded metal blades varies from .1 percent to .2 percent of critical damping.
- Structural damping of bonded composite blades varies from .25 to 2 percent of critical damping, depending upon the material used and its orientation.
- Aerodynamic damping varies from zero to .7 percent of critical damping.

A combined blade structural and aerodynamic damping value may be as follows:

Bonded metal blades

Min. value	Max. value
.1%	.9%

Bonded composite blades

Min. value	Max. value
.25%	2.7% (depending on fiber orientation)

Typical model blades indicate .1 percent for aluminum structural damping alone and .4 percent for PRD blades; therefore, these values should be used for tail rotor blade computations.

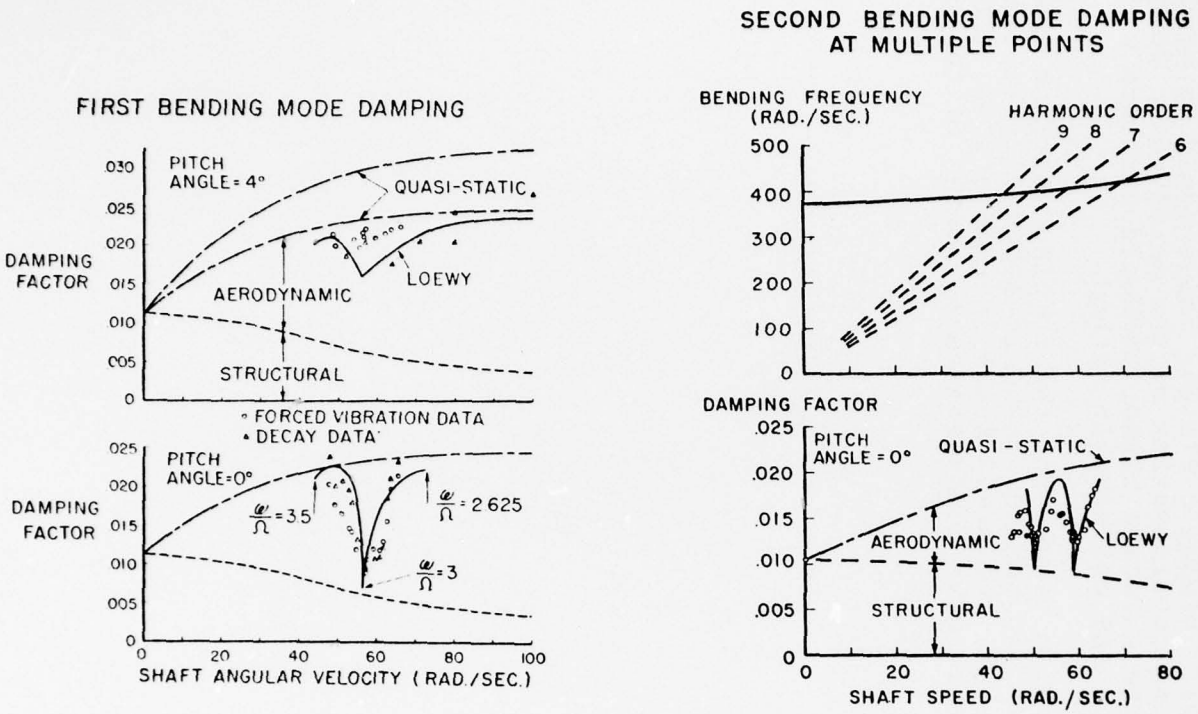

Figure A-2. Damping factors

It would appear from the above that for metal blades a value of less than 1 percent for the total of structural and aerodynamic damping could be used to calculate the necessary forcing functions to deice the blade.

For the composite blade, a similar value could be used based on the fact that no consideration of the aerodynamic forcing functions of the existing higher harmonic airloads were included in the BHT calculation method.

The present design values for the forcing function loads for the various deicing schemes could be reduced by at least 50 percent. However, for preliminary investigations, the value of 2 percent will give conservative estimates of the required force level.

APPENDIX B

POWER EFFECT OF ICE ACCUMULATION

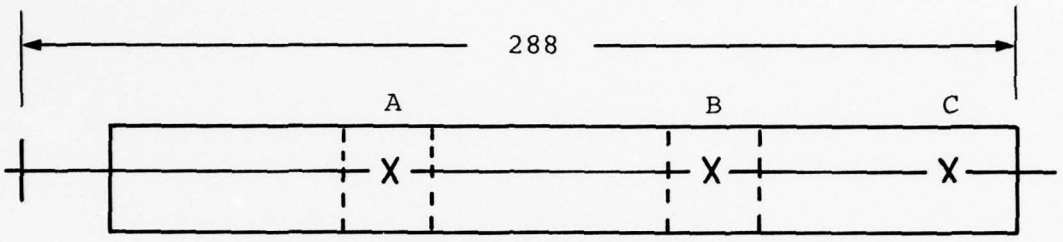

For collective mode 8.4/rev

Nodal points @ station 95.5
199.5
276

Assume:

- Area of noniced nodes is 18 inches wide
- Ram air temperature rise at tip prevents ice formation inboard to .85 R

Therefore:

- Node at tip is $\frac{276}{288} = 0.958R$
- Tip node may be ignored

Node A:

Station is 95.5/288 = .332R

Node B:

Station is 199.5/288 = .692R

$$\Omega R = 700 \text{ ft/sec}$$

$$R = 24 \text{ ft}$$

$$\Omega = 700/24 = 29.2 \text{ rad/sec}$$

$$V_A = .332 \times \Omega R$$

$$V_A = .332\ \Omega R$$

$$V_A^2 = .111(\Omega R)^2$$

$$C_{D_A} = 1.5\ C_D \qquad \text{(References 4 through 10)}$$

$$S = \frac{23}{12} \times 12/144 = .16 \text{ sq ft}$$

For totally iced blade

$$Q_b = C_{D_B} \frac{\rho}{2} SV^2 r$$

$$= 1.5 C_D \frac{\rho}{2} c dr (\Omega r)^2 r$$

$$Q_b = 1.5 C_D \frac{\rho}{2} c \Omega^2 \int_o^R r^3 dr$$

$$= 1.5 C_D \frac{\rho}{2} c \Omega^2 \frac{r^4}{4} \Bigg]_o^R$$

$$Q_b = .374 C_D \frac{\rho}{2} c (\Omega R)^2 R^2$$

For noniced blade

$$\Delta Q_b = C_D \frac{\rho}{2} SV^2 r$$

$$\Delta Q_b = C_D \frac{\rho}{2} c dr (\Omega r)^2 r$$

$$Q_b = C_D \frac{\rho}{2} c \Omega^2 \int_o^R r^3 dr$$

$$Q_b = C_D \frac{\rho}{2} c \Omega^2 \frac{r^4}{4} \Bigg]_o^R$$

$$= .25 C_D \frac{\rho}{2} c (\Omega R)^2 R^2$$

For blade iced at nodes

$$\Delta Q_b = \Delta Q_A + \Delta Q_B$$

$$= \Delta D_A \times .332R + \Delta D_B \times .692R$$

$$\Delta Q_b = .5C_{D2}\frac{\rho}{2}(.0625Rc)(.111)(\Omega R)^2(.332R) + .5C_{D2}\frac{\rho}{2}(.0625Rc)$$

$$(.48)(\Omega R)^2(.692R)$$

$$= .001159C_{D2}\frac{\rho}{2}cR^2(\Omega R)^2 + .0104C_{D2}\frac{\rho}{2}R^2c(\Omega R)^2$$

$$\Delta Q_b = .0116C_{D2}\frac{\rho}{2}cR^2(\Omega R)^2$$

$$\text{Increase} = \frac{.2500 + .0116}{.2500} = \frac{.2616}{.2500} = .045$$

$$= 4.5\% \text{ Q increase}$$

For the Type III aerodynamic flap shaker

- Increase in blade basic Q due to presence of tip flap

$$\Delta Q_{Flap} = \Delta C_{D2}\frac{\rho}{2}SV^2 \times R_{Flap}{}^x$$

$$\Delta Q_{Flap} = .50C_{D2}\frac{\rho}{2}(.0625cR)(.94)(\Omega R)^2(.969)R$$

$$= .0284C_{D2}\frac{\rho}{2}c(\Omega R^2)R^2$$

$$Q_b = .479\frac{\rho}{2}C_Dc(\Omega R)^2R^2$$

$$S = cx\frac{18}{288}R$$

$$= .0625cR$$

$$V = \frac{279}{288}\Omega R$$

$$= .969\Omega R$$

$$V^2 = .94(\Omega R)^2$$

$$\Delta C_D = .50C_D$$

$$Rx = .969R$$

$$\text{Ratio increase} = \frac{.479 + .0284}{.479} = \frac{.5079}{.479}$$

$$= 1.06 \text{ increase in power}$$

APPENDIX C

STATIC STRESS EFFECTS

The static stress effects of the five systems were estimated and are described below:

CONCLUSIONS

Type I (Ref: Figure 5) - Shakers on tail rotor gearbox

Shakers mounted on a tail rotor gearbox produce oscillatory loads on the tail rotor blade. From a static strength point of view, this does not have any significant effects. This conclusion is valid for all ships under consideration (already designed).

Type II (Ref: Figure 6) - Shakers on main rotor gearbox

Shakers mounted on the main rotor gearbox (left and right) produce some oscillatory loads on the main rotor blade. From the static strength point of view, the main rotor blade and hub assembly will encounter insignificant effects. This conclusion is valid for all ships under consideration (already designed).

Type III (Ref: Figure 8) - Main rotor blade excited by aerodynamic tab

The location of the deicing tab at the tip of the blade causes approximately 15 to 20 percent increase in centrifugal force and beamwise moments. Furthermore, the mass balance cg will be shifted aft of its present location, which definitely will cause an adverse effect in overall performance of the rotor.

Reviewing the analysis of a UH-1N, it appears that in order to keep present positive margins of safety for the main rotor blade and yoke assembly, strengthening of these parts will be necessary.

This device is the least desirable compared to the others being considered at this time.

Type IV (Ref: Figure 9) - Excitation at antinodal point

This shaker is installed inside the blade near the root end where the blade is attached to the hub. Since its weight (8 to 10 pounds) is located near the blade root end at 57 inches from C_L hub, the resulting ΔCF (centrifugal force) is about 3100

pounds. Because of the increase in centrifugal force, the retention bolt will need to be strengthened. If the shaker is located at a greater radius on the blade, the ΔCF must be considered for each case. Possibly the shaker may replace balance weights used in the blade, or weights used to achieve a high inertia rotor. It might be possible to replace static weights in the tips of some blades with an equivalent shaker weight that causes no ΔCF; no change in static stress would result.

Type V (Ref: Figure 13) - Excited at antinodal point

The shakers are located at the 28.0-inch radial station of the blade at the root end and weigh approximately 10 pounds. Inspection shows that the concentration of the deicing weight at the root end will make an insignificant difference in the shifting of the mass balance cg of the blade.

From the static strength point of view, this device is the most suitable among all the five designs considered for deicing purposes.

ANALYSIS

Type III

Main Rotor Blade Excited by Aerodynamic Tab

Assume the weight of the shaker device cg at 300.0-inch from the centerline of the hub.

$$\Delta_{CF} = \frac{(10.0)(300)}{386}\left[\left(\frac{2\pi \times 362}{60}\right)^2\right] = 11{,}170 \text{ lb}$$

Yoke Assembly

Assume beamwise moments increase approximately 5 percent and that the chordwise moments stay the same.

$M_B = -(281{,}922)(1.05) = -296{,}108$ in.-lb

$M_C = 1{,}103{,}129$ in.-lb

$C_F = 339{,}599 + 11{,}170$ (1) $= 350{,}769$

$EI_B = 43.5 \times 10^6$ lb-in.^{2}, $EI_C = 12{,}900 \times 10^6$ lb-in.^{2}

$EA = 244.8 \times 10^6$ lb

$F_{BU} = 191{,}000$ PSI, $F_{Tu} = 130$ KSI

(1) $= \Delta_{CF}$

Analysis

$$f_b = \frac{296,108(.73)(16.0)}{43.5} = 79,506, \quad R_{bu} = .624$$

$$f_t = \frac{350,769(16.0)}{244.8} + \frac{(1,103,129)/7\text{-}1(16.0)}{\frac{244.8}{2}} = 43235 \text{ PSI}$$

$$R_{tu} = .50$$

$$M.S = \frac{1}{.624+.50} - 1 = \underline{\underline{-.12}}$$

Assume weight of shaker device at station 288 = 10 lb

$$\Delta_{CF} = \frac{(10.0)(288.)}{386}\left[\left(\frac{2\pi x356}{60}\right)^2\right] = 10,370 \text{ lb}$$

Main Blade Bolt

From Δ_{CF} calculations, it appears that bolt loads will increase roughly 10 percent.

$$P_S = (106,350)(1.10) = 117,000 \text{ lb}$$

Area of bolt

O.D. = 2.499 in.

I.D. = 2.0 in. $A = \left[\pi/4\ 2.499^2 - 2.0^2\right] = 1.76 \text{ in.}^2$

$$f_{s_{av}} = \frac{117,000}{1.76} = 66,470 \text{ PSI}$$

$$M.S = \frac{109,000}{(1.50)(66470)} - 1 = \frac{+0.09(av)}{(Shear\ av)}$$

(2)

$$f_{s_{N.A}} = 2(66,470) = 132,940 \text{ PSI}$$

$$M.S = \frac{109,000}{(1.50)(132,940)} - 1 = \frac{-.45}{Shear\ @\ N.A}$$

(2)

Yoke

Load Cond. 3

$$C_F = 127,000 + 15,550 \text{ (1)} = 142,550 \text{ lb}$$

$$M_C = 500,000 \text{ in.-lb}, \quad M_B = 1.15(386,000) = 443,900 \text{ in.-lb}$$

(1) Δ_{CF} due to deicing device

(3) Assumed beamwise moment increased 15 percent

(2) Ultimate Design Load Factor

Section Properties and Allowables

$A = 2.499$ in.^{2}, $I_C = 45.34$ in.^{4}

$F_{BU} = 217$ KSI $F_{tu} - 180$ KSI

$I_B = 14.85$ in.^{4}

Analysis

$$f_b = \frac{443{,}900(2.25)(1.5)}{14.85} \text{ (2)} = 100886 \qquad R_b = .465$$

$$f_t = \left[\frac{142{,}550}{2(2.499)} \quad \frac{500{,}000(4.025)}{45.34}\right] 1.5 \text{ (2)}$$

$$= 109{,}360 \text{ PSI}$$

$$R_t = .607$$

$$M.s = \frac{1}{Rb+Rt} - 1 = \underline{\underline{-.07}}$$

(2) Ultimate load factor

Type IV - Antinodal excitation

Drive shaft size = .575 in.

Material steel

$\text{Area} = (.7854)(.575)^2 = 0.260$ in.^{2}

Δw_1 for blade seg. from sta. 24.50 in. to $\approx$49.5 in.

$= (0.26)(.285) = .0741$ lb/in.

Δw_2 for blade seg. from blade sta. $\approx$ 49.5 in. to 63.50 in.

i) Δw_{2-a} tungsten tube reinforced by steel

Steel area $= (1.625^2-1.50^2)(.7854) = .306$ in.^{2}

$= (.306)(.285) = .0875$ lb/in.

ii) Δw_{2-b} tungsten wt $\alpha = 68^{o}$

$= 1/2(.75)^{2}(2.37-.694)(.69) = 0.325$ lb/in.

iii) Δw_{2-c} aluminum block wt

Area $= \frac{(2.50+1.50)}{2}\ 14.0 = 28$ in.^{2}

$\Delta w_{2c} = 28(.10)$

$= 2.80$ lb

$= .20$ lb/in.

Δwt increase from sta 49.5 to 63.5

$= .20$ lb/in.$+.325$ lb/in.$+.0875 = 0.6125$ lb/in.

Δwt/blade $= (.0741)(14.0)+.6125(14) = 9.612$ lb

Δwt/blade = assuming all accessories included = 10 lb

Calculation of C.G. of shaker device weight from hub

$$\text{C.G. (Location)} = \frac{.6125(24.5+25+14.0/2)+.074(24.5+\frac{25.1}{2})}{.6125+.074}$$

54.35 in. from $\mathbb{C}_L$ hub

$$\Delta_{CF} = \frac{10(54.35)}{386}\left[\left(\frac{2\pi(356)}{60}\right)^{2}\right]$$

$= 1955$ lb limit

$= 2933$ lb (ULT)

Analysis of Retention Bolt Pin

Material 4340 steel, H.T. 180 KSI

$F_{su} = 109$ KSI

$V_{\text{total shear}} = 98,600+2,933 = 101,533$ lb

O.D. $= 2.499$ $\quad A = 1.763$

I.D. $= 2.00$

$2t = 0.499$ $\quad D/t = 10$

$$f_{s_{N.A}} = \frac{(2.01)(101,533)}{1.762} = 115,823$$

$$M.S\ @\ N.A = \frac{109,000}{115,823} - 1 = \underline{\underline{-.06}}$$

Type V (UH-1) Aircraft

Effect of deicing device weight on mass C.G. balance of rotor.

Sta. 24.5 - 28.5

Weight of deicing device = 10 lb

$$W = \frac{10}{4} = 2.5 \text{ lb/in.}$$

Assume 10 lb acts at 3.75 in. from leading edge.

Since mass cg = $\frac{\Sigma WR\bar{x}cg}{\Sigma w_R}$

Inspection shows that the concentration of the deicing device weight of approximately 10 pounds located at radial station 28.0 in. will make insignificant difference in mass balance C.G. of a blade of 264-inch radius.

In conclusion, the overall effect from the static strength point of view is negligible.

Calculation of weight of shaker

$$W = \left[\alpha R^2 + (3.0^2 - 2.65^2)\right].7854 \quad \ell\rho$$

$$\alpha = 30^o$$

$$R = 3.26 \text{ in.}$$

$$\ell = 2.60 \text{ in.}$$

$$\rho = .285$$

$$W = \left[.524(3.26)^2 + 1.553\right] (2.60).285$$

$$= 5.27 \text{ lb}$$

Assume that the total Δ_{wt} of the deicing device ≈10 lb

Δ centrifugal force calculations

$$\Delta_{CF} = \frac{\Delta WR}{386}\left[\left(\frac{2\pi RPM}{60}\right)^2\right]$$

Location of deicing shaker (R) ≈ 28.0 in. radial sta.

RPM = 356

$$\Delta_{CF} = \frac{(10)(28.0)}{386}\left[\left(\frac{2\pi x356}{60}\right)^2\right]$$

= 1008 lb limit

= 1512 lb (ULT.)

Retention Pin Analysis

Material, 4340 steel H.T. 180 KSI

Max. shear load in pin = 98600 lb

Effects of deicing device on pin loads

CF = 1512 lbs

Moment (max) @ ℄ grip = (1512)(6.0) = 9072 in.-lb

Total loads on pin

Shear load = 98600 + 1512 = 100,112 lbs

Moment = 9072 in.-lb

Section properties

O.D. = 2.45 A = 1.879 in.^{2} I = 1.129 in.^{4}
I.D. = 1.90 D/t = 8.90
2t = .55

$F_{BU} = F_{tu}$ = 180 KSI, F_{su} = 109 KSI

Analysis

$$f_{b_u} = \frac{9072(1.225)}{1.129} = 9843 \text{ PSI} \qquad R_b = .055$$

$$f_{su_{(av)}} = \frac{100,112}{1.879} = 53,279 \text{ PSI} \qquad R_s = .544$$

$$f_{su(N.A)} = 2(53,279) = 106,560 \text{ PSI}$$

at

$$M.S = \frac{109,000}{106,560} - 1 = \frac{+0.02}{\text{(N.A. Shear)}}$$

APPENDIX D

RELIABILITY COMPUTATIONS

TABLE D-1. TYPE I - TAIL ROTOR GEARBOX WITH ATTACHED SHAKERS

Failure/$1x10^6$ Hr	Quantity/ Aircraft	Description	Total Failure/ $1x10^6$ Hr
291.0	4	Bearing, Sealed	1164.0
7.0	2	Housing	14.0
4167.0	2	Electric Motor	8333.0
140.0	1	Wire Harness to Motor	140.0
17.0	5	Connecters	85.0
118.0	2	Accelerometers	236.0
.5	20	Miscellaneous Hardware	10.0
274.0	1	Wire Harness to Accel.	274.0
195.0	2	Shaft and Eccen.	190.0
100.0	1	Ice Detector	100.0
--	1	Controller	2400.0
			12946.0

MTBF = 77.2 hr

TABLE D-2. TYPE II - MAIN ROTOR GEARBOX WITH ATTACHED SHAKERS

Failure/$1x10^6$ Hr	Quantity/ Aircraft	Description	Total Failure/ $1x10^6$ Hr
291.0	4	Bearing Sealed	1164.0
204.0	4	Gear	816.0
7.0	2	Housing	14.0
4167.0	2	Electric Motor	8333.0
140.0	1	Wire Harness to Motor	140.0
17.0	5	Connectors	85.0
118.0	2	Accelerometer	236.0
.5	20	Miscellaneous Hardware	10.0
274.0	2	Wire Harness to Accelerometer	548.0
95.0	2	Shaft and Eccen.	190.0
100.0	1	Ice Detector	100.0
2400.0	1	Controller	2400.0
			14036.0

MTBF = 71.25 hr

TABLE D-3. TYPE III - MAIN ROTOR BLADE EXCITED BY AERODYNAMIC TAB

Failure/$1x10^6$ Hr	Quantity/ Aircraft	Description	Total Failure/ $1x10^6$ Hr
17.0	3	Electrical Connecter	51.0
274.0	1	Wire Harness to Slipring	274.0
4.0	1	Standpipe	4.0
.6	2	Drive Pin	1.2
87.0	1	Slipring	87.0
118.0	2	Accelerometer	236.0
622.0	2	Solenoid	1244.0
33.0	2	Spring	66.0
3.0	2	Mounting Bracket	6.0
27.0	4	Rod End Bearings REM6ATL10	108.0
30.0	2	Idler Link	60.0
4.0	2	Faflon Bearing	8.0
4.0	4	Faflon Bearing BJL16TF22-11	16.0
30.0	2	Bellcrank	60.0
2149.0	2	Aerodynamic Tab and Mounting System	4298.0
168.0	2	Tip Cover/Tab Support	336.0
274.0	2	Wire Harness to Solenoid and Accelerometer	548.0

TABLE D-3. CONC.

Failure/$1x10^6$ Hr	Quantity/ Aircraft	Description	Total Failure/ $1x10^6$ Hr
17.0	4	Electrical Connecters	68.0
.5	36	Miscellaneous Hardware	18.0
100.0	1	Ice Detector	100.0
2400.0	1	Controller	2400.0
			9989.2

MTBF = 100.1

TABLE D-4. TYPE IV - MAIN ROTOR BLADE EXCITED AT ANTINODAL POINT

Failure/$1x10^6$ Hr	Quantity/ Aircraft	Description	Total Failure/ $1x10^6$ Hr
4.0	4	Bushing	16.0
233.0	2	Eccentric	466.0
476.0	2	Angular Cont. Bearing	952.0
233.0	2	Drive Shaft	466.0
204.0	4	Gear	816.0
318.0	2	Oil Seal	636.0
7.0	2	Gear Case	14.0
4167.0	2	Electric Motor	8333.0
7.0	2	Support Block	14.0
600.0	2	Lubricant and Seals	1200.0
118.0	2	Accelerometer	236.0
274.0	2	Wire Harness to Shaker & Acc.	548.0
17.0	4	Connecters	68.0
17.0	3	Connecters	51.0
274.0	1	Wire Harness to Slipring	274.0
4.0	1	Standpipe	4.0
.6	2	Drive Pin	1.2
87.0	1	Slipring	87.0
.5	20	Miscellaneous Hardware	10.0

TABLE D-4. CONC.

Failure/$1x10^6$ Hr	Quantity/ Aircraft	Description	Total Failure/ $1x10^6$ Hr
100.0	1	Ice Detector	100.0
2400.0	1	Controller	2400.0
			16692.2

MTBF = 59.9 Hr

TABLE D-5. TYPE V - HUB EXCITED BY SHAKER

Failure/$1x10^6$ Hr	Quantity/ Aircraft	Description	Total Failure/ $1x10^6$ Hr
291.0	4	Bearing, Sealed	1164.0
204.0	4	Gear	816.0
7.0	2	Housing	14.0
4167.0	2	Electric Motor	8333.0
274.0	2	Wire Harness to Motor and Accel.	548.0
17.0	4	Connecters	68.0
118.0	2	Accelerometer	236.0
17.0	3	Connecters	51.0
274.0	1	Wire Harness to Slipring	274.0
4.0	1	Standpipe	4.0
.6	2	Drive Pin	1.2
37.0	1	Slipring	87.0
.5	20	Miscellaneous Hardware	10.0
95.0	2	Shaft and Eccen.	190.0
100.0	1	Ice Detector	100.0
2400.0	1	Controller	2400.0
			14296.2

MTBF = 69.9 Hrs

APPENDIX E

MAINTAINABILITY COMPUTATIONS

TABLE E-1. TYPE I - TAIL ROTOR GEARBOX WITH ATTACHED SHAKER

Nomenclature	MTBF $1x10^{-6}$	Quantity/ Aircraft	Elap. Hr	No. Men	MMH/FH $1x10^{-6}$
Bearing, Sealed	291.0	4	.12	1	140.0
Weight, Eccentric	98.0	2	.12	1	24.0
Housing	7.0	2	.18	1	3.0
Motor, Electric	95.0	2	.10	1	19.0
Harness, Wire	140.0	1	.80	1	112.0
Connector, Electric	17.0	5	.15	1	13.0
Accelerometer	118.0	2	.23	1	54.0
Miscellaneous Hardware	0.5	20	.25	1	0.3
Drive Shaft	98.0	2	.27	1	53.0
					418.3
Control Unit and Panel Unit					39

.000456 MMH/FH

This analysis is based on removal and replacement time only.

TABLE E-2. TYPE II - MAIN ROTOR GEARBOX WITH ATTACHED SHAKERS

Nomenclature	MTBF $1x10^{-6}$	Quantity/ Aircraft	Elap. Hr	No. Men	MMH/FH $1x10^{-6}$
Bearing, Sealed	291.0	4	.27	1	314.0
Gear	204.0	4	.27	1	220.0
Housing	7.0	2	.32	1	4.0
Electric Motor	95.0	2	.21	1	40.0
Wire Harness to Motor	140.0	1	.80	1	112.0
Electric Connector	17.0	5	.15	1	13.0
Accelerometer	118.0	2	.23	1	54.0
Miscellaneous Hardware	0.5	20	.25	1	3.0
Drive Shaft	45.0	2	.27	1	24.0
Eccentric	45.0	2	.27	1	24.0
					808
Control Unit and Panel Unit					39
					.000848 MMH/FH

This analysis is based on removal and replacement time only.

TABLE E-3. TYPE III - MAIN ROTOR BLADE EXCITED BY AERODYNAMIC TAB

Nomenclature	MTBF $x10^{-6}$	Quantity/ Aircraft	Elap. Hr	No. Men	MMH/FH $x10^{-6}$
Electrical A/F Connector	17.0	3	.50	1	26.0
Wire Harness to Slip Ring	274.0	1	.80	1	20.0
Standpipe	4.0	1	.39	1	22.0
Drive Pin	0.6	2	.39	1	0.47
Slip Ring	87.0	1	.39	1	34.0
Accelerometer	118.0	2	--	-	---
Solenoid	622.0	2	.35	1	435.0
Spring	33.0	2	--	-	---
Mounting Bracket	3.0	2	--	-	---
Rod End Bearing (REM6ATC10)	27.0	4	.31	1	33.9
Idler Link	30.0	3	.31	1	18.6
Faflon Bearing	4.0	2	.37	1	3.0
Faflon Bearing (BJC16TF22-11)	4.0	4	.41	1	6.6
Bellcrank	30.0	2	.37	1	2.2
Aerodynamic Tab and Mount System	2149.0	2	.40	1	1719.0
Tip Cover/Tab Support	168.0	2	.29	1	97.0
Wire Harness to Solenoid	274.0	2	.80	1	438.0
Electric Rotating Connectors	17.0	4	.30	1	20.0

TABLE E-3. CONC.

Nomenclature	MTBF $x10^{-6}$	Quantity/ Aircraft	Elap. Hr	No. Men	MMH/FH $x10^{-6}$
Miscellaneous Hardware	0.5	36	.37	1	6.6
					2882.3
					or (.00288)
Controller and Instrument Panel Unit (Ref: Compass Control)					.00003
					.002919

This analysis considers only removal and replacement.

TABLE E-4. TYPE IV - MAIN ROTOR BLADE EXCITED AT ANTINODAL POINT

Nomenclature	MTBF $x10^{-6}$	Quantity/ Aircraft	Elap. Hr	No. Men	MMH/FH $x10^{-6}$
Bearing, Sealed	291.0	4	3.8	2.9	12827.0
Gear	204.0	4	3.8	2.9	4496.0
Housing	7.0	2	3.8	2.9	154.0
Electric Motor	95.0	2	.24	1	46.0
Wire Harness to Motor and Accelerometer	274.0	2	.39	1	214.0
Connectors (Rotating)	17.0	4	.24	1	16.0
Wire Harness to Slip Ring	274.0	1	.80	1	219.0
Standpipe	4.0	1	.39	1	2.0
Drive Pin	0.6	2	.39	1	--
Slip Ring	87.0	1	.39	1	34.0
Miscellaneous Hardware	0.5	20	.37	1	4.0
Accelerometer	118.0	2	.28	1	66.0
Connectors (A/F)	17.0	3	.50	1	26.0
					18104.0
Control Unit and Panel Unit					39.0
					18143.0

This analysis considers only removal and replacement time.

NOTE: This configuration requires blade removal.

TABLE E-5. TYPE V - MAIN ROTOR HUB EXCITED BY SHAKER

Nomenclature	MTBF $x10^{-6}$	Quantity/ Aircraft	Elap. Hr	No. Men	MMH/FH $x10^{-6}$
Bushing	4.0	4	-	-	--
Eccentric	233.0	2	.18	1	84.0
Angular Contact Bearing	476.0	4	.23	1	44.0
Drive Shaft	233.0	2	.23	1	107.0
Gear	204.0	4	.23	1	188.0
Oil Seal	318.0	2	.23	1	146.0
Gear Case	7.0	2	.25	1	4.0
Electric Motor	95.0	2	.23	1	44.0
Support Block	7.0	2	.21	1	3.0
Lubricant	600.0	2	.12	1	144.0
Accelerometer	118.0	2	.18	1	42.0
Wire Harness to Shaker and Accelerometer	274.0	2	.20	1	110.0
Connectors (Top)	17.0	4	1.43	1	97.0
Connectors (A/F)	17.0	3	1.43	1	73.0
Wire Harness to Slip Ring	274.0	1	.80	1	219.0
Standpipe	4.0	1	.39	1	2.0
Drive Pin	0.6	2	.39	1	--
Slip Ring	87.0	1	.39	1	34.0

TABLE E-5. CONC.

Nomenclature	MTBF $x10^{-6}$	Quantity/ Aircraft	Elap. Hr	No. Men	MMH/FH $x10^{-6}$
Miscellaneous Hardware	0.5	20	.25	1	3.0
					1344
Controller and Panel Unit (Ref: Compass Control)					39.0

This analysis considers only removal and replacement.

APPENDIX F
WEIGHT ANALYSIS OF SKETCHES

Type I - YAH-63 Tail Rotor

Item	ΔWeight, lb	Cumulative Weight, lb
Shaker		
Motor	.706	.706
Bearings 2 @ .23	.46	1.166
Case		
$\pi(3)(.25)(2.5)(.01) = .589$ $\pi(2)(.25)(.625)(.1) = .098$ $\pi(2)(.5)(1.56)(.1) = .490$ $(.75)(.75)(2)(.1) = .112$	1.289	2.455
Studs and bolts		
$(12)(1.125)(\ )(.125)^2(.285) =$	.189	2.644
Eccentric Weight		
Shaft $\left[\pi(.3937)^2 - (.1875)^2\right]$ $(2.75)(.283) = .293$		
Weight $\left[(1.5)(\pi)(1.25)^2\frac{90}{360}+(1.25)(.563)\right.$ $\left.(1.5)\right].283 = .820$	1.113	
Sub-total	3.757	3.757
2 of the above required		7.514
Fitting		
$(.25)(24)(1.5)(.1) =$	.9	
$(1.75)(.375)(4)(.1) =$	.26	
$(2)(3)(.5)(4)(.25)(.1) =$	.3	
Sub-total	1.46	8.974

Item		ΔWeight, lb	Cumulative Weight, lb
Control System			
Dual shaker electronic control unit	≈	4.0	
Control unit	≈	1.25	
Wiring	≈	.70	
	Sub-total	5.95	
		Type I Total	14.924

Type II - AH-1G Main Rotor Gearbox - Symmetric Mode

Item		ΔWeight, lb	Cumulative Weight, lb
Shaker			
Motor		2.75	2.75
Bearings 305 = .52 Fafnir 302 = .18		.70	3.45
Gears			
$(\pi)(1.75)(.25)(.5)(.283)$ $\pi(.75)(.188)(.5)(.283)$	= .194 = .063	.257	3.707
Case			
$\pi(5.5)(3.56)(.25)(.1)$	= 1.538		
$\pi\left(\frac{5.25}{2}\right)^2(.25)(.1)(2.15)$	= 1.164		
$\pi(1.5)(.25)(1)(.1)$	= .1178		
$\pi(3.56)(.43)(1)(.1)$	= .481		
$\pi(3.5)(.312)(1)(.1)$	= .343		
$3(.5)(5.25)(.1)$	= .788	3.951	7.658
Studs and bolts	=	.14	7.798
Eccentric weight			
Shaft			
$(4.625)(\pi)(.375)^2(.283)$	= .578		
Weight	=6.4	6.978	
	Sub-total	14.776	14.776
Attachment fitting			
(4) (1)(.375)(2)(.1)	=	.30	
Bolts	=	.15	
	Sub-total	.45	15.226
2 of the above required			30.452

Item		ΔWeight, lb	Cumulative Weight, lb
Control system			
Dual shaker electronic control unit	=	5.0	
Control unit	=	1.5	
Wiring	=	.70	
	Sub-total	7.20	
	Type II Total		37.652

Type III - Aerodynamic Flap UH-1 Blade Tip

Item	ΔWeight, lb	Cumulative Weight, lb
Flap		
$(6)(18)\left(\frac{3}{144}\right)$ =	2.25	2.25
Torque rod		
$\pi(.125)^2(18)(.285) = .252$		
$\pi(.25)^2(3)(.285) = .168$	.420	2.670
Torque rod fittings		
$(2)(.375)(1.25)(.283)$ =	.265	2.935
Push rod		
$\pi(.125)^2(5)(.283)$ =	.07	3.005
Idler arm		
$(.5)(.25)(1.5)(.1)$ =	.019	3.024
Solenoid		
$\pi(.75)(1.5)(.433) = 1.53$ $\pi(.125)^2(2.5)(.253) = .031$	1.561	4.585
Solenoid bracket =	.20	4.785
Tip cap		
$\frac{2+2+2.525+1+2+1}{2}(22)(.12)(.1)$ =	1.39	6.175
Inboard attachment bracket		
$\frac{1.5+1.0}{2}(6.5)(1)(.1)$ =	.81	6.985
Inboard rib		
$\frac{1+1+2.5+1+14.5}{2}(.12)(15)(.1)$ =	1.8	8.785

Item	ΔWeight, lb	Cumulative Weight, lb
Outboard rib	1.40	10.185
Skin(s)		
(2)(19.5)(16)(.06)(.1) ≈ .375	.374	10.559
Gussets		
4(7)(3)(.5)(.040)(.1) ≈ .334 4(4)(4)(.5)(.040)(.1) ≈ .128	.296	10.855
Bolts	.50	11.355
2 of the above required		22.71
Slip ring installation	15.00	37.71
Control box	1.0	
	Type III Total	38.71

(No delta weight added to rotor for increased centrifugal force.)

Type IV - Inblade Shaker UH-1 Blade

Item	ΔWeight, lb	Cumulative Weight, lb
Shaker		
Motor	1.50	1.5
Bearings	.70	2.2
Gears	.258	2.458
Case	2.80	5.258
Studs and bolts	.14	5.398
Eccentric weight		
Weight		
$(.5)(1)(1.43)(14)(.633) = 6.33$		
Tube		
$\pi(1.5)(.060)(14)(.283) = 1.12$		
Shaft		
$(28)\pi(.562)(.125)(.283) = 1.75$		
Bearing = .46		
Bolts = .14		
Sub-total	9.8	
	15.198	15.198
Blade fitting		
$\frac{(.81+.375)}{X}(x)(2)(16)(.1) =$	3.79	
$(2)(.5)(1.5)(2)(.1) =$	.30	
Bolts	.18	
Sub-total	4.27	19.468

Item	ΔWeight, lb	Cumulative Weight, lb
Attachment bracket		
(3.0)(.4375)(2)(.1) =	.26	19.728
2 of the above required		39.456
Slip ring assembly	20.00	
Sub-total		59.456
Control system		
Dual shaker electronic control	5.00	
Control unit	1.50	
Wiring	1.20	
Sub-total	7.70	
Type IV (Inblade Shaker) Total		67.156

Type IV - Exterior Blade Shaker

Installation weight from above		67.156
Add 4 pounds for covers	4.00	
Type IV (Exterior Blade Shaker) Total		71.156

Type IV - Blade Tip Shaker

Assume a blade tip shaker is to be used replacing existing tip weights. Use AH-1G as an example.

Assume shaker is similar to UH-1 design.*

Shaker weight (2 required)	39.4	
Remove tip weight (equivalent to shaker weight)	-32.0	7.4
Slip ring assembly	20.0	
Sub-total		27.4

Control system

Dual shaker electronic control	5.0	
Control unit	1.5	
Wiring	4.0	
Sub-total	10.5	
Type IV (Blade Tip Shaker) Total		37.9

*Not critical because AH-1G has 32 pounds at tip weights.

Type V - Hub Modal Excitation

Item	ΔWeight, lb	Cumulative Weight, lb
Shaker (same as Type II)	14.776	14.776
Attachment bolt		
$(12)\pi(.25)^2(.283)$	.667	15.443
Spacer		
$\pi(1)(.87)(.1)$	.273	15.716
Bonded block		
$(5)(.5)(2.5)(.1)$	.625	
Sub-total	16.341	16.341
2 of the above required		32.682
Slip ring	20.00	
Sub-total		52.682

Control system

Dual shaker electronic control	5.0	
Control unit	1.5	
Wiring	.70	
Sub-total	7.20	
Type V Total		59.882

APPENDIX G

BREADBOARD SYSTEM TESTS

1.1 DUAL MOTOR DRIVEN SHAKER CONFIGURATION

A breadboard control system was fabricated and tested. It consisted of dual motor-driven shakers mounted on a cantilevered beam and associated electronic controller unit. The objectives of these tests were to address the requirements between the two shaker units, and to identify possible problem areas.

1.1.1 Description of Test Configuration

1.1.1.1 Motor Controller System Description

A schematic diagram of the D.C. motor controller is shown in Figure G-1. The system consists of two identical D.C. motor speed control channels (designated master and slave) and a means of deriving relative frequency and phase error between the two. This error is then used to modify the speed of the slave motor until synchronization between the master and slave motors occurs.

Mounted on each motor shaft is a 40-tooth steel gear. A magnetic pickup is also mounted on each motor in close proximity to the gear teeth. A pulse is generated as each gear tooth rotates past the magnetic pickup. The frequency of the resulting train of pulses (40 pulses/revolution) is thus proportional to the shaft speed of the particular motor. The pulses are filtered and a D.C. analog voltage proportional to motor speed is obtained. This motor speed voltage is then utilized as conventional tachometer feedback.

One tooth on each gear is longer to produce a larger magnitude pulse during each revolution. Phase error between the master and slave motors is thus determined by the relative displacement in time between the two reference pulses. A voltage proportional to the phase and frequency error is derived and used to modify the speed of the slave motor. Synchronization occurs whenever the two reference pulses are aligned with respect to time.

The controller circuits were mechanized utilizing standard off-the-shelf components. The breadboard electronics are shown, along with the mechanical configuration, in Figure G-2.

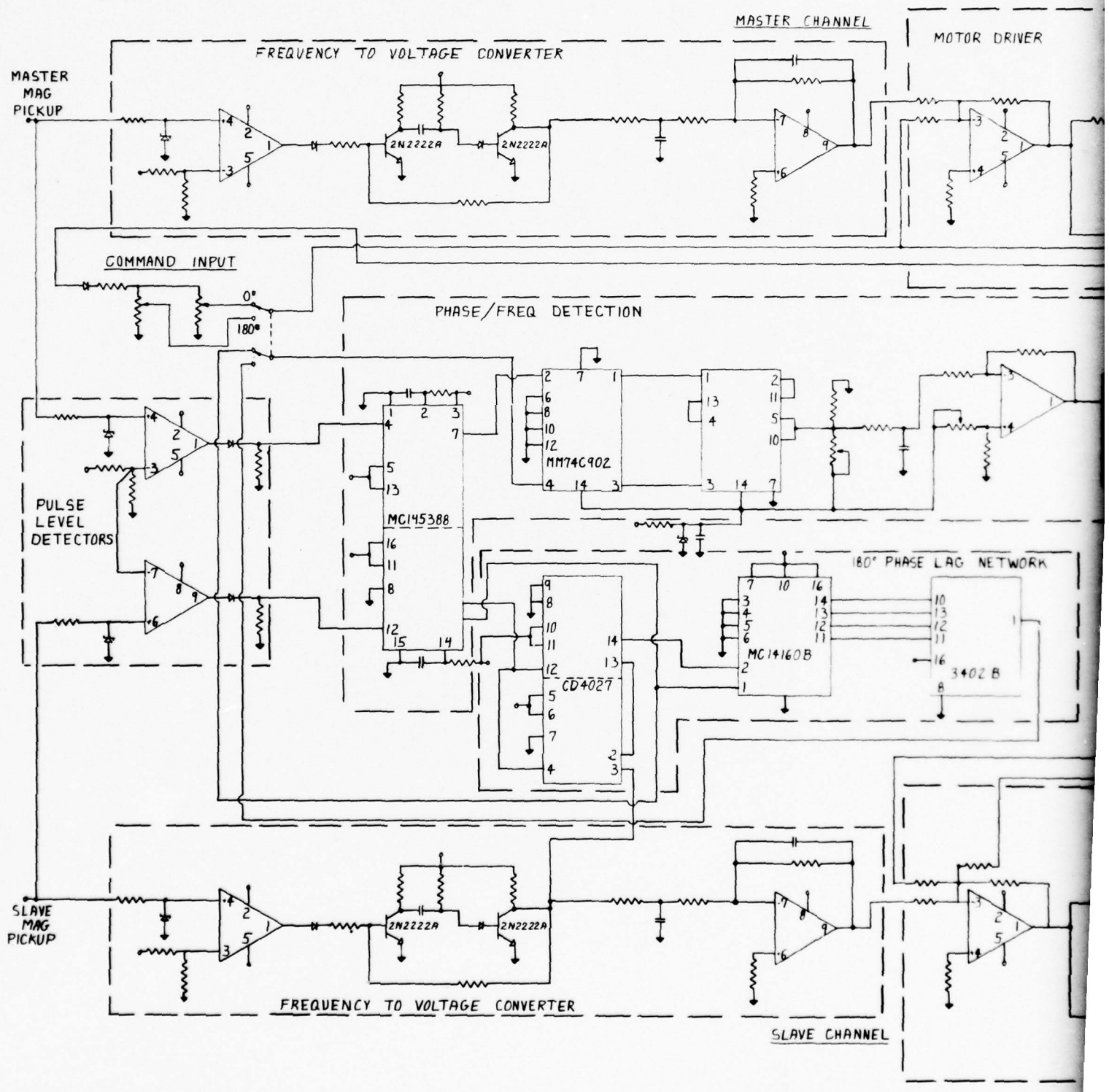

Figure G-1. Dual motor controller

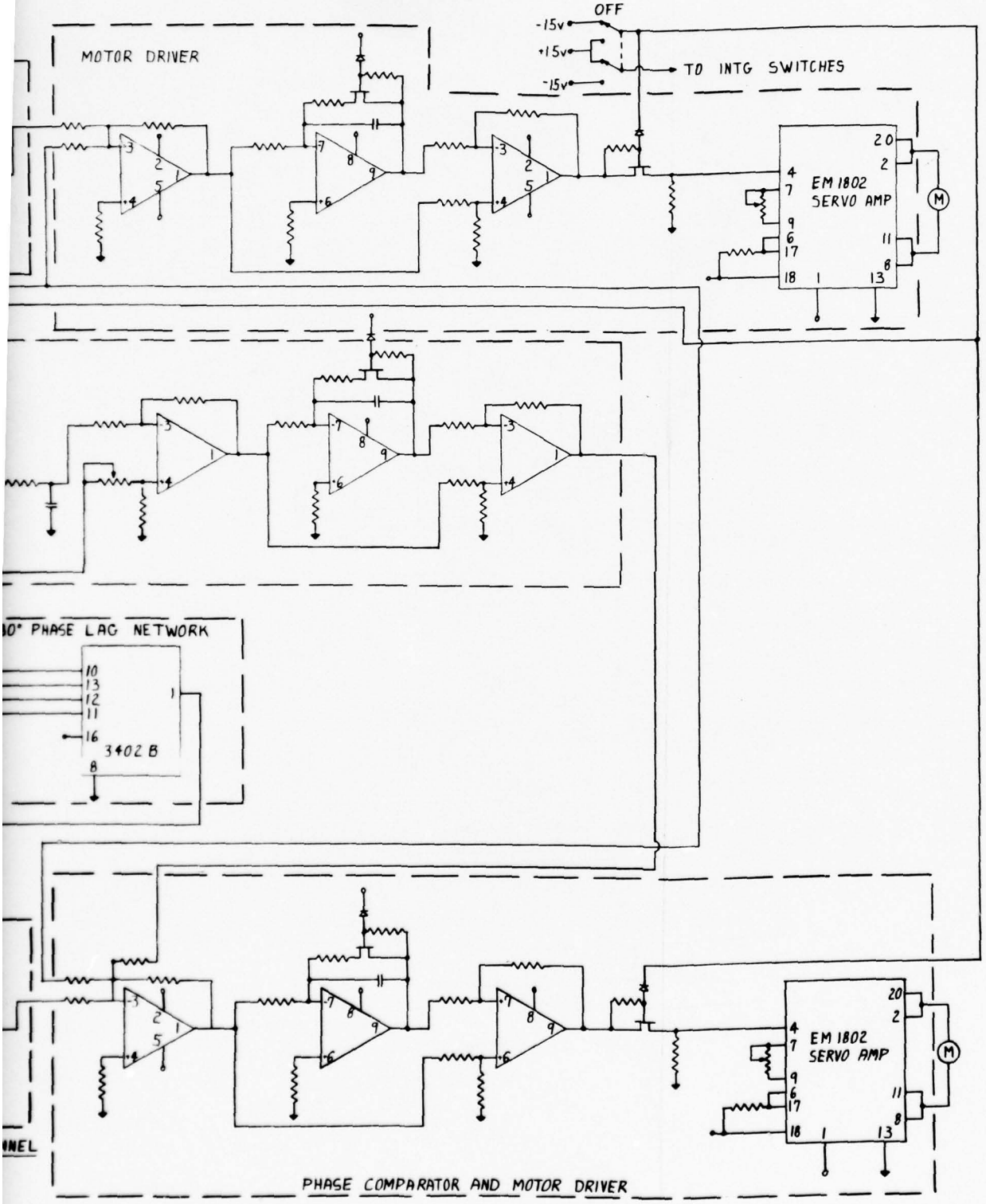
MOTOR DRIVER
OFF
-15v
+15v
-15v
TO INTG SWITCHES
EM 1802
SERVO AMP
M
0° PHASE LAG NETWORK
3402 B
EM 1802
SERVO AMP
M
PHASE COMPARATOR AND MOTOR DRIVER
R CONTROLLER

SK C3 41777

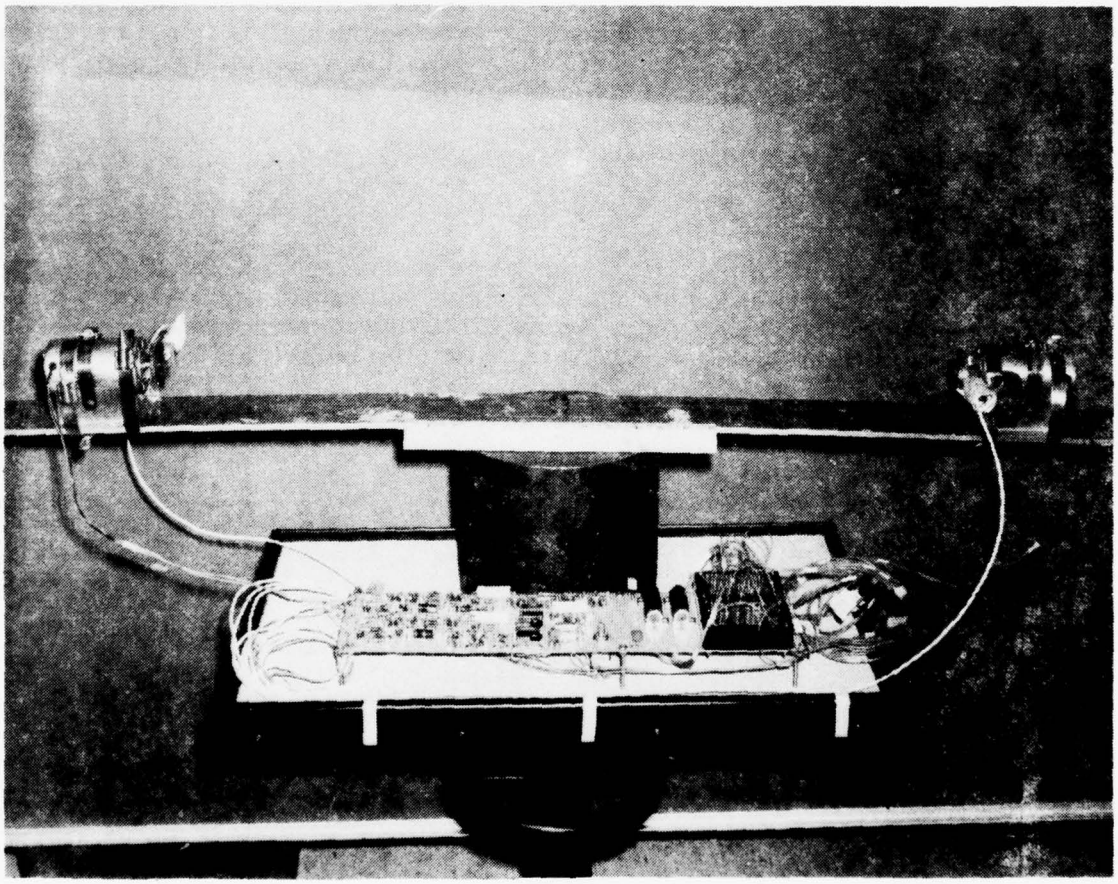

Figure G-2. Electro-mechanical breadboard

1.1.1.2 Test Set-up

A cantilevered beam was used to represent a scaled-down mechanical version of the rotor blade. The beam is an aluminum bar 106 inches long, 1/4 inch thick, and 3-3/8 inches wide. Beam characteristics were tailored to approximate the frequency and deflection required for a full-scale blade. Two small (1/12 hp) permanent magnet motors with eccentric weights attached directly to the motor shafts are mounted on the beam at an antinode to provide a symmetrical mode excitation of the beam. Motor speed and location on the beam were varied initially to determine the frequency and antinode location at which the beam resonance occurred. At the frequency and for the eccentric weight and arm used (.175 ounce at a radius of .5 inch) the force generated is approximately .75 pound.

1.1.1.3 Test Results

Beam resonance was found to occur at a motor speed of 2325 RPM. Synchronization between motors occurred approximately 1.5 seconds after rotor turn on. Approximately 2 seconds after synchronization, maximum deflection of the beam was achieved, which was .3 inch peak-to-peak at the tip. The following figures are oscilloscope pictures obtained during operation of the system. Figure G-3 shows pulse-to-voltage converter output and input to the master motor.

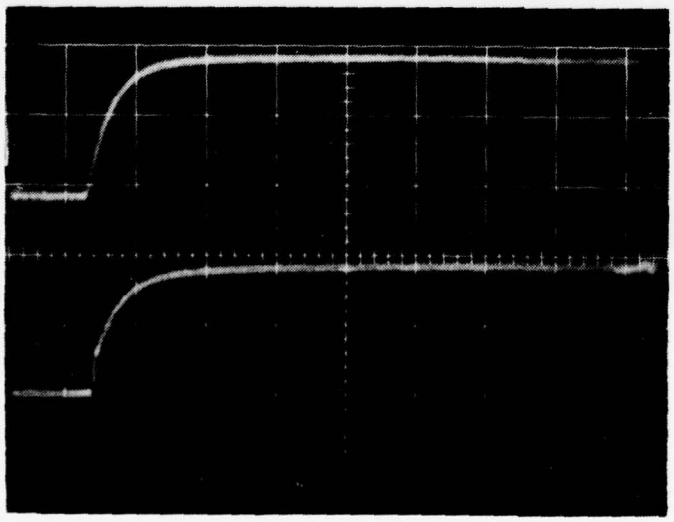

Upper Trace

Input Signal to Master Motor

Vertical = 5v/cm
Horizontal = 0.5 sec/cm

Lower Trace

Pulse to Voltage Converter Output - Master Motor
Vertical = 5v/cm
Horizontal = 0.5 sec/cm

Figure G-3. Converter output and input signals to master motor

Figure G-4 is the same data for the slave motor. Note the speed correction in the pulse to voltage converter output due to the phase/frequency error between the master and slave.

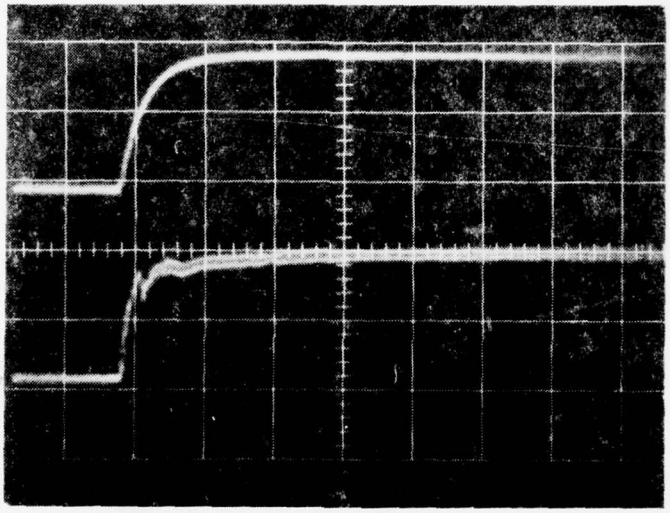

Upper Trace

Input Signal to Slave Motor
Vertical = 5v/cm
Horizontal = 0.5 sec/cm

Lower Trace

Pulse to Voltage Converter Output - Slave Motor
Vertical = 5v/cm
Horizontal = 0.5 sec/cm

Figure G-4. Converter output and input signals to slave motor

Figures G-5 and G-6 are the outputs of the master and slave magnetic pickups. The larger amplitude pulses are the result of one longer tooth on the gear, as previously described. The time interval between pulses represents 9^{o} of revolution.

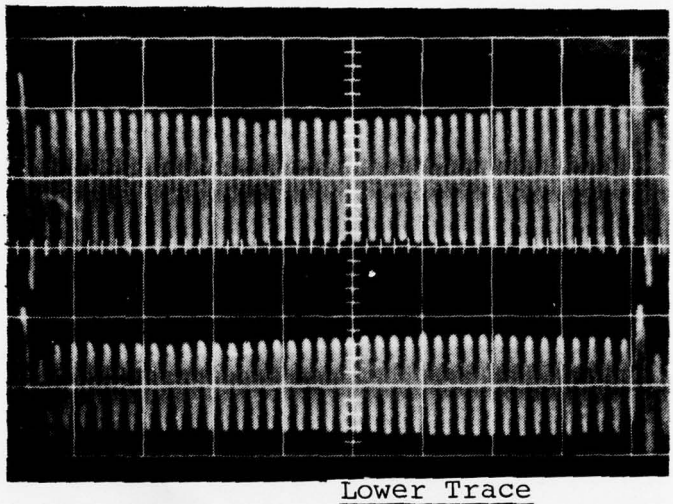

Upper Trace

Master Magnetic Pickup
Output
  Vertical = 5v/cm
  Horizontal = 2 sec/cm
  uncalibrated

Lower Trace

Slave Magnetic Pickup
Output
  Vertical = 5v/cm
  Horizontal = 2 sec/cm
  uncalibrated

Figure G-5. Magnetic pickup signal 2 sec/cm

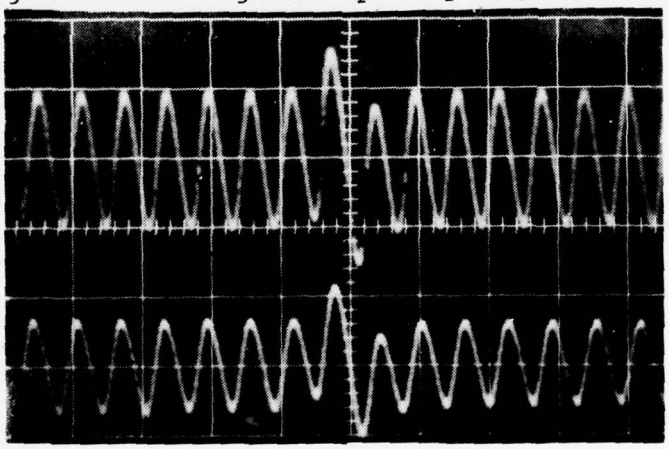

Upper Trace

Master Magnetic Pickup
Output
  Vertical = 5v/cm
  Horizontal = 1 sec/cm

Lower Trace

Slave Magnetic Pickup
Output
  Vertical = 5v/cm
  Horizontal = 1 sec/cm

Figure G-6. Magnetic pickup signal 1 sec/cm

Figure G-7 shows the relative phase error between the master and slave motors at synchronization. As shown by the figure, phase error is approximately 0.5 degree. Figure G-8 shows the output of the phase/frequency detector during start up of the motors. Note that the detector output is essentially at zero error level within 1.5 seconds of motor turn on.

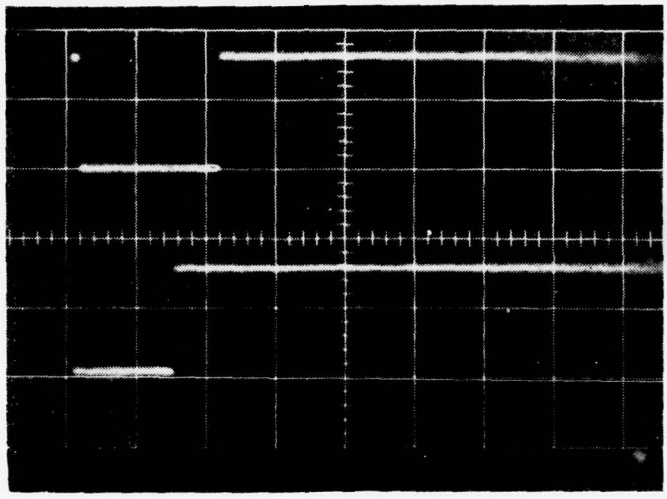

Upper Trace

Master Reference Pulse
After Shaping
Vertical = 10v/cm
Horizontal = 50μsec/cm

Lower Trace

Slave Reference Pulse
After Shaping
Vertical = 10v/cm
Horizontal = 50μsec/cm

0.0258 second = 360 degrees

Figure G-7. Phase error between master and slave motor

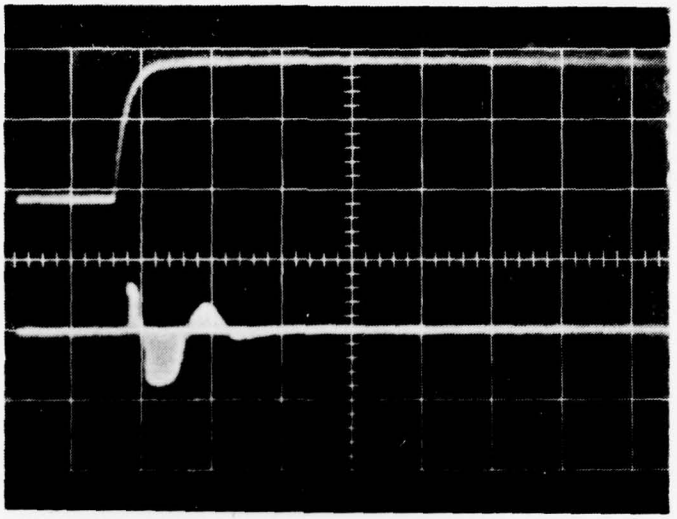

Upper Trace

Input Signal to Slave Motor

Vertical = 5v/cm
Horizontal = 1 sec/cm

Lower Trace

Phase/Frequency Detector Output
Vertical = 1v/cm
Horizontal = 1 sec/cm

Figure G-8. Phase/frequency detector output

Subsequent testing of the system was done using the beam suspended by a spring which represents a free-free beam. The purpose here was to evaluate both symmetric and asymmetric mode excitation and 180-degree out-of-phase motor control.

1.1.2 Conclusions

Although the tests were conducted using a model that may not accurately represent a scaled version of the rotor system, tests duplicated the problems involved of maintaining synchronized speed and phase control of dual eccentric weight shakers mounted in a vibratory environment.

The electronic controller unit performed satisfactorily with the phase relationship between eccentric weights held to less than 1 degree. Also, it is considered the system contains all of the functions required to maintain synchronous speed and phase control of dual motor-driven eccentric shakers in a vibratory environment. Although the specific method of mechanizing the system could differ, the concept of both speed and phase control loops for system control is considered necessary. It may be desirable to reduce response time for synchronizing the system.

The concept applies to both the dual blade mounted or dual gearbox mounted shaker systems.

The single eccentric weight configuration works well and deletes the gearing requirements of a dual weight type.

The breadboard system did not include certain functions that are considered necessary for a development system. These are:

- Automatic duty cycle timing with operator override.
- System monitor and automatic shutdown for fail-safe operation.

1.2 HYDRAULIC ACTUATOR SHAKER CONFIGURATION

The feasibility of using a hydraulic actuator shaker located in the nonrotating control system for deicing purposes was tested. Objectives of the tests were to determine if it was possible to drive the actuator at the required frequencies with a usable stroke displacement needed for blade deicing, and to determine the effect of external loading on the frequency response of the actuator.

1.2.1 Description of Test Configuration

A functional block diagram of the configuration used in this test is shown in Figure G-9. A variable frequency signal is applied to the valve driver electronics whose output drives the actuator valve. A linear voltage differential transformer (LVDT) provides the feedback for closed loop operation. Load

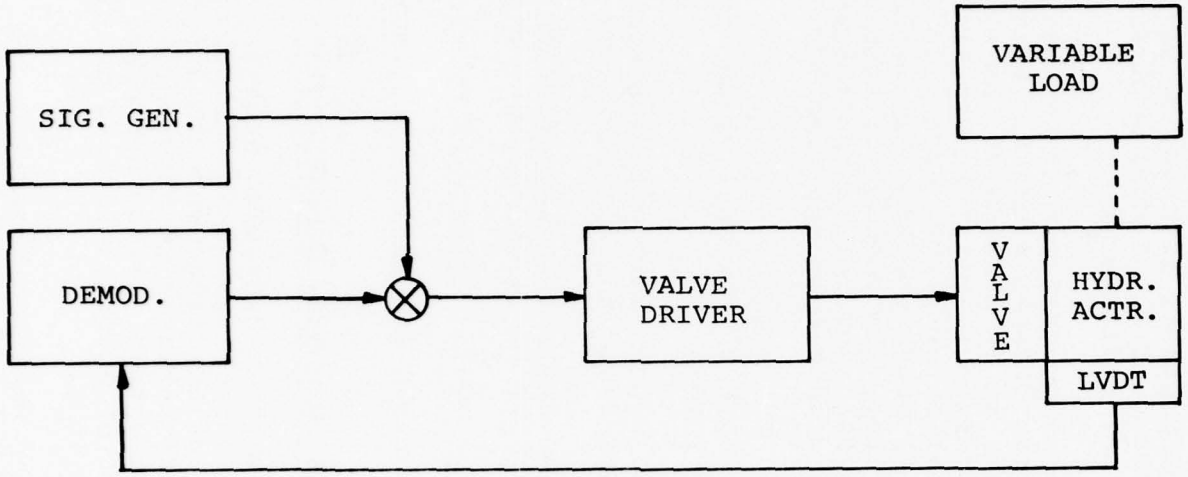

Figure G-9. Block diagram of test configuration

conditions for the actuator were no-load, 100-pound, and 300-pound loads. The actuator is shown in Figure G-10.

1.2.2 Test Results

Frequency sweeps were made from 0 to 50 Hz under no-load, 100-pound load, and 300-pound load conditions to evaluate actuator response and stroke displacement. Frequency response data are shown in Table G-1 for a 3000 psi system with a 100-pound load. Performance using a 300-pound load is essentially the same.

TABLE G-1. FREQUENCY RESPONSE FOR ACTUATOR AND SERVO CONTROL (3000 PSI, 100-POUND EXTERNAL LOAD)

Frequency (Hz)	Displacement (± in.)
15	0.055
20	0.037
25	0.026
30	0.021
40	0.012
50	0.008
55	0.007

1.2.3 Conclusions

It is possible to drive the hydraulic actuator with a usable displacement out to 50 Hz. It is recognized that the test configuration did not properly simulate an aircraft configuration (i.e. spring rates, etc.), but it does appear to be a possible approach. Here again, the breadboard system did not include the functions of failure monitoring for automatic shutdown, duty cycle timing, and operator override which are considered necessary for a development system.

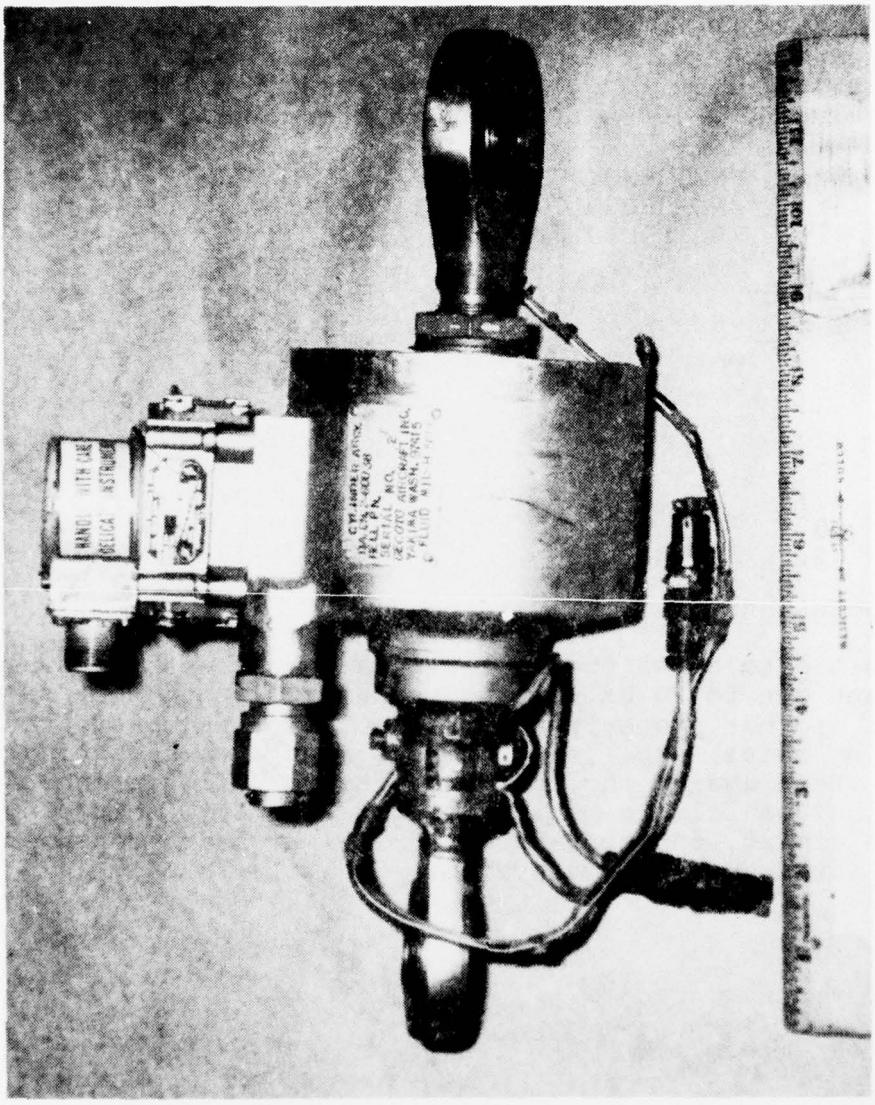

Figure G-10. Hydraulic actuator

APPENDIX H

MAIN AND TAIL ROTOR MODE SHAPES

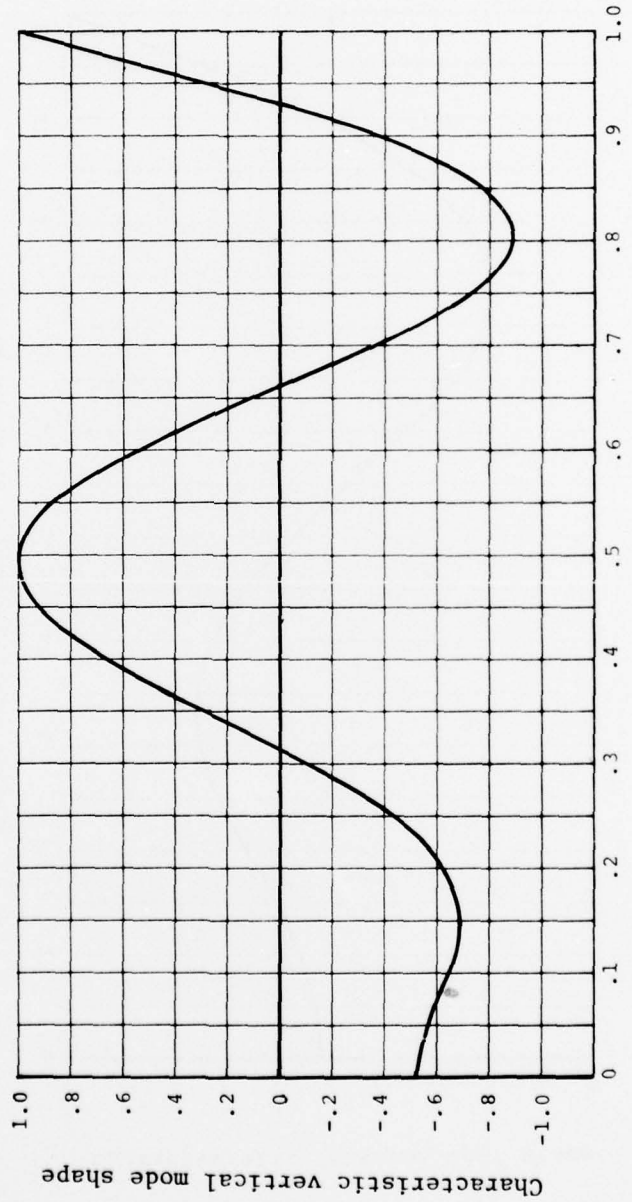

Figure H-1. UH-1 symmetric mode @ 2546 CPM main rotor

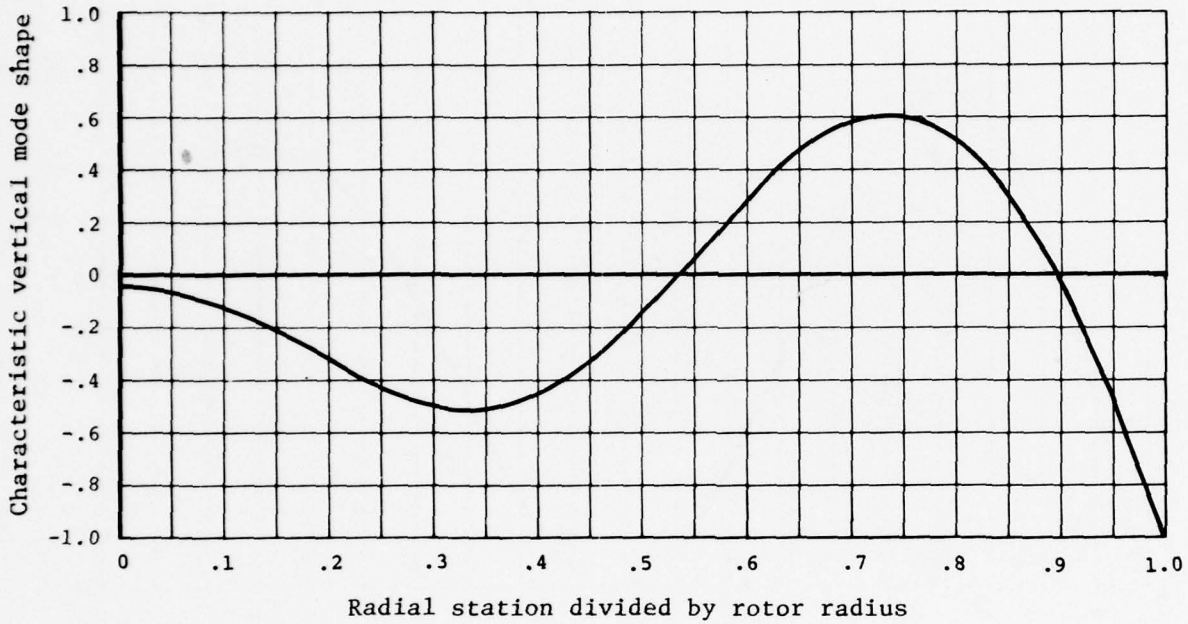

Figure H-2. UH-1 symmetric mode @ 1752 CPM main rotor

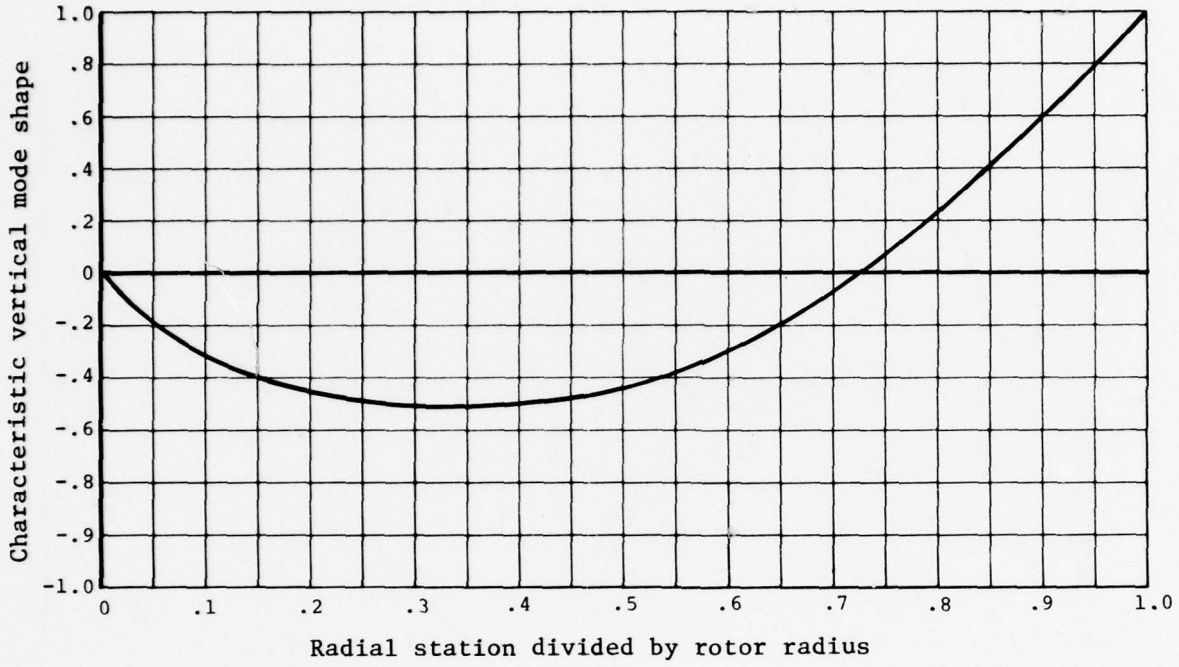

Figure H-3. UH-1 asymmetric mode @ 4005 CPM tail rotor

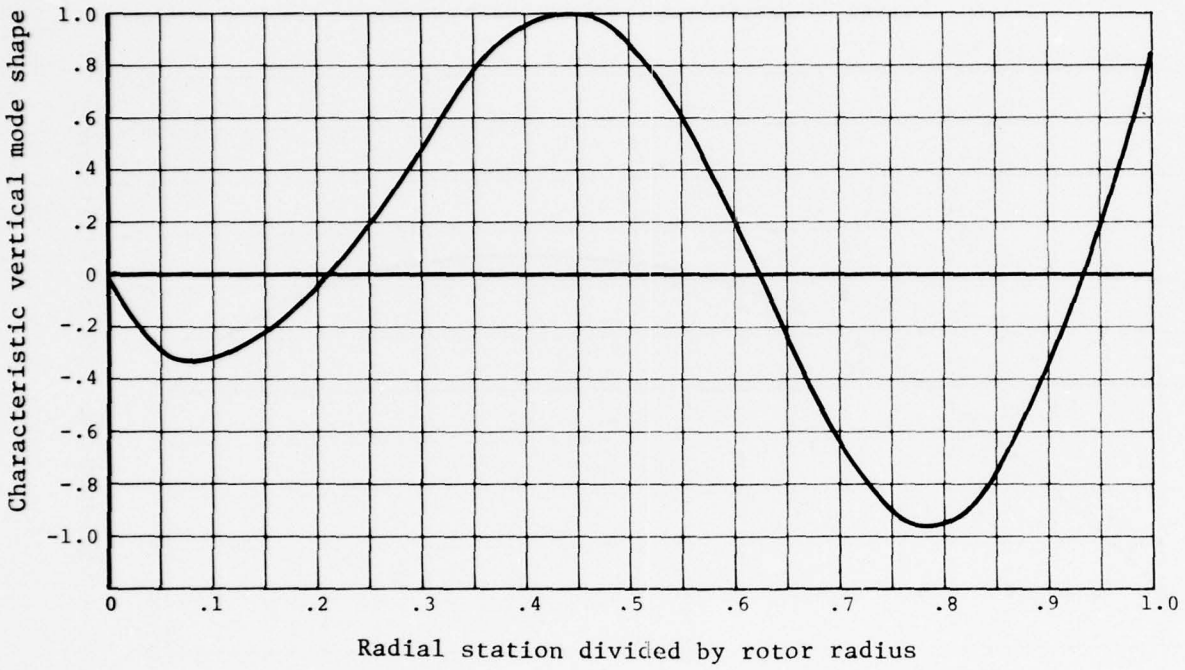

Figure H-4. AH-1 asymmetric mode @ 2571 CPM main rotor

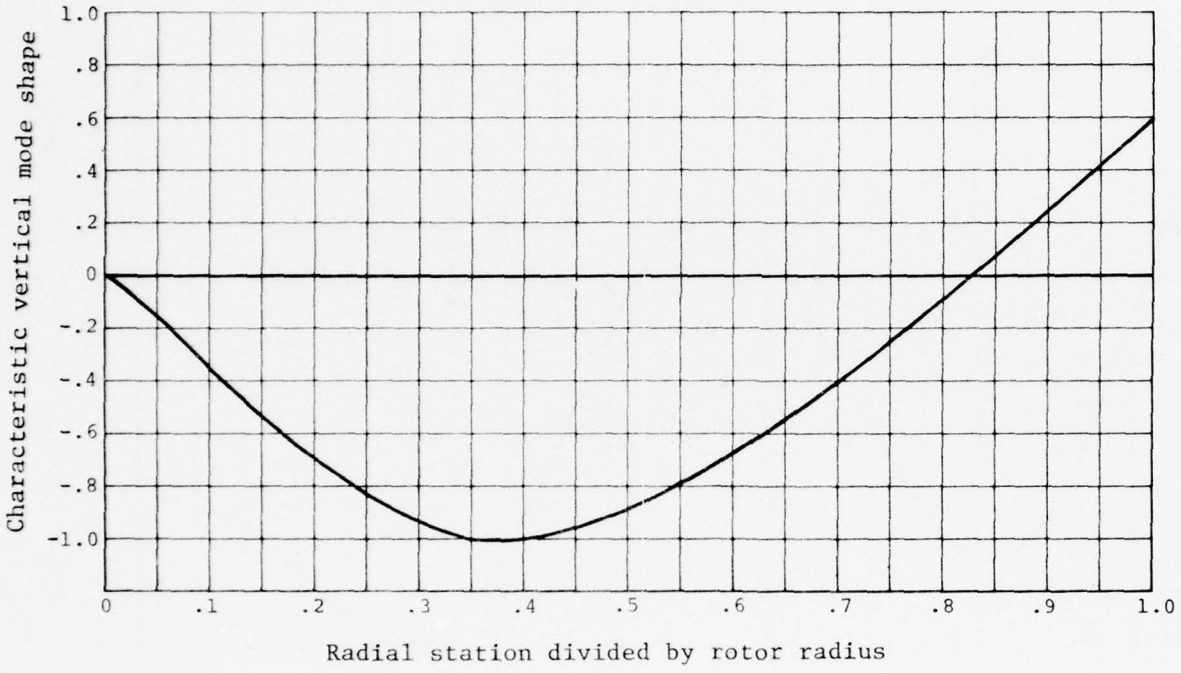

Figure H-5. AH-1 asymmetric mode @ 1724 CPM tail rotor

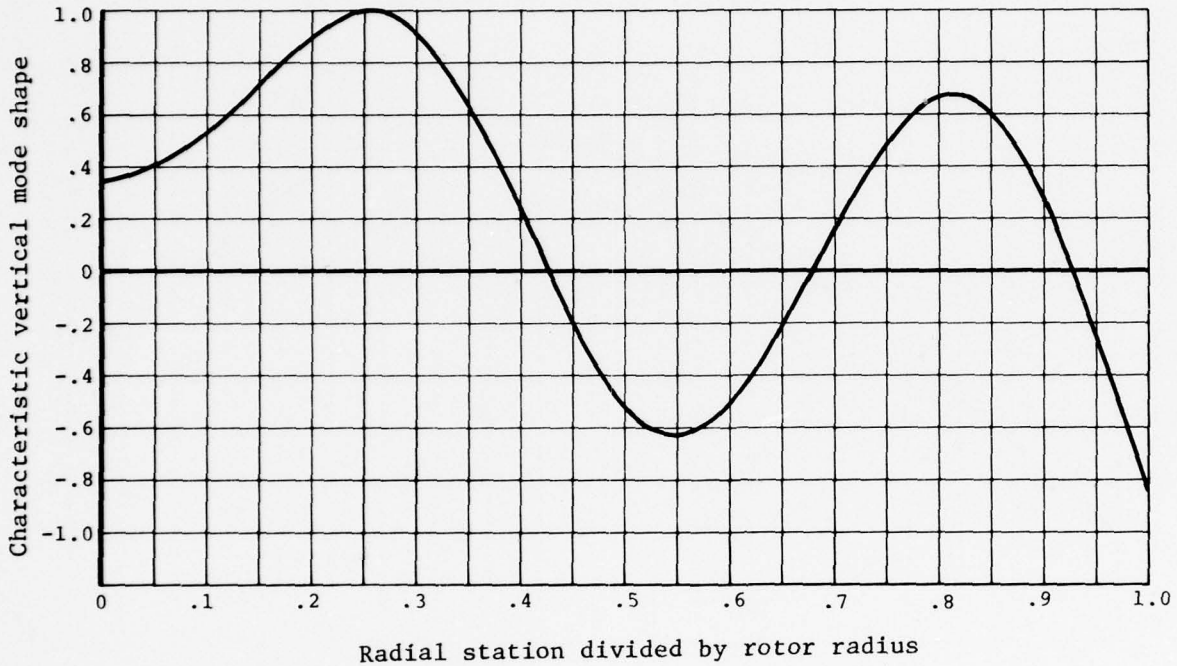

Figure H-6. OH-58A symmetric mode @ 3168 CPM main rotor

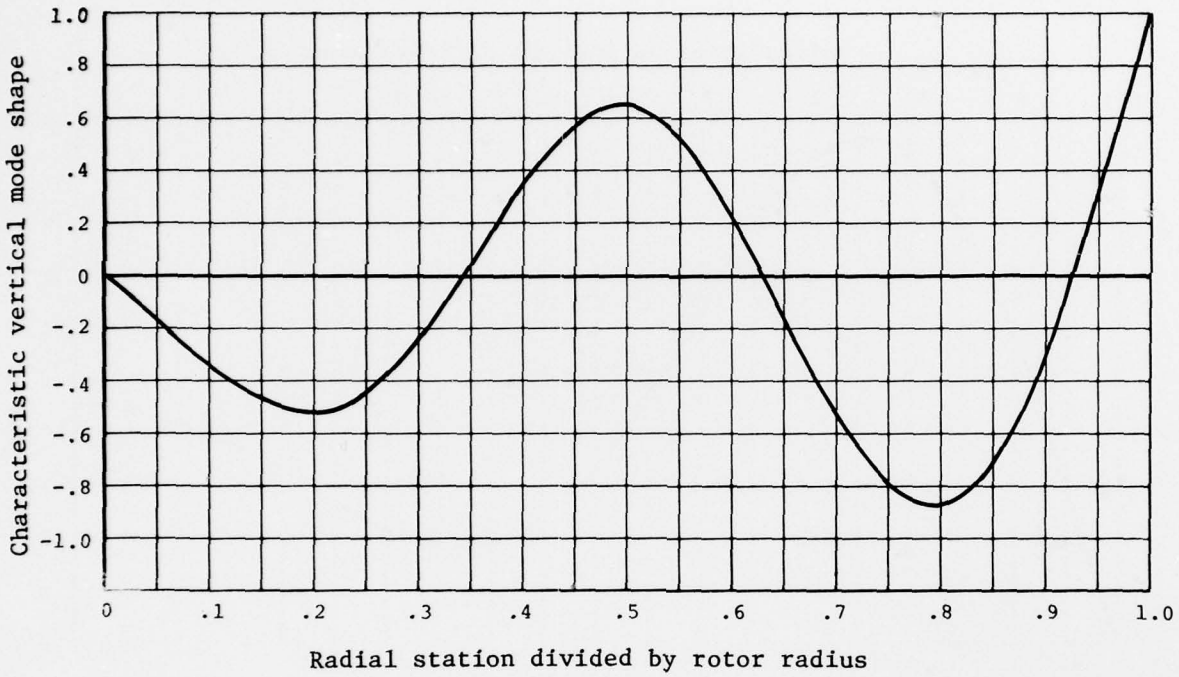

Figure H-7. OH-58 asymmetric mode @ 2694 CPM main rotor

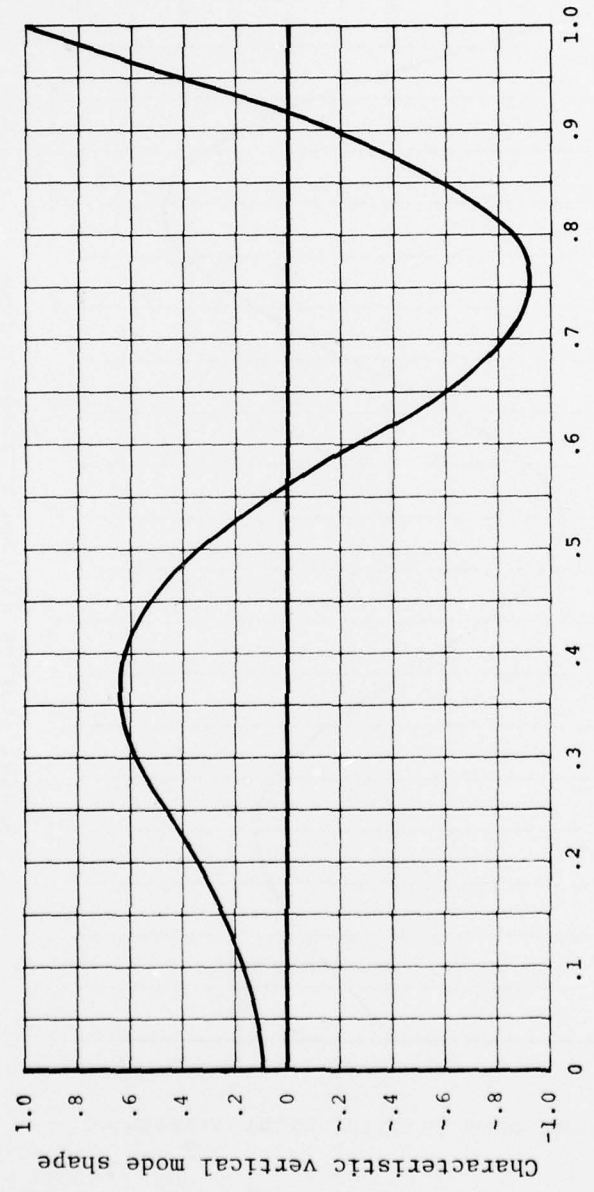

Figure H-8. OH-58 symmetric mode @ 2248 CPM main rotor

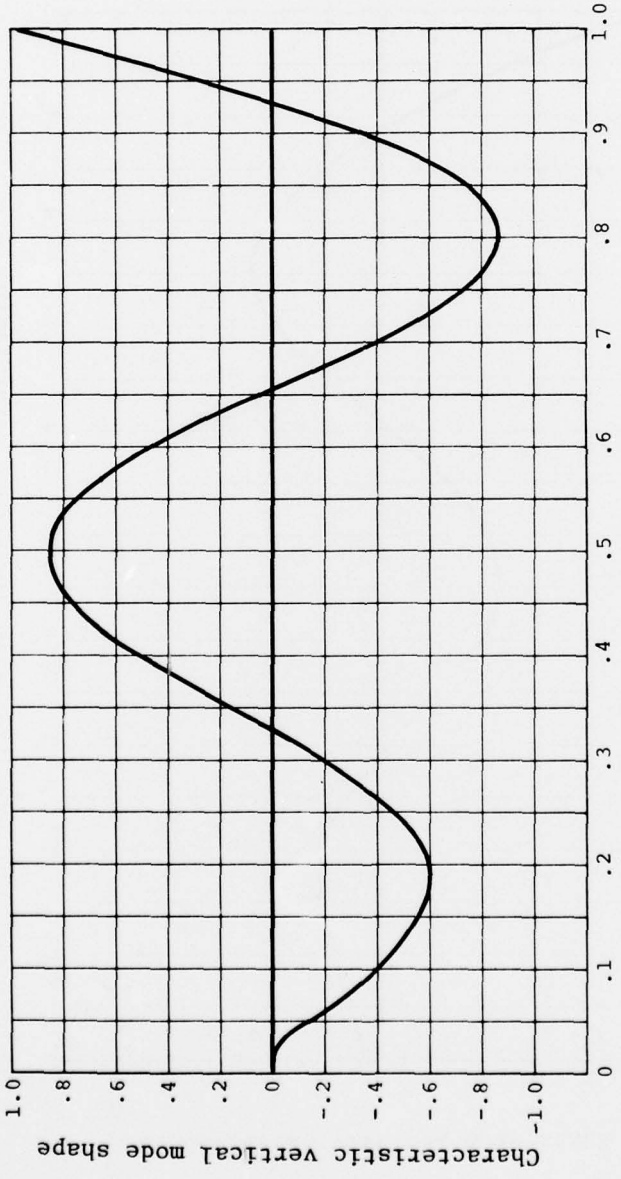

Figure H-9. CH-47 scissors mode @ 1888 CPM

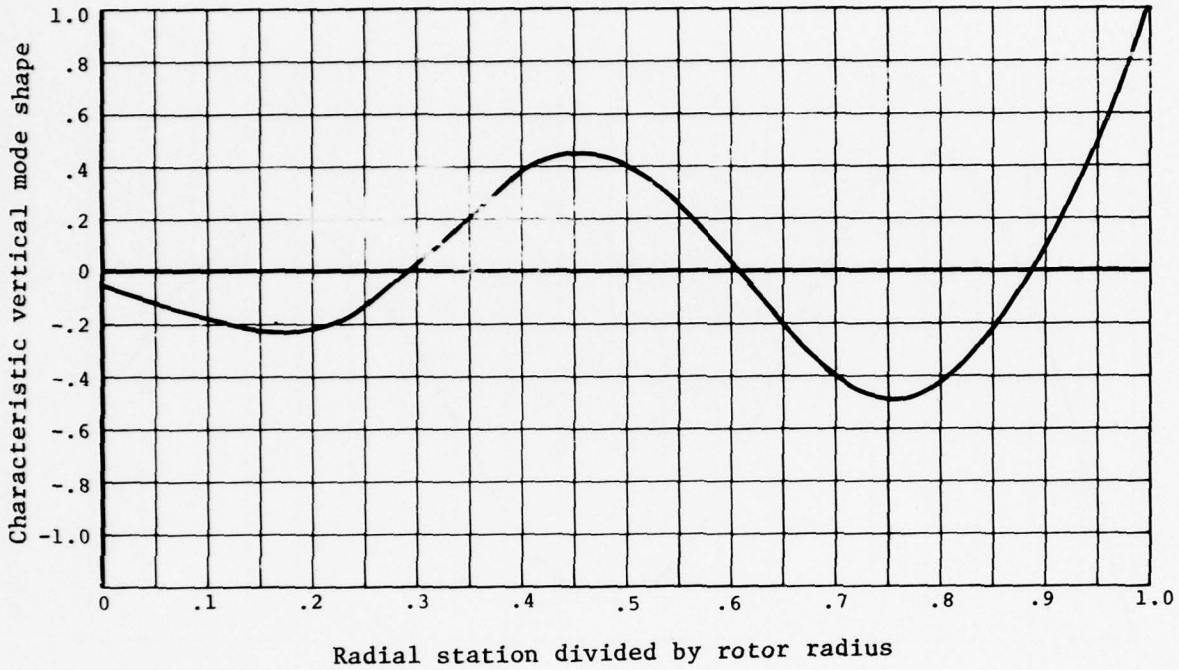

Figure H-10. YAH-63 symmetric mode @ 2138 CPM main rotor

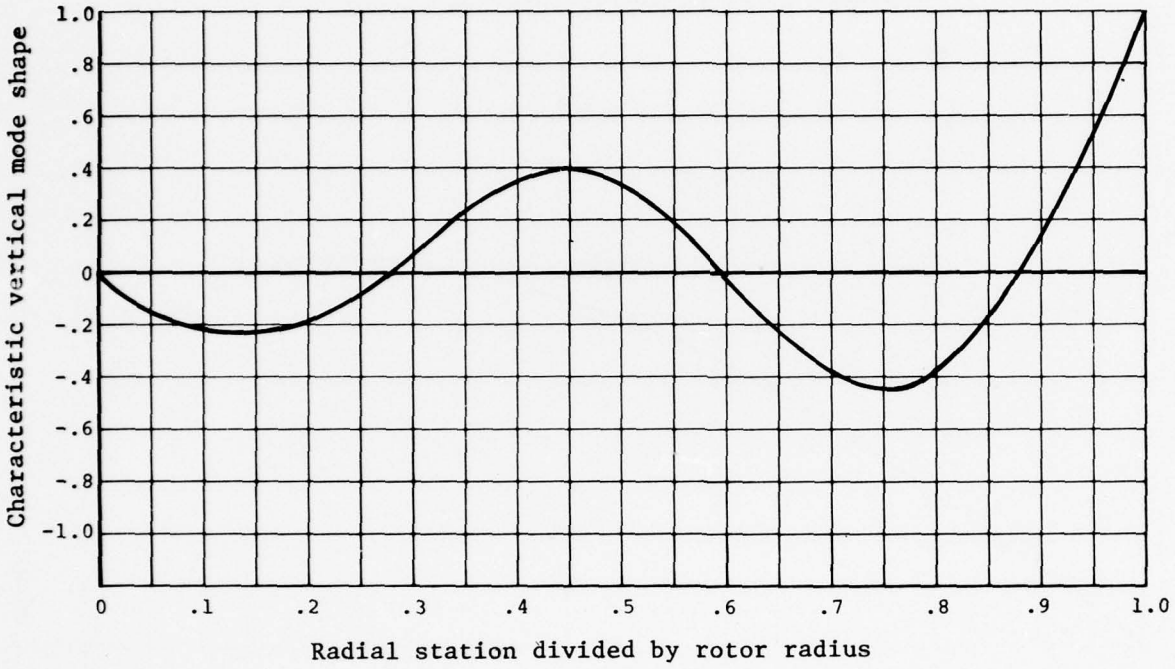

Figure H-11. YAH-63 asymmetric mode @ 2011 CPM main rotor

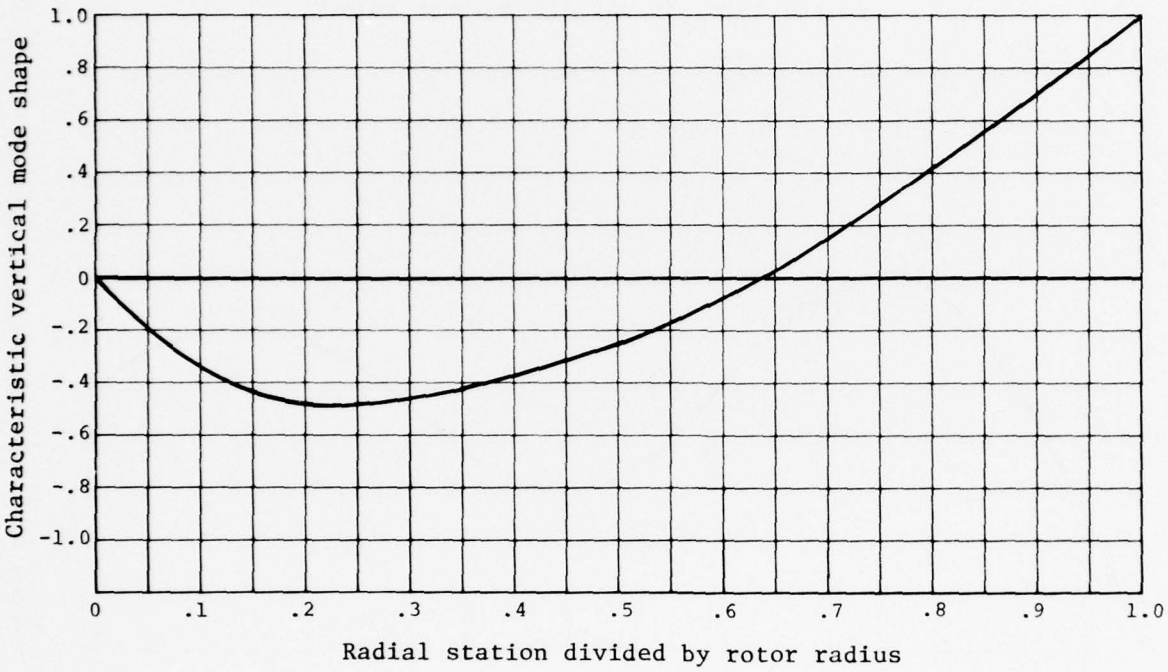

Figure H-12. YAH-63 asymmetric mode @ 3686 CPM tail rotor

LIST OF SYMBOLS

A	Area (in^2)
B	Number of blades
C	Rotor chord (in)
C_D	Drag coefficient
C_{D_A}	Section drag coefficient at point A
C_{D_B}	Section drag coefficient at point B
CF	Centrifugal force (lb)
ΔCF	Incremental centrifugal force (lb)
F	Force (lb)
F_{BU}	Ultimate allowable bending stress (psi)
F_{SU}	Ultimate allowable shear stress (psi)
F_{TU}	Ultimate allowable tensile stress (psi)
fb	Bending stress (psi)
fs	Shear stress (psi)
ft	Tensile stress (psi)
g	Acceleration of gravity (386 in/sec^2)
GI	Generalized inertia for mode ($lb\text{-}in\text{-}sec^2$)
I_B	Moments of inertia along beamwise axis (in^4)
I_C	Moments of inertia along chordwise axis (in^4)
k	Vertical impedance of fuselage/pylon (lb/in)
M_B	Beamwise bending moment (in-lb)
M_C	Chordwise bending moment (in-lb)
MS	Shape where force applied (in)
M.S.	Margin of safety
Q_A, Q_B	Torque of blade element (ft-lb)
Q_b	Torque/blade (ft-lb)
R_b	fb/F_{Bu}
R_s	fs/F_{Su}
R_t	ft/F_{Tu}
S	Element area (ft^2)
V_A, V_B	Velocity of point A (ft/sec)
X, x	Displacement (in)
Z	Vertical deflection at hub (in)
$Z_n(0)$	Vertical mode shape for nth mode
α_o	Slope of lift curve, $d\ C_L/d\alpha$
ΔL	Change in lift (lb)
δ	Modal participation factor
ε_n	Generalized coordinate of the nth node
ζ	Damping factor
ρ	Air density (slugs)
Ω	Rotor angular velocity (rad/sec)
ω	Frequency (rad/sec)
ω_n	Natural frequency (rad/sec)